FRICTION, WEAR, AND LUBRICATION IN VACUUM

by

Donald H. Buckley

Prepared at NASA Lewis Research Center

Library of Congress Catalog Card Number 72-174581

PREFACE

This publication is intended as a review of studies and ob-
servations on the friction, wear, and lubrication behavior of ma-
terials in a vacuum environment. The specific subject of adhe-
sion was not included. There is a general discussion of the
subject, however, with reference to friction and adhesive wear.
The intent in this document was to satisfy two interests in the
field of tribology: that of the basic researcher and that of the
engineer confronted with lubrication design problems. Vacuum
provides the basic researcher with a tool that enables him to
eliminate normal environmental effects and their influence on
friction, wear, and lubrication. It offers a means of examining
the basic properties of materials that influence tribological
characteristics. For the engineer, it is one more environment
with which he must concern himself in the design of lubrication
systems. It is hoped that this document will have something to
offer both.

CONTENTS

INTRODUCTION

ADHESION THEORY OF FRICTION

In order to gain a fundamental understanding of the friction and wear behavior of materials in a vacuum environment, it is important to consider those factors that determine and influence friction and wear in general. The topographical, physical, mechanical, and chemical nature of the surface influence the friction and wear behavior of solid bodies in contact. Further, bulk properties such as deformation characteristics, fracture behavior, and structure will exert an effect on friction and wear.

The first step to gaining insight into the friction and wear behavior of solid surfaces in contact is to examine the surface profile or topography. Most solid metal surfaces used in engineering applications are not atomically flat. A surface, when examined microscopically or with a profilometer, even though highly polished, has an irregular nature. The surface consists of high and low spots as shown schematically in figure 1(a). The nature of the irregularities will be influenced to some degree by the method of surface preparation: Mechanically prepared sur-

(a) Asperities.   (b) Cleavage steps.

(c) Contacting asperities.   (d) Plowing.
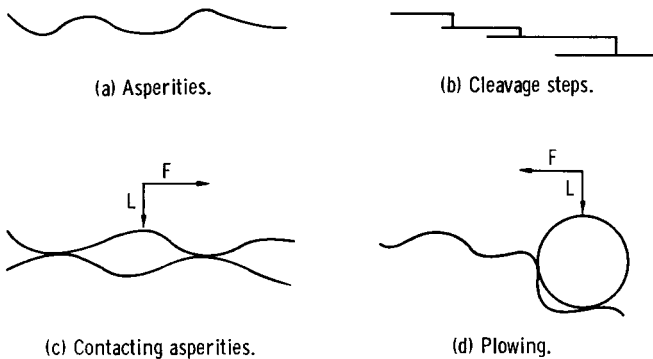
Figure 1. - Nature of surfaces and surface interactions.

1

faces tend to be the most rough, and electropolished surfaces tend to be the least. The surface high spots or protuberances are called asperities. Surface irregularities determine the nature of solid-state contact.

Although most surfaces have asperities of varying heights and degrees, atomically flat surfaces can be and have been generated. When diamond, sapphire, lithium fluoride, or sodium chloride is fractured along a cleavage plane, an atomically flat surface can result. Even metals such as zinc can, at cryogenic temperatures, be cleaved along its basal plane producing atomically smooth flat surfaces. In the cleavage process, however, steps result on the surface as shown in figure 1(b). These steps develop in the cleavage process because in cleaving large areas, fracture cracks develop between adjacent parallel cleavage planes and leave steps in the surface. Between such steps the surfaces may be atomically flat. Thus, even if atomically flat steps are developed as shown schematically in figure 1(b), when two such surfaces are placed into contact with one another, the presence of the steps will prevent complete contact over the apparent contact area unless bifurcation was done in such a manner as to permit the two surfaces to remate in the same manner in which separation occurred.

When two solid surfaces whose surface profiles are like that shown in figure 1(a) are brought into contact, the interfacial contact is as shown in figure 1(c). As shown, the real or actual contact is only a small portion of the apparent contact area. The points or high spots that make solid contact are the asperities. If a very light load L is applied to the surfaces in contact, these surface asperities will at first deform elastically. If the load is sufficiently light, these local regions will always deform elastically. However, because the amount of real contact area is generally small, not only elastic but plastic deformation of these surface irregularities occurs as well. In addition, elastic deformation occurs in the bulk of the asperity while plastic flow is occurring in its surficial layers.

The deformation process of the surface asperities will continue until the load is supported, that is, until the real contact

area is sufficiently large such that the applied force is below the elastic limit or yield pressure in compression. When the two surfaces in contact are of the same material, the deformation will occur to both surfaces. Where the surfaces are of different materials, the deformation will generally take place in the weaker of the two materials or in the material with the lower elastic limit.

When one of the surfaces in figure 1(c) is pulled tangentially over the other, there is a resistance to this tangential motion, which is simply the frictional resistance of the two bodies to such motion. The friction of a material pair in contact is usually expressed as the coefficient of friction. The friction coefficient may be written simply as

$$\mu = \frac{F}{L}$$

where μ is the friction coefficient, F is the friction force, and L is the normal load. The greater the normal load, the greater the friction force. The friction force in this relation is determined by the true interfacial contact area A and the shear strength S of the weakest material in the surficial region.

$$F = AS$$

The contact area is proportional to the applied normal load L and the deformation or strain containing both an elastic and plastic component D.

$$A = \frac{L}{D}$$

When the applied normal load is removed, elastic recovery occurs. The true contact area, then, can be represented by the contact area determined by plastic deformation. From these relations, it can be readily seen that the coefficient of friction may be expressed as

$$\mu = \frac{S}{D}$$

This relation is applicable when there is negligible plastic flow of the materials in contact. If, however, one surface will flow into another, such as a steel ball would do on a sheet of lead (see fig. 1(d)), the friction in addition to a shearing component will have a plowing component. The plowing component will simply be the force required to deform the material ahead of the ball in figure 1(d).

Much of our present understanding of the basic concepts of friction was formulated by Leonardo da Vinci in the late fifteenth century (ref. 1), by the French engineer Amontons at the end of the seventeenth century (ref. 2), and by Coulomb in the eighteenth century (ref. 3). Coulomb originally believed that adhesion contributed to the friction of solid bodies in còntact, but he later discounted this theory in favor of the concept that friction was the physical resistance to the pulling of the mechanically interlocked asperities over one another. Bowden and Tabor later established that Coulomb's original concept with respect to friction being related to adhesion at the asperities was correct (ref. 4).

According to the adhesion theory of friction as proposed by Bowden and Tabor, adhesion occurs at the contacting asperities, and the force required to shear the adhered junctions S will be the shear strength in the surficial region.

SURFACE FILMS IN A NORMAL ENVIRONMENT

The surfaces of most solids in air at atmospheric pressure contain films. Most metal surfaces, for example, are represented by figure 2. The bulk metal or alloy has a near surface region of highly worked metal, which develops in the process of forming the surface. Depending on the nature of the surface processing, the structural makeup of this layer will vary. For metals that are prone to develop surface textures, such as the hexagonal metals, these textures may be present on the surface.
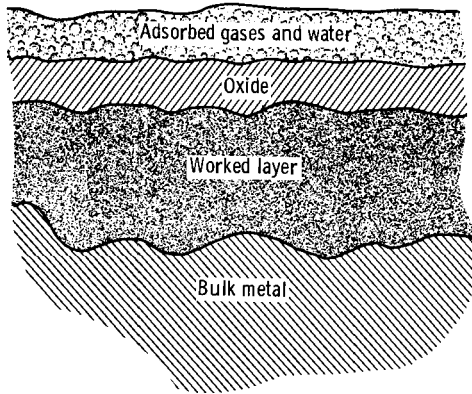
Figure 2. - Schematic representation of rubbing metal
   surface.

The nature of reactivity of the metal surface depends largely on
the physical and chemical nature of surface layer.

   Metal oxide films. - With single-crystal metal surfaces,
the surface activity to form oxides (as shown in fig. 2) will de-
pend on orientation. The data of table I indicate the zones on
single-crystal spheres where preferred oxidation in air occurs

TABLE I. - OXIDATION OF METAL SINGLE CRYSTALS

IN AIR (REF. 5)

Metal	Crystal structure	Active regions	Inactive regions
Al	Face-centered cubic	(100)	(111)
Cu	Face-centered cubic	(100) (210)	(311) (111)
Au	Face-centered cubic	No change to 550° C	
Pb	Face-centered cubic	(100) (311)	(111) (210)
Ni	Face-centered cubic	(100) (110)	(111)
Ag	Face-centered cubic	(100)	(111)
Cr	Body-centered cubic	No preference	None
Fe	Body-centered cubic	(100) (111)	Region between (100) and (110)
Cd	Close-packed hexagonal	Six areas 45° to (0001)	(0001)
Zn	Close-packed hexagonal	Hexagonal ring cen-tered at (0001)	(0001)

(ref. 5). In the table these are called active regions.

With polycrystalline metal surfaces where different orientations are present on the surface, the nature of the oxide film will vary from grain to grain because of the differences in surface energies as demonstrated by the data of table I. The lower energy, more densely packed { 111} planes in the face-centered-cubic (FCC) system are less reactive with oxygen than the less densely packed { 100} and { 110} planes. The grain boundaries themselves on the polycrystalline metal surface tend to interact with oxygen because of the high energy in these regions.

Alloying elements can markedly alter the nature of the surface oxide. Auger emission spectrometer analysis of stainless steels has shown chromium to be present on the surface and, on oxidation, to form chromium oxide. With alloys, it is possible to have an oxide present on the surface that is principally the reaction product of oxygen with the solvent, with the parent metal, with a solute element, which may be present in minor amounts, or with a mixture of oxides of the metallic elements present in the alloy. Thus, the oxide region of figure 2 may be complex, and it is well established as being present on all metal surfaces except gold.

Other films. - The top layer in figure 2 represents gases and adsorbed water vapor by the metal oxides. Many of the gases present in a normal air environment will chemisorb rapidly to the common oxides found on friction and wear surfaces. Table II presents some of these gases and metal oxides and the heats of chemisorption together with the speed of adsorption (ref. 6). Thus, one can see that the surfaces of metals are thoroughly covered with films.

The presence of environmental constituents are not only present on metal surfaces but on nonmetal surfaces as well. For example, the presence of water vapor on graphite is essential to its lubricating properties. Carbon, in general, contains chemisorbed oxygen that frequently can only be removed by heating it to temperatures in excess of 1500° C (1793 K), whereupon the oxygen evolves as carbon monoxide.

With ionic crystals, the presence of adsorbed surface spe-

TABLE II. - CHEMISORPTIONS ON OXIDES AT ROOM

TEMPERATURE (REF. 6)

Gas	Oxide	Initial heat of adsorption, kcal/mole	Velocity of adsorption
O_2	NiO	54	Initially rapid adsorption, then slow
	Cr_2O_3	--	Same as NiO
	Fe_2O_3	--	Same as NiO
	MnO	24	Small, very rapid adsorption
	$ZnO \cdot Cr_2O_3$	42·0	Extremely rapid
CO	NiO	26	Rapid adsorption; coverage <1.5 percent at 20° C (293 K)
	CoO	20	Rapid adsorption; coverage 3 percent at 25° C (298 K) and 0.1 mm (N/m^2) pressure
	ZnO	9 to 13	Rapid; reversible adsorption
	Cu_2O	20	Rapid adsorption; 30 percent coverage at 20° C (293 K) and 0.2 mm (N/m^2) pressure
	MnO	64·4	Rapid adsorption
	Cr_2O_3	28	Adsorption 90 percent complete in 5 min
	$ZnO \cdot Cr_2O_3$	14·9	Adsorption 90 percent complete in 5 min
CO_2	NiO	28	10 Percent limiting coverage at 20° C (293 K)
	CoO	23	6 Percent limiting coverage at 20° C (293 K)
N_2O	NiO	--	Instantaneous reversible adsorption
	CoO	13	Instantaneous reversible adsorption
C_2H_4	CoO	13	Completely reversible at 20° C (293 K)
	ZnO	25·2	90 Percent of charge adsorbed in 2 min
	$ZnO \cdot Cr_2O_3$	11	Charge adsorbed in 8 min
	Cu_2O	20	Rapid adsorption
SO_2	Cu_2O	37	Rapid adsorption

cies not only influences the surface properties of the crystals but
also affects the mechanical behavior of the solids. The effect of
environmental constitutents on the behavior of ionic solids is
discussed in detail in the literature (refs. 7 to 11).

When two metal surfaces are brought into contact, the as-
perities will be covered by the oxides and adsorbed films. If the
load is sufficiently high, such that the surfaces deform plasti-
cally at the interface, metal to metal adhesion can occur through
the surface films present. The imposition of tangential motion
on the surfaces in contact will result in the shear of the weakest
region in the surficial layer. The shear force required coupled
with the real area in contact, as discussed earlier, will deter-
mine the friction force.

Metal oxides, in general, have higher shear strengths than
the corresponding parent metal (see table III; refs. 12 and 13).
The only metal oxides in table III that have lower shear strengths
than the parent metal are molybdenum and silver. Thus, in
most instances, for two solid metal surfaces in contact, tangen-
tial motion will result in the shear of the weakest bonds formed
at the interface which, in general, will be the metallic bonds
rather than the oxide. The oxide, however, reduces the amount
of metal-to-metal bonding that can occur and thereby reduces,
also, the true metal-to-metal contact area and the cross-
sectional interfacial area of metal that must be sheared. The
effect of the oxides and other surface contaminating films on
metal surfaces is very important to the understanding of the dif-
ferences in the friction behavior of metallic surfaces in air and
vacuum.

Solid solubility concept. - Based on the fact that shear will
occur in metallic junctions, Ernst and Merchant (ref. 14) calcu-
lated the friction coefficients for various metal pairs using the
relation $\mu = S/H$ where S is the shear strength of metal at the
interface and H the hardness of the metal. (Hardness, instead
of deformation or strain, was used in the previous relation for
friction coefficient.) The friction coefficients, which they deter-
mined from the relation S/H and experimentally, are presented

TABLE III. - RELATIVE SHEAR STRENGTHS

MEASURED FOR VARIOUS METALS AND

METAL OXIDES IN COMPRESSION

TWISTING (REFS. 12 AND 13)

Metal	Shear strengths for metal at high pressures, S_s, kg/mm^2	Metal oxide	Shear strengths for metal oxides at high pressures, S_s, kg/mm^2
Al	31.0	Al_2O_3	94
Cu	49.0	Cu_2O	103
Ni	87.0	NiO	119
Fe	100.0	Fe_2O_3	167
Cr	122.0	Cr_2O_3	134
Mo	121.0	MoO_3	111
W	128.0	WO_3	140
Ag	47.0	Ag_2O	35
Pb	6.8	PbO	24
		PbO_2	99
		Pb_3O_4	81
Co	63.0	Co_2O_4	117
Zn	18.4	ZnO	126
Ti	130.0	TiO_2	145
Zr	45.0	ZrO_2	121

in table IV. In table IV(a) the metal pairs in contact were capable of forming solid solutions. Examination of the predicted and observed friction coefficients indicates good agreement. With the surface films present, the friction coefficient for metals or alloys in contact rarely exceed a value of 1.5.

In table IV(b) a comparison is made between predicted and observed friction coefficients for pairs of metals that exhibit almost mutual insolubility. Here the predicted and observed friction values vary considerably. Ernst and Merchant were indicating with table IV the effect of mutual solubility on friction. Although, in general, the friction properties of insoluble pairs are lower than for mutually soluble metal pairs, care must be taken in using bulk properties, such as solid solubility, for pre-

TABLE IV. - COMPARISON OF

PREDICTED[a] AND OBSERVED

FRICTION COEFFICIENTS

(REF. 14)

(a) Pairs forming solid solu-
tions at room temperature

Pair	Friction coefficient	
	Predicted	Observed
Al-Fe	1.05	1.05
Al-Zn	.85	.82
Co-Fe	----	.54
Co-Cu	.90	.89
Co-Al	1.05	1.01
Cu-Cd	.83	.85
Cu-Zn	.85	.86
Zn-Fe	.85	.85
Zn-Sb	.85	.85

(b) Pairs almost mutually in-
soluble at room temperature

Cd-Al	<0.83	0.57
Cd-Bi	<.83	.79
Cd-Fe	<.83	.64
Cd-Zn	<.83	.62
Cu-Fe	<1.35	1.05
Zn-Bi	<.86	.70

[a]Based on μ = S/H and
S = 0.427 L/3ρ $\log_e$ T$_m$/T.

dicting surface behavior. As will be shown later, adhesion and
high friction can occur for insoluble as well as soluble metal
pairs.

When two solid surfaces are in contact, some degree of me-
tallic adhesion will almost always occur. The function of bound-
ary lubricants is to reduce this adhesion as much as possible.
The presence of lubricating films on metal surfaces will reduce
the friction coefficients for metals in contact to values consider-

ably below those presented in table IV. With effective boundary lubricants, such as fatty acids, friction coefficients for metals in contact will generally be 0.1 or less. With poorer fluid lubricants present on metal surfaces, friction coefficients may be as high as 0.2. These organic films further reduce the amount of metallic contact occurring across the interface. They act with the metal oxides present in reducing metallic contact, the total adhesion, and consequently the friction force.

The presence of adsorbed surface films greatly influences the friction behavior of nonmetals, also. The degree to which these films reduce friction will be discussed in reference to vacuum results. The presence of surface active agents on nonmetals, particularly on ionic solids, can influence the mechanical behavior of these solid surfaces. If surface active species can influence deformation, they can also influence friction. Surface active films can influence the deformation behavior of ionic solids by various mechanisms. These include (1) strengthening by dissolution of the solid surface or the Joffe effect (ref. 15); (2) surface hardening or Roscoe effect (refs. 16 and 17); and (3) surface softening or Rebinder effect (refs. 9 and 11).

The Rebinder effect. - The Rebinder effect has been studied most and, because of its significance to the friction behavior of solids, will be discussed in some detail here. The first disclosure of this effect was reported in 1928 by Russian researchers (refs. 9 and 11). Although considerable information was generated in this area by the Russian laboratories, particularly by the founder of the concept (Rebinder), little support was given to it outside Russia until recently.

The Rebinder effect has been shown in the deformation of ionic solids such as lithium fluoride (ref. 18) and magnesium oxide (ref. 19). This increase in ductility or ability to deform plastically in the presence of adsorbed surface species has also been observed in metals (refs. 11, 17, and 20). It has been observed in the covalent material germanium and in metal carbides (ref. 21).

Some sliding friction experiments have been conducted with the ionic solid lithium fluoride to determine the influence of sur-

(a) Dry air.
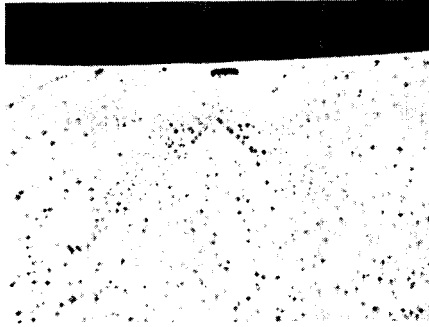
(b) Water.
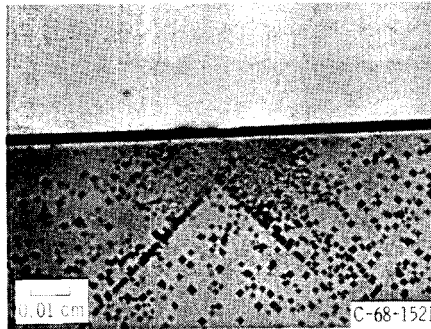
(c) Water and 5.0×10^{-6} N myristic acid.

Figure 3. - Cross section of wear tracks on lithium fluoride in sliding friction experiments. Load, 200 grams (2.0 N); 1.6-millimeter-diameter sapphire ball; temperature, 20° C (293 K); sliding velocity, 0.005 millimeter per second. Ball made a single pass across surface covered with three different media: air, water, and water with myristic acid.

face films on friction and deformation. A sapphire ball was slid
across a freshly cleaved lithium fluoride (100) surface. The
lithium fluoride specimen was then cleaved normal to the sliding
track and etch pitted. The subsurface deformation and the de-
velopment of cleavage cracks is shown in figure 3(a). Examina-
tion of figure 3(a) reveals that slip has taken place along the
{011} and {101} sets of planes. Since these are the slip planes,
plastic deformation might be expected to occur in such a fashion.
In addition to the slip bands, cleavage cracks developed along
the {011} slip bands and have their origin at the surface.
Cracks can form in lithium fluoride at the intersection of {110}
slip planes according to the equation

$$\frac{1}{2} a[011] + \frac{1}{2} a[101] = \frac{1}{2} a[110]$$

It is important to note from the etch pitted slip bands in fig-
ure 3(a) that a brittle material such as lithium fluoride will de-
form plastically in sliding.

In order to show the marked influence that atmospheric
constituents can have on the mechanical behavior of ionic crys-
tals in sliding friction studies, equivalent experiments were
conducted with lithium fluoride in water. Rather than simply
comparing behavior in moist air with that in dry air, water was
used. The lithium fluoride crystals were cleaved in water and
friction experiments were conducted with water present on the
crystal surface. The crystals were then cleaved normal to the
wear track and etched. The track subsurface deformation is
shown in figure 3(b). Note that, although slip bands are evident
from the dislocation etch pits along the (110) plane, a subsurface
crack has formed in the crystal. This crack lies in a (001)
plane. In dry air (fig. 3(a)) the crack formed at the surface
along (110) planes rather than in the subsurface. With the plas-
tic deformation of lithium fluoride, cracks can develop along a
(100) plane with the intersection of {110} slip bands in accor-
dance with the equation

$$\frac{1}{2} a[110] + \frac{1}{2} a[1\overline{1}0] \rightarrow a[100]$$

The crack developed in figure 3(b) was the result of both com-
pressive forces acting on the crystal surface in the form of the
normal load and tangential forces associated with sliding.

Figure 3(c) is a sliding friction track in cross section after
a sliding friction experiment was conducted in a 5.0×10^{-6} normal
solution of myristic acid. In the presence of the acid, there was
no evidence of either surface or subsurface crack formation as
seen in figures 3(a) and (b). In figure 3(c) the subsurface depth to
which the (011) slip bands extend is appreciably greater than that
observed in the other two environments. Thus, a greater de-
gree of plasticity appears to exist in the presence of the myris-
tic acid. The energy associated with the sliding friction process
appears to have been absorbed completely in plastic behavior.

The influence of environment on the behavior of ionic solids
is further shown in some sliding friction experiments conducted
on the (111) cleavage face of calcium fluoride. Figure 4 pre-
sents deformation data as a function of the molar concentration
of dimethylsulfoxide in water. The data indicate that with de-
creasing concentrations of dimethylsulfoxide or increasing con-
centrations of water, the width of the wear track increases.
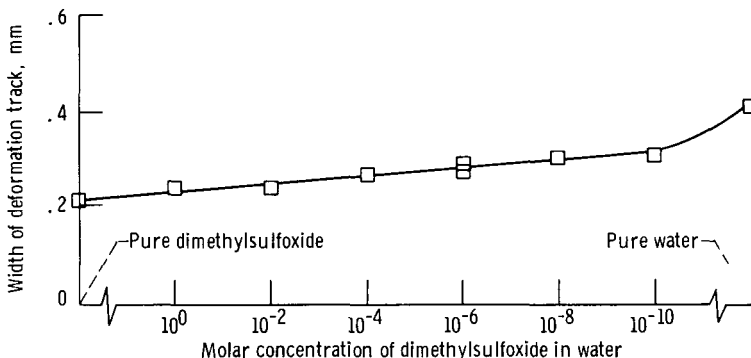
Figure 4. - Dislocation track width for sapphire ball sliding on (111) cleavage
surface of calcium fluoride in various concentrations of dimethylsulfoxide
in water. Sliding velocity, 0.005 centimeter per second; load, 300 grams
(2.9 N); ambient temperature, 20° C (293 K).

This increase in the width of the wear track may be attributed to an increase in the plasticity of the surface.

The foregoing discussion on the influence of surface films on the deformation and fracture of lithium fluoride and calcium fluoride indicates that the presence of surface films on ionic solids influences not only surface behavior but also subsurface behavior. Not only does the ability of surface films to influence deformation behavior influence friction because it determines true contact area, but also it influences the wear of solid surfaces in contact. The presence of surface or subsurface cracks can, with repeated traversals over the same surface, give rise to the formation of wear particles. This has been demonstrated with the ionic solids lithium and calcium fluorides. Deformation results with calcium fluoride indicate the extreme sensitivity of ionic solids to small changes in environmental constituents.

RELATION OF ADHESION TO STATIC AND DYNAMIC FRICTION

When two solids are placed in contact, the contact occurs across the interface between surface asperities. Plastic flow of these metal asperities will then occur, and a certain amount of metal-to-metal contact will take place through any surface films present. The force required to initiate motion between the two solid surfaces will represent the static friction force. Once one of the solid surfaces is in motion, the friction force measured is the dynamic friction. In general, the static friction coefficient for solids in contact is higher than the dynamic friction coefficient. There are a number of factors that account for the difference.

Static friction. - The first major difference between the two types of friction is the times that asperities or microjunctions are in contact. When two solid bodies are placed into contact under a load, first elastic and then plastic deformation will occur. The solids generally will undergo further deformation while standing in contact. This time-dependent additional deformation of the solids in contact under an applied stress is re-

ferred to as creep. Creep may be exhibited in the elastic range, where the creep strain may be completely (or nearly so) recovered on the removal of the stress, or in the plastic range, where the creep deformation is permanent. For creep deformation in the plastic range an elastic component also exists, but it may be trivial by comparison with the plastic (ref. 22). Metals are particularly prone to creep.

Adhesion at the interface will increase with increasing interfacial contact area as creep in the microjunctions continues. With increasing adhesion there should be a corresponding increase in the static friction. This in fact has been observed, as is shown by the data of figure 5 (from ref. 23), where the static-friction coefficient is plotted as a function of contact time.

The data of figure 5 do not show the static friction becoming less dependent on contact time with prolonged contact times. The curve should resemble creep curves. Static-friction curves obtained by Ishlinski and Kraghelsky (ref. 24) show that it does. After some period of time the static-friction coefficient becomes less dependent on contact time, and the slope of the curve changes. Adhesion and static-friction coefficient measurements are therefore extremely dependent on the time the solid surfaces
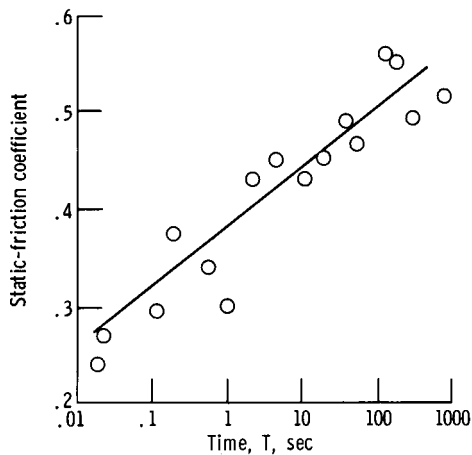
Figure 5. - Static-friction coefficient as function of time for unlubricated steel sliding on steel (ref. 23).

are in contact.

With metals more prone to creep than nonmetals, it might be anticipated that greater differences would exist between the static and dynamic-frictions of metals than of nonmetals. This is in fact what is generally observed.

The static-friction coefficient of materials not only is important in the initiation of relative motion between surfaces but also manifests itself during relative motion between solid surfaces in the so-called stick-slip phenomenon. This phenomenon is particularly prevalent with metal surfaces in contact. If one surface is slowly moved across another and if the friction force is recorded during movement, the friction force will rise to some high value and then drop very suddenly. This process will continuously repeat itself. With relative motion strong bonds of adhesion will form across the interface, motion will momentarily stop, and the friction force, or force required to overcome the bonding of the adhered junctions, will continue to increase until the bond forces of adhesion are exceeded. When this occurs the bonds will break, and motion will occur with an accompanying sudden decrease in friction. The process continuously repeats itself. The stick portion of the process is in reality a measure of the force necessary to overcome static friction.

Dynamic friction. - In dynamic-friction measurements, adhesive junctions between solid surfaces are continuously being made and broken very rapidly, and the dynamic-friction coefficient represents an averaging of the making and breaking of adhesive contacts.

Factors that influence dynamic friction. - When two surfaces are in dry sliding contact, very high interfacial temperatures are momentarily generated at the contacting microjunctions or asperities. These temperatures may reach 1000° C (1293 K) (ref. 4). Because they occur with junction contact and are of short duration, they are called flash temperatures. In addition, the energy put into the surface as a result of the friction process will generally increase the temperature in the surficial layers.

These temperatures will be influenced by the normal load, slid-
ing velocity, the nature of the solids, and the properties of sur-
face films. With increasing sliding velocity, the surface tem-
peratures increase until the melting point of the lower melting
material is reached. When this occurs, a marked decrease in
the friction force will occur because the liquid metal will have
much lower shear strength than the same metal in the solid
state.

    The coefficient of friction for metal surfaces in contact can
be markedly influenced also by the normal load applied to the
surfaces in contact. Figure 6 is a plot of the coefficient of fric-
tion for copper sliding on copper as a function of applied load
(ref. 25). At very light loads the coefficient of friction is ap-
proximately 0.4. This lower friction represents basically the
friction properties of the copper oxide films present on the two
surfaces. As the load is increased, metallic contact begins to
occur through the oxide films, and the friction coefficient begins
to increase and continues to do so with increased loading as more
and more metal to metal contact occurs.

    Although oxides can be penetrated on metal surfaces to re-
sult in an increase in friction, even the oxides themselves are
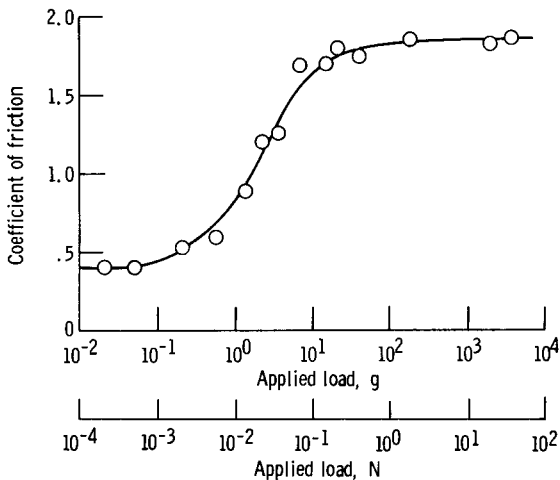
Figure 6. - Coefficient of friction as function of load for
copper sliding on copper (ref. 25).
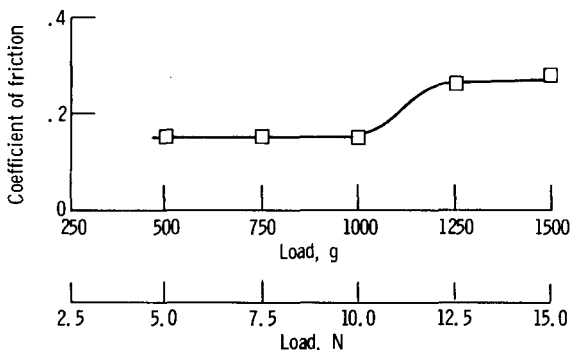
Figure 7. - Coefficient of friction as function of load for
sapphire sliding on sapphire in air (760 torr). Sliding
velocity, 0.013 centimeter per second; ambient temper-
ature, 25° C (298 K).

sensitive to load.   Figure 7 for single-crystal aluminum oxide
(sapphire) sliding on itself in air shows the effect of loading on
friction coefficient.   At the lighter loads the friction coefficient
was 0.15.   With increased loading and penetration of adsorbed
water vapor and oxygen, the friction coefficient rose to a value
of 0.25.   As will be shown later, complete removal of these
chemisorbed surface films in vacuum will result in a fourfold in-
crease in friction coefficient of aluminum oxide.

As already mentioned, sliding speed, may also influence the
coefficient of friction between two surfaces (see fig. 8).   At very
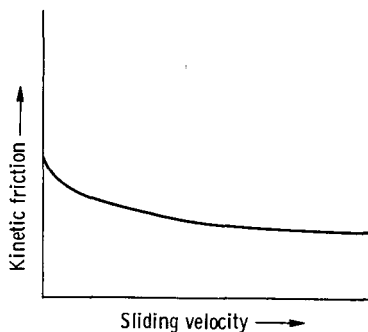
Figure 8. - Typical plot of kinetic
coefficient as function of sliding
velocity (ref. 26).

high sliding velocities, if localized melting on the surface of the materials in contact does not occur so as to result in a marked decrease in friction coefficient, other changes can take place in the materials. Sufficient interfacial heating, which will increase with increasing sliding speed, can produce these localized changes. One such change would be a metallurgical transformation. Another can be diffusion of alloy constituents to the surficial region.

WEAR AND VARIOUS TYPES OF WEAR

The wear of solid surfaces in contact can be caused by one or a combination of wear mechanisms. The most common types of wear are abrasive, adhesive, corrosive, erosive, and fatigue.

ABRASIVE WEAR

Abrasive wear occurs when two solid surfaces are in contact and one of the two solids is considerably harder than the other. The harder surface asperities will press into the softer surface with plastic flow of the softer surface occurring around the asperities from the harder surface. When a tangential motion is imposed, the harder surface will move, shearing and removing the softer material. Abrasive wear is the mechanism involved in the finishing of many surfaces. Filing, sanding, and grinding of surfaces all involve the process of abrasive wear. The mechanism of wear in these processes may not, however, be exclusively abrasive wear. Chemical interaction of surface oxides frequently are involved, which can give rise to an element of corrosive wear. The fatigue mechanism may also be involved.

Kruschov and Babichev (ref. 27) found that the resistance of metals to abrasive wear was related to their relative hardness. Figure 9 is a plot of what they term abrasive wear resistance as a function of metal hardness. The relation is readily apparent. In general, the abrasive wear behavior of materials is proportional to the load applied to the surfaces in contact, proportional to the distance of sliding, and inversely proportional to the hardness.
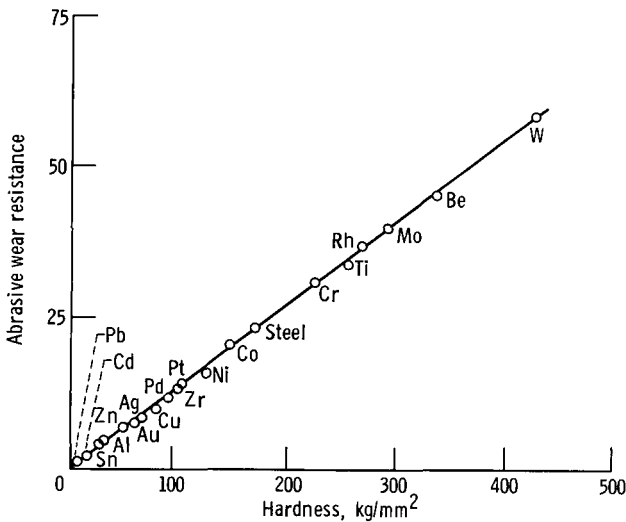
Figure 9. - Wear resistance of various metals and steel (ref. 27).

The abrasion of metal surfaces can result in the development of preferred surface orientations or texturing (ref. 28). These preferred surface orientations can, as will be discussed with reference to the vacuum results, markedly influence friction and wear behavior.

CORROSIVE WEAR

Corrosive wear occurs when the environment interacts with solid surfaces in contact to contribute to the attrition of the surfaces. If two surfaces react actively with the environment, the rubbing of surfaces together in such an environment can result in the continuous formation and removal of reaction products. Since the material of the surfaces in contact are contained in the reaction product, material is being removed from the surface. With rubbing, fresh surface is continuously being exposed for further reaction. If the reaction products are solids, they are generally moved out of the contact zone as solid wear particles. When the reaction products are gaseous, corrosive wear may occur very rapidly. An example of this situation occurs when solid carbon is used in air above 680° C (953 K).

ADHESIVE WEAR

Adhesive and fatigue wear are important to the behavior of materials in contact in vacuum as they are the most frequent types of wear encountered in a vacuum environment. A detailed discussion of these types of wear at this point will eliminate the need for the same in discussing vacuum data.

Adhesive wear is the most detrimental and is frequently encountered. It can very rapidly destroy such mechanical components as bearings, gears, and seals. Adhesive wear involves the adhesion of solid surfaces across an interface with subsequant subsurface fracture in one or both materials. Material may be transferred from one surface to another, from each surface to the other, or back and forth from one surface to another. The transfer process of course is a material removal process. Figure 10 shows schematically how the process can occur. In order for adhesive wear to take place, fracture must occur in the subsurface of one or both materials. If fracture occurred at the adhesive junction, that is, at the interface between the two surfaces, no adhesive wear would occur. This, of course, means that when adhesive wear takes place, the adhesive junction between the two solid surfaces is stronger than some region subsurface where fracture has taken place.

Considering adhesive wear in a stepwise manner, the first step necessitates that adhesion take place between the two solids in contact. This can occur in an ordinary environment by the

Motion ⟶
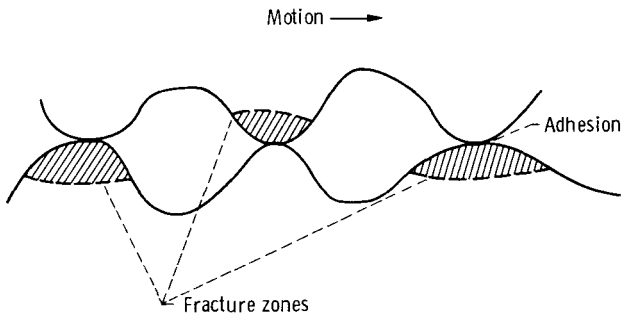
Figure 10. - Adhesive wear.

penetration of surface films with deformation of the solids in contact. It can occur in vacuum with the simple approach of two clean surfaces.

Interatomic bonds in adhesion. - The plot of figure 11 shows the interatomic forces acting across the interface where nascent surfaces come into contact. An atom from each of the two surfaces in contact will form a bond which will be in equilibrium at some distance r_1. The equilibrium distance of separation occurs at the minimum in the potential energy, the distance at which the attractive forces just balance the repulsive forces. If the atoms are moved together under applied force in the form of load, a strong repulsive force arises. When the atoms are pulled apart, the force required for separation, which will influence cohesive or friction forces, will first go through a maximum σ_{max} and then fall off asymptotically to zero (see fig. 11). The value of σ_{max} corresponds to the ultimate strength or theoretical strength at a distance of r^1 on a strain of $\left(r^1 - r_0\right)\!/r_0$.

A line may be drawn tangent to the resultant force curve at $r = r_0$. The modulus of elasticity is defined as the ratio of stress to strain. Thus, in figure 11, the modulus is given by E
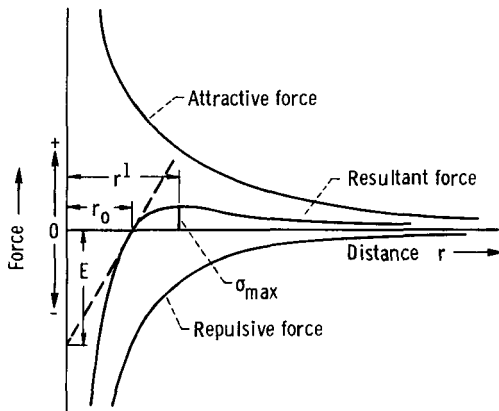
Figure 11. - Interatomic forces between two atoms as function of distance of separation.

where

$$E = \frac{d\sigma}{\frac{dr}{r_0}} = \frac{d\sigma r_0}{dr}$$

or the slope of the curve at $r = r_0$ multiplied by r_0. The inter-
cept of this line of tangency on the force axis is also E by the
rule of similar triangles (ref. 29). The elastic-stress range in
real metals, for example, is only about 1/100th to 1/1000th the
value σ_{max} in figure 11. The modulus of elasticity is, how-
ever, the only commonly measured mechanical property which
directly reflects these interatomic forces.

   If two solid surfaces in contact were perfect solids and if
the bonds formed across the interface in the microjunctions were
perfect, the force necessary to separate or move the surfaces
apart could be determined using the theoretical strength of the
interatomic junctions from σ_{max} (fig. 11) and knowledge of the
true contact area:

$$\sigma_{max} = \sqrt{\frac{ES}{a}}$$

where E is the elastic modulus, a is the lattice parameter of
the crystalline solids, and S is the surface energy. If values are
used in this equation, the theoretical strength is found to be ap-
proximately equal to $E/10$. For iron, by way of example, it
would be 2×10^6 kilograms per square centimeter. The strength
of real solids such as iron, are considerably below this value.
The deviation of real solids from ideal will result in a greater
true contact area when surfaces are pressed together under load
because plastic flow will occur at much lower applied stress. At
the same time, however, the shear strength is less. Thus, one
might expect that the friction behavior of wiskers (crystalline
solids with a minimum of defects) might not be too different from
less perfect solids of the same material.

Relation between cohesion and elasticity. - Based on the foregoing considerations, a relation might be anticipated between the mechanical property of elastic modulus and the more basic property of cohesive energy. Figure 12 is a plot of Young's modulus of elasticity as a function of cohesive energy for various face-centered-cubic metals. Where bonding occurs across an interface for like metals in contact, if the contact area were the same in each case, the force to fracture the cohesive bonds of lead would be considerably less than the force to fracture iridium cohesive bonds (ref. 30). Since, however, the elastic modulus for lead is considerably less than that for iridium, the contact area under a given load will also be larger, and this increases the force necessary to fracture cohesive junctions where the applied load is the same for the two metals.

It was mentioned earlier that, for adhesive wear to occur, interfacial bonding between the two surfaces in contact must be stronger than cohesive bonding in one of the two solids. LEED
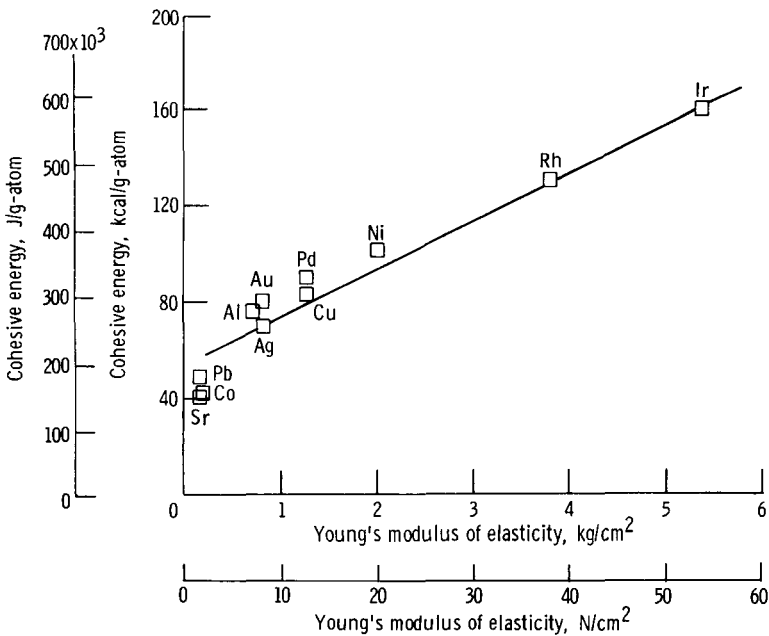
Figure 12. - Relation of Young's modulus to cohesive energy for various face-centered cubic metals.

(low energy electron diffraction) studies with various face-centered-cubic metal crystals in contact show that, for dissimilar metals in contact, the adhesive junction at the interface is stronger than the cohesive junctions in the cohesively weaker of the two solids in contact. The data of table V present results considering the effects of orientation, the effect of alloying, and the effect of dissimilar metal pairs. In each case of adhesive contact, the cohesively weaker of the two face-centered-cubic metals transferred to the cohesively stronger.

LEED patterns are presented in figure 13 showing the changes in the diffraction pattern of the nickel (111) surface as a result of adhesive contact. Figure 13(a) shows a clean nickel (111) surface before adhesive contact. In figure 13(b) that same surface is shown after being contacted by copper. Copper adherred to the cohesively stronger nickel. The copper accounts

TABLE V. - METAL TRANSFER OBSERVED IN

ADHESION OF FACE-CENTERED-

CUBIC METALS

Metal couple	Metal which trans-ferred to the other surface
Orientation effects	
(100) Au to (100) Cu	Au
(100) Au to (110) Cu	Au
(100) Au to (111) Cu	Au
Effects of alloy constituents	
(111) Au to (111) Cu-Al alloys[a]	Au
Other dissimilar metal pairs	
(111) Au to (111) Ni	Au
(111) Ag to (111) Ni	Ag
(111) Cu to (111) Ni	Cu
(111) Al to (111) Ni	Al
(111) Au to (111) Ag	Ag
(111) Au to (111) Al	Al
(111) Pt to (111) Al	Al

[a]0.1 to 10 at. % Al.

(a) Before contact.

(b) Contacted by copper.

(c) Contacted by lead.

(d) Contacted by platinum.

C-69-1792
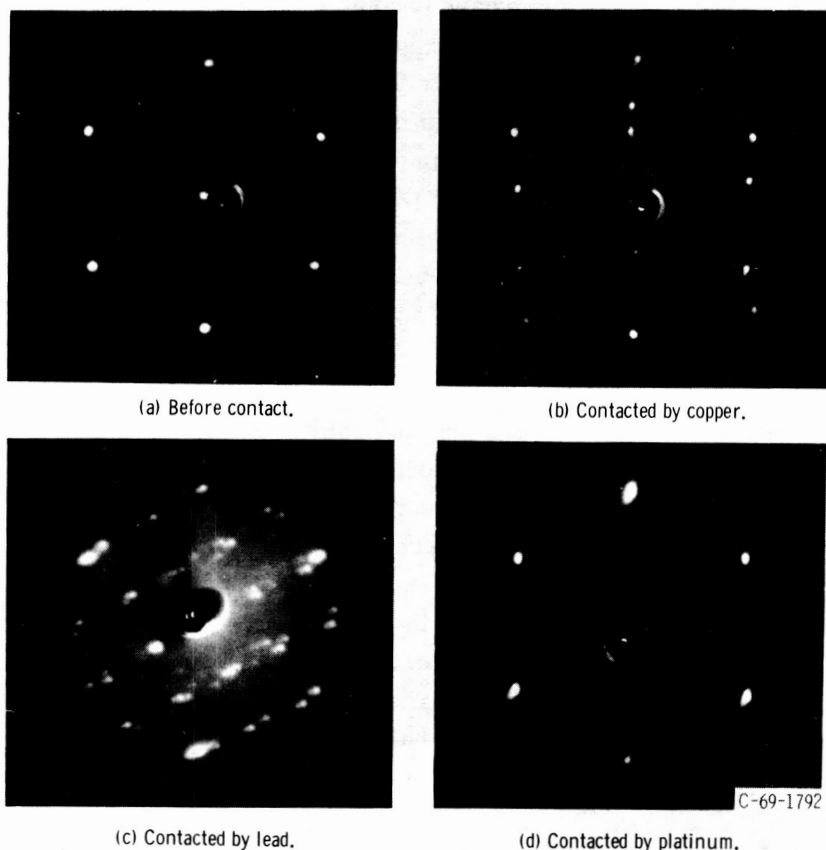
Figure 13. - LEED photographs of nickel (111) surface before and after adhesive contact with various metals. Contact load, 20 dynes (20×10^{-5} N) at 20° C (293 K); contact time, 10 seconds at 10^{-10} torr.

for the additional diffraction spots in figure 13(b) not seen in figure 13(a). The regular arrangement of the spots indicates that the copper is present on the nickel in an ordered fashion.

Figure 13(c) represents the surface of figure 13(a) after adhesive contact with lead. Note the large number of additional diffraction spots due to the presence of the lead on the nickel. Again, the cohesively weaker metal, lead in this instance, transferred to the cohesively stronger nickel.

The diffraction pattern of figure 13(d) shows the change in the LEED pattern of the nickel (111) surface after adhesive contact with a platinum (111) surface. There are no new diffraction

spots, and the nickel spots have become elongated (compare (a) and (d) of fig. 13). On tensile fracture of the adhered pair, nickel transferred to the cohesively stronger platinum. The elongation of the diffraction spots is due to lattice strain produced by the tensile fracture in the nickel.

When two solid surfaces are placed into contact and adhesion occurs across the interface, the theoretical strengths of, for example, metals cannot be used because the real strength of the junction will be so much less. There are three principal reasons why the theoretical strength and the real strength of the junctions will be different:

First, with real metals, on the application of stress in the form of load to the surfaces in contact and the removal of load, there will not be complete elastic recovery, even where the stresses applied are very low in relation to the yield strength.

Second, real crystalline solids exhibit substantial anisotropy. With iron, for example, the modulus of elasticity normal to the (111) plane is 3.0×10^6 kilograms per square centimeter, and that normal to the (100) plane is 1.3×10^6 kilograms per square centimeter, or less than half the (111) plane. The usually used value for friction and wear surfaces of 2.0×10^6 kilograms per square centimeter actually is an average of these two extremes and all other intermediate orientations. Thus, for two identical microjunctions topographically under the same load, the final area in true adhesive contact will differ simply if the orientation of the grains vary.

Third, the theoretical strength and the real strength of the junction differ because of the presence of defects. This is one of the most important reasons in considering both adhesive and fatigue wear. The defects can be point defects, such as vacancies and interstitials, or line defects, such as dislocations and other surface defects produced at the interface between the two contacting solids. These defects may be very much like those encountered at a grain boundary.

In the loading process used when two solid surfaces are placed into contact, energy is stored in the bodies. If the load is sufficiently light and only elastic deformation occurs, the

energy input is equal to that stored up and the process is reversible. Where the energy exceeds a critical point, instability results and the bodies can relax to a more stable state by plastic flow or fracture or by flow followed by fracture. For flow followed by fracture, that portion of stored energy which is dissipated by relaxation is an irreversible process.

Fracture will occur in one or both of the solid bodies in contact in the weakest zones of the surficial regions. The fracture process is a progressive separation of bonds starting at some site, surface or subsurface, where the dissipation of the input energy associated with sliding or rolling contact under load cannot be dissipated. When a sufficient amount of energy, which cannot be dissipated as heat, has been accumulated at a particular site, fracture will occur. This may be at the adhesive junction, in which case no adhesive wear will occur; or it may occur in the subsurface regions, in which case a particle may be removed from a surface. Fracture is most likely to be initiated at some imperfection in the surficial layers because bond energies are weaker at these sites than in the normal structure.

The adhesive wear particle. - At this point it is well to consider those phenomena that occur in materials that give rise to the formation of an adhesive wear particle. As already discussed, the first thing that must happen is adhesion. What gives rise to the removal of material from one surface after adhesion has taken place? The answer to this question is dictated by the mechanisms of fracture and those factors that influence fracture mechanisms. Since nearly all materials are the subject of adhesive wear, the fracture mechanisms that can give rise to the generation of a wear particle in the various classes of materials will vary. Many of the fracture concepts to be discussed will relate to wear by fatigue as well as adhesion.

With metals, if single-crystal surfaces are in sliding contact, deformation will occur by slip. This involves the gliding of one slip plane over another. With tangential motion of two surfaces in contact, slip sometimes will continue until complete separation has occurred. The termination of the slip process occurs when the two parts are formed from a single one of the

two crystals in contact. This is commonly referred to as shearing fracture. It can occur, for example, where a hexagonal metal is involved with basal planes parallel to the surface. Thus, slip in an asperity of a hexagonal metal can, when carried to completion by the sliding process, give rise to an adhesive wear particle due to shearing fracture along the preferred (0001) slip plane. This would be adhesive wear in its simplest form.

In most engineering applications, metals or alloys used are in a polycrystalline form whose preferred slip planes are not parallel to the surface but rather are at a variety of orientations. Sliding or rolling on these surfaces as encountered in friction and wear devices can produce preferred orientations on the surface by the process of texturing. This is shown by the sketch in figure 14 for a hexagonal metal such as beryllium. Once such surface texturing has occurred, the polycrystalline surface may behave with respect to shearing fracture like the single-crystal surface.

In light of the foregoing discussion, it might be anticipated that the friction force between hexagonal metals such as beryllium, where texturing has occurred as shown in figure 14 and where slip occurs only along the basal planes, will be nearly the same for single crystals and polycrystals. This, in fact, has been observed where the basal plane in the single crystal is parallel to the surface (ref. 31).
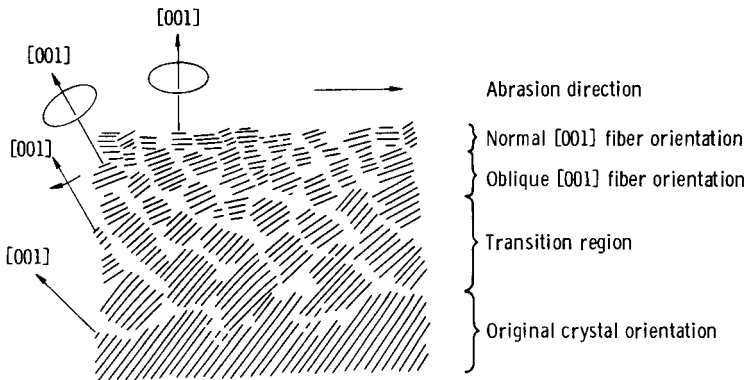
Figure 14. - Diagrammatic form of fragmented surface region of abraded beryllium crystal (ref. 28).

With metals having slip systems other than the basal slip mechanism, the shearing process is complicated by slip plane and slip plane dislocation interaction. For example, with face-centered-cubic metals Lomer-Cottrell locks, due to the insection of {111} slip plane dislocation, will give rise to work hardening and an increase in the force to shear.

Particle generation by cleavage. - Fracture by cleavage can also occur in the surficial regions of metals in contact giving rise to wear particles. This usually occurs at low temperatures with separation taking place along well defined crystallographic planes producing the type of surface referred to in reference to figure 1(b). No face-centered-cubic metal is known to fail by this mechanism. Further, in sliding friction experiments with iron-silicon crystals (a body-centered-cubic alloy), no evidence for cleavage has been observed at -195° C (78 K) during the process of sliding (ref. 32).

Fracture for a number of materials, whether by initiation of cleavage cracks or in a plastic manner along slip planes, occurs along well defined planes. The planes involved for some typical materials are shown in table VI (ref. 33).

There is a marked difference in micromechanism of fracture that occurs in surficial layers of metals, inorganic crystalline solids indicated in table VI, and brittle amorphous materials. In amorphous materials, the strain rate is proportional to the applied stress, and strain may be somewhat uniformly distributed. The viscosity of brittle materials shows a notable temperature dependency. Glass, for example, on changing from 80° to 60° C (353 to 333 K) will undergo a 10 000-fold increase in its viscosity coefficient. At room temperature, flow in glass is practically nil and there is no possibility of relieving stresses by flow. Metals and inorganic crystalline solids, however, are relatively insensitive to temperature with respect to resistance to plastic flow. It is believed that, in metals and inorganic crystalline solids, the origin of microcracks lies in the hetergeneous nature of the plastic flow process of these materials under applied stresses.

TABLE VI. - MODE OF FRACTURE OF METAL CRYSTALS

AND MINERALS (REF. 33)

Crystal structure	Material	Cleavage or fracture plane	Slip plane
Face-centered cubic	Co	Not observed	(111)
	Al	Not observed	(111)
	Al-Zn solid solution	(111)	(111)
Body-centered cubic	Fe	(001)	(011)(123)(112)
	Fe-Si alloy	(001)	(011)(123)(112)
	Fe-Si alloy containing over 4 percent Si or at low temperature	(001)	(011)
	Mo	(001)	(011)(123)(112)
	Cr	(001)	?
Close-packed hexagonal	Mg	$(0001)(10\bar{1}1)(10\bar{1}2)(10\bar{1}0)$	(0001)
	Zn	(0001)	(0001)
	Zn containing 0.13 percent Cd	$(0001)(10\bar{1}0)$	(0001)
	Zn containing 0.53 Cd	(0001)	(0001)
Body-centered rhombohedral	Bi	(111)	(111)
Hexagonal	Te	$(10\bar{1}0)$	(0001)
Cubic	Rock salt	(001)	(011)
	Rock salt at low temperature	(001)(011)	(011)
	Solid solution of $SrCl_2$ in rock salt	(001)	
	Solid solution of $SrCl_2$ in rock salt at low temperature	(001)	(011)

There are mechanisms other than simple slip or cleavage that can give rise to the formation of a wear particle in crystalline solids. These more complex modes will occur with materials commonly encountered in friction and wear surfaces.

Effect of inclusions. - The presence of obstacles in metals can give rise to dislocation coalescence and the initiation of subsurface crack nuclei. The development of such voids is shown

in figure 15 (ref. 34). This mechanism of crack initiation can be started by such obstacles as oxide inclusions in metals such as copper (ref. 35) and in iron by nitrogen and carbon (ref. 36).

This type of subsurface void development can occur very readily for surfaces in sliding or rolling contact. Oxide inclusions are very prevalent in the near surface layers of relatively soft metals because these oxides can be buried by the sliding process. Further, with bearing and gear steels, carbide inclusions are always present. Thus, where adhesion occurs with

(a) Extra row of atoms put in lattice to form edge dislocation.

(b) Collapse of atoms to more stable positions leaving crack nucleus below extra row of atoms.

Obstacle   Obstacle

(c) Dislocation pileup against obstacles (with enough applied force, end pairs can coalesce).

(d) Coalescence of two dislocations.

(e) Coalescence of three dislocations.
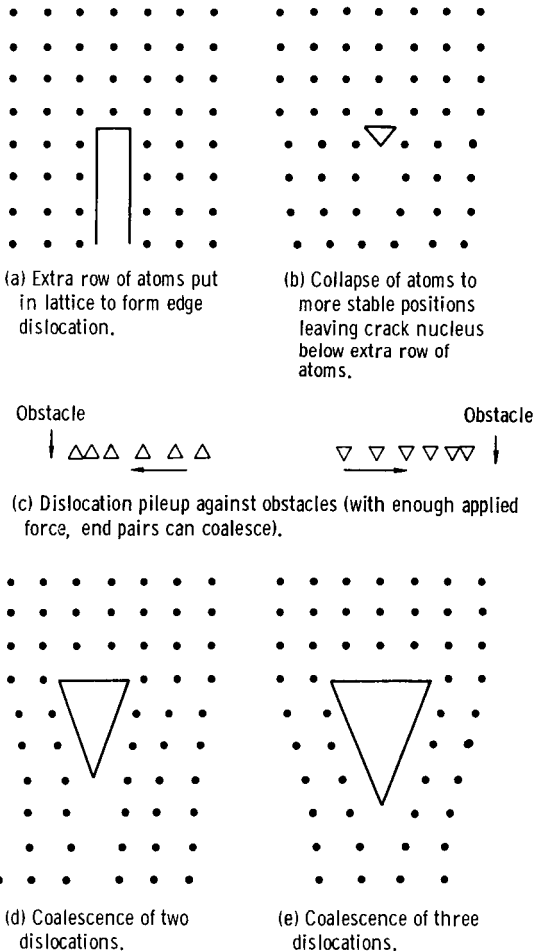
Figure 15. - Formation of crack nuclei as result of dislocation coalescence (ref. 34).

such subsurface voids present, the weakest region may not be
the adhesive interfacial area but rather the cohesive subsurface
region about the void. On application of a force, the fracture
progresses from the subsurface void to the surface by fracture
of cohesive bonds more readily than by fracture of the adhesive
interfacial bonds. This results in the generation of an adhesive
wear particle. Surfaces that are subjected to repeated loading
can develop wear particles readily because, with repeated rolling
or sliding, the material zone between the void and surface may
undergo an exhaustion in ductility. This will result in the forma-
tion of disordered layers and the propagation of the subsurface
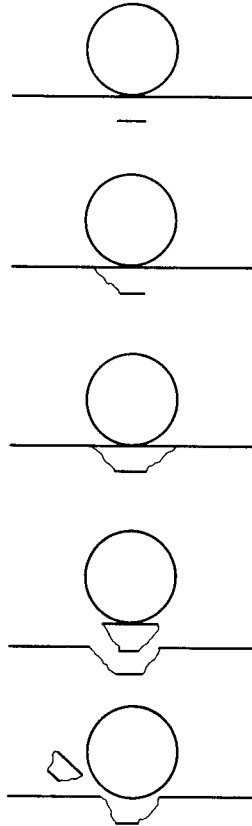
Figure 16. - Generation of
wear particle.

void to the surface as shown in figure 16. The ultimate result as shown in figure 16 is the development of the adhesive or fatigue wear particle.

There are other mechanisms that can initiate subsurface cracks and the start of the formation of an adhesive or fatigue wear particle. These mechanisms are presented schematically in figure 17. The mechanisms were summarized by Cottrell (ref. 37) in reference to bulk material behavior but they can be applied here equally well to near surface phenomena. The subsurface crack developed from sliding on a lithium fluoride surface (fig. 3(b)) resulted from the coalescence of $(10\bar{1})$ slip plane dislocations to form a crack along a (001) cleavage plane as shown schematically in figure 17(b). All the possible forms of crack initiation shown in figure 17 can occur for solids in sliding

(a) Crack formed by pileup of dislocations in slip band against grain boundary.

(b) Coalescence of two slip dislocations to form crack dislocation on cleavage plane.

(c) Coalescence of two slip bands to form cleavage crack.

(d) Crack resulting from shear on two bands.

(e) Crack formed at tilt boundary.
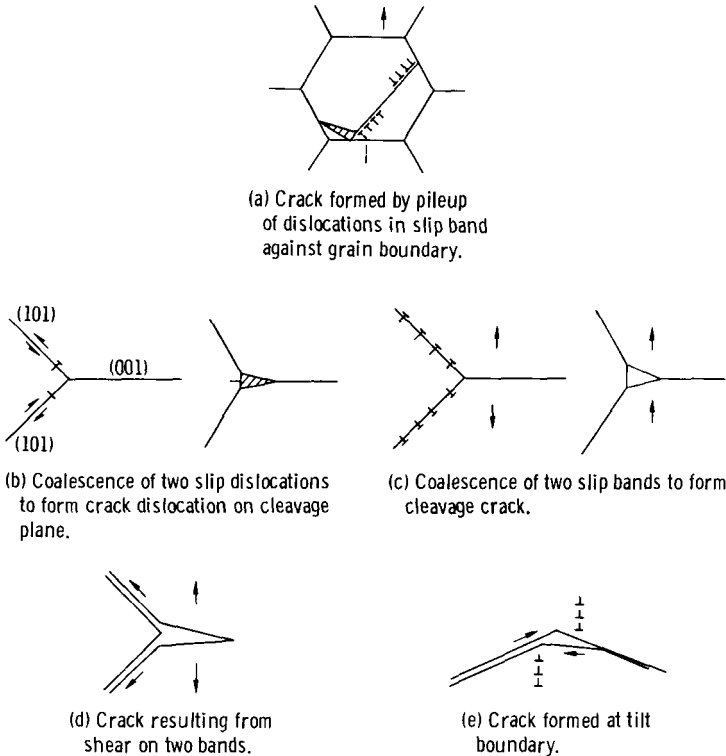
Figure 17. - Mechanisms of crack initiation (ref. 37).

or rolling contact.

In surface microjunctions where plastic flow is very local-
ized, there is plastic instability. This plastic instability can con-
centrate shear on certain planes. Fracture can intiate along
these bands of concentrated flow.

Most fracture initiation and fracture mechanics studies have
been conducted for brittle solids and not until recently has much
attention been paid to ductile fracture behavior. It is the ductile
fracture behavior that is most frequently encountered with sur-
faces where friction and wear is involved. With respect to really
brittle solids, the Griffith theory (ref. 38) is applicable to frac-
ture, and the mechanics of fracture by this mechanism have been
extensively examined for such materials by Irwin and associates
(refs. 39 to 41).

Ductility in metals. - With most crystalline solids in sliding
or rolling contact, plastic deformation is observed. Even with
relatively brittle solids, such as aluminum oxide and lithium
fluoride, plastic flow exerts an influence on observed sliding be-
havior. Metals, which are generally considered ductile, vary in
their ductility, and these variations can influence the mode of
fracture. In general, metals that deform by slip or less than
five independent systems cannot undergo significant plastic de-
formation before fracture. This is the so called Von Misés
criterion. This accounts for the relatively brittle behavior of
hexagonal metals such as zinc at low temperatures. Basal slip
provides only three slip systems. At higher temperatures where
other systems may be activated, these metals exhibit excellent
ductility. In body-centered-cubic (BCC) metals, the type of met-
als most commonly encountered in friction and wear surfaces,
the Von Misés criterion is met at all temperatures. Neverthe-
less, with most body-centered-cubic metals, a ductile-brittle
transition is observed. This, of course, will influence the na-
ture of the fracture observed.

Alloying can influence the ductile-brittle transition behavior
of metals such as iron. Stoloff (ref. 42) has shown that, for iron
base solid solutions, the alloying elements, cobalt, silicon, va-
nadium, and aluminum, suppress dislocation tangle formation

and markedly increase both yield stress and the ductile-brittle transition temperature. Nickel, in contrast, has little influence on dislocation substructure and is not as effective in this respect.

Thus far, adhesion and the generation of subsurface defects that can give rise to the generation of adhesive wear particles have been discussed as if they were two independent processes. The adhesion process itself may, however, give rise to the development of subsurface defects.

Lattice mismatch. - When clean copper and clean gold are placed in contact in a vacuum environment so as to maintain clean surfaces, adhesion occurs across the interface. If the same atomic planes in copper and gold are used and the crystallographic directions are matched across the interface, LEED studies have shown that the gold will transfer epitaxially to the copper (ref. 30). The transfer of the gold to the copper might be anticipated from the earlier discussion on cohesive energy (see fig. 12). Because the gold is bonded epitaxially to the copper and the gold has lattice parameters which differ from copper, the gold atoms must undergo strain to enable them to take on the lattice characteristics of the copper. The manner in which this occurs is shown in figure 18.

Figure 18 indicates the atomic arrangement in an ordered copper-gold alloy and the arrangement of gold on the copper surface in an epitaxial manner. Lattice strain and fracture of cohesive bonds occur as indicated.

Where the lattice mismatch between the two surfaces in contact is relatively large as it is for gold on copper, the mismatch cannot be entirely accommodated simply by strain. When the atomic disregistry becomes sufficiently large, misfit dislocations like those shown in figure 19 will develop.

In reference to figure 19, if an arbitrary point on the surface is selected where atoms match across the interface and there is general lattice mismatch, as the matched pair of atoms is moved away, each successive row will enounter an increase in the degree of mismatch. If the lattice parameters do not differ greatly and therefore the mismatch is not large, as is the case
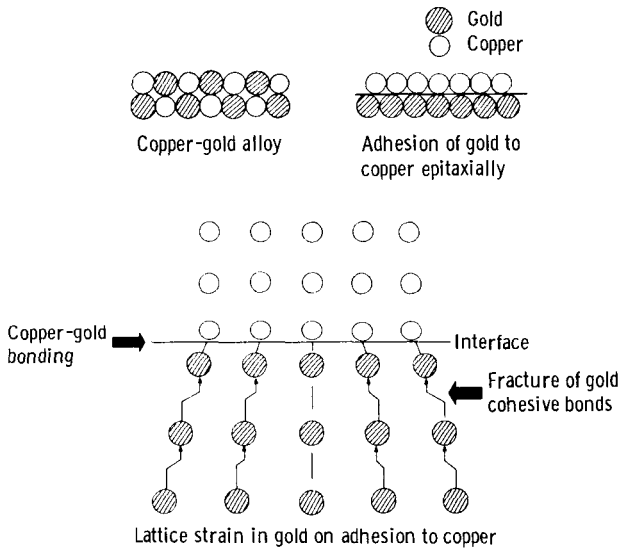
Figure 18. – Atomic arrangement and lattice bonding.

with gold and silver, the mismatch may be accommodated by strain. Where the mismatch is large, as is the case for gold and copper, misfit dislocations will develop near the interface (see fig. 19) because strain alone cannot satisfy the atomic disregistry. The presence of such defects has been discussed in the literature in reference to the deposition of one material on an-
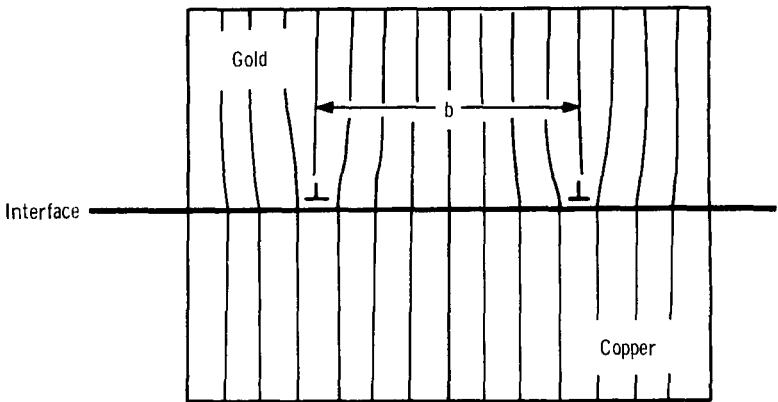
Figure 19. – Accommodation of lattice mismatch in copper-gold contact with misfit dislocation.

other (refs. 43 to 46).

The presence of the interfacial misfit dislocations in fig-
ure 19 would reduce the number of gold bonds across the inter-
face. The average strength of the adhesive bond would be greater
than the cohesive strength of the weaker of the metals (namely,
gold) and fracture would occur in the gold. Thus, the process of
materials adhering one to another may in and of itself introduce
defects which will reduce the strength of one of the materials sub-
surface and give rise on tensile fracture to the formation of ad-
hesive wear.

If what has been said thus far is correct, then it might be an-
ticipated that the greater the degree of lattice mismatch, the
greater should be the concentration of subsurface defects (i. e. ,
misfit dislocations) and this should affect the force necessary to
fracture two surfaces in adhesive contact. Table VII presents the
results of adhesion measurements for various face-centered-
cubic metals to a gold (111) surface. Adhesive contact was made
to the gold with the (111) surfaces of gold, silver, aluminum, and
copper. Where the lattice misfit was less than 1 percent, the ad-
hesive forces exceeded 400 dynes (400×10^{-5} N) with an applied
force of only 20 dynes (20×10^{-5} N). With copper in contact with

TABLE VII. - EFFECT OF LATTICE MISFIT ON

ADHESION OF GOLD TO VARIOUS FACE

CENTERED CUBIC METALS

Metal	Lattice parameter, Å (or 10^{-10} m)	Percent mis-fit with (111) Au	Force of adhesion of Au (111) to (111) metal surface,[a] dyne (or 10^{-5} N)
Au	4.078	0	>400
Ag	4.086	.19	>400
Al	4.049	.71	>400
Cu	3.615	11.1	80

[a]Applied load 20 dynes (20×10^{-5} N); contact time, 10 sec;
    ambient temperature, 20° C (293 K); ambient pressure,
    10^{-11} torr.

the gold and where the lattice misfit was in excess of 11 percent, the adhesive force measured was only 80 dynes (80×10^{-5} N). Even with a consideration of differences in cohesive energies and deformation characteristics as were presented in figure 12, the degree of lattice misfit and, therefore, the presence of surficial defects appear to have an influence on adhesive behavior.

FATIGUE WEAR

The concept of fatigue wear is normally associated with friction, wear, and lubrication with repeated cycling in bearing or gear components (ref. 47). For example, one of the major concerns of bearing designers in the fatigue life of bearings. The bearings operate in a normal environment and are well lubricated. After a repeated number of stress cycles of the bearings during operation, the bearings will fail by fatigue. Material will have become dislodged, in the case of a ball bearing either from the ball or race, destroying the usefulness of the bearing.

Wear by fatigue can also occur during dry solid-state contact. It can occur in vacuum for materials that do not adhere strongly because of the presence of surface films or where there is a lubricant film. When two surfaces are in rubbing contact, the surface microcontacts are subjected to both compressive and tensile forces. This fact has been determined experimentally by Radchik and Radchik (ref. 48). Thus, with repeated passes, surface and subsurface cracks can develop that may lead to the generation of free wear particles.

In fatigue, failure in the material arises because of stress-reverse effects, that is, fracture can develop under alternating stresses with a peak level that could be safe if imposed in only tension or compression. The number of stress cycles of some given amplitude that a material can sustain before failure is termed the fatigue life with the life varying with the level of stress imposed.

The beginning of the formation of wear particles by fatigue is the surface or subsurface crack. The dislocation origin of some of these cracks has already been discussed with reference

to figures 15 and 17. The Cottrell and Hull (ref. 49) mechanism
exists in metals where slip can occur on more than one set of
planes. This gives rise to the formation of cracks by slip-plane
dislocation interaction.

The Mott (ref. 50) mechanism requires for its operation a
screw dislocation which terminates in the surface at one end and
at some internal cavity at the other. The cavity can result from
the approach of two edge dislocations of opposite sign to within
10 Å (100 nm) of each other. When this occurs a crack can de-
velop that will widen with the addition of other dislocations glid-
ing on the same planes. The ability to cross slip is an important
factor in the Mott mechanism because, under alternating
stresses, the screw dislocation will complete a circuit by cross
slipping from one plane to another.

A fatigue crack forming mechanism which is particularly
likely with hexagonal metals is that shown schematically in fig-
ure 20. This type of crack will form where a polygon boundary
terminates inside the crystal; there will then exist large tensile
stresses across the plane on which it ends. Such cracks have
been observed on hexagonal metals subjected to deformation
(ref. 52).

A number of other processes can give rise to the initiation
of fatigue cracks or subsurface cracks that can weaken materials
in the surficial region and generate wear particles by fatigue or
adhesive wear. These include vacancy clustering as a void form-
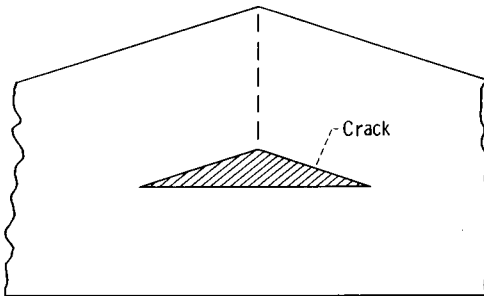

Figure 20. - Possible mechanism of cracking along slip
plane due to wall of similar edge dislocations in hex-
agonal metals such as beryllium (ref. 51).

ing mechanism (ref. 51), reversed slip acting as stress raisers (ref. 53), random cross slipping (ref. 54), and edge-screw dislocation interactions (ref. 55).

Once an atomic crack has formed by one of the mechanisms mentioned earlier, the question arises as to what propagates the crack such that a free wear particle is generated. With brittle materials such as glass, the continuum approach taken by Griffith (ref. 38) is applicable to crack propagation. This method of approach is primarily for amorphous materials because it does not take structure into consideration. The real strength of solids is considerably below that of the theoretical strengths calculated from the theory of atomic cohesion. It was this difference that gave rise to the concept of the presence of dislocations in solids.

Fatigue in brittle materials. - The Griffith concept is based on the premise that microcracks already exist in an isotropic material and considers the propagation of the crack under an applied stress. The simplest approach is to consider a crack present in a two-dimensional flat plate. If the crack is elliptical, then when a stress is applied the elastic strain energy in the region of the crack can be determined. This results in an increase in the radius of the crack tip dimensions. When the energy put into the material by the applied stress exceeds the surface energy of the material, the crack surface area will increase.

The Griffith concept applies to the situation where no plastic deformation occurs. Where plastic deformation does occur, some of the energy put into the material will be absorbed in plastic flow in the regions of the crack tip. This requires that an additional term be introduced into the Griffith approach to account for this factor. With brittle materials, crack propagation usually takes place at high velocities. In plastic materials, the rate is controlled by internal stresses in the plastic zone of the crack tip. Since the properties in this zone are highly structure sensitive (depending on orientation, on dislocation structure, and on dislocation mobility) the actual course and velocity of the crack may be quite irregular and intermittent.

Fatigue in ductile materials. - With materials in sliding or rolling contact, most of which are subject to plastic behavior,

the Orowan (ref. 56) work hardening of plastic regions model may be applicable. According to this concept, there is an elastic matrix, which for contacting solids may be considered to be the material in the microjunction. With alternating stresses, a core or central region of the elastic matrix may undergo plastic deformation with the alternating strain. A fatigue crack will develop when the number of stress cycles which have been applied are sufficient to raise the stress in the junction by progressive work hardening to the point where the static fracture stress has been reached.

The subsurface zone where a fracture crack may form will have a large influence on the size of the wear particle. The deeper the crack, the larger will be the wear particle when the crack has propagated to the surface. With surfaces in rubbing or sliding contact, this zone will be dictated by the applied load and the friction force. Hamilton and Goodman (ref. 57) have analyzed the zones of maximum subsurface stress. The zone of this maximum stress may move from the subsurface to the surface when the friction force exceeds a certain value. This variation in the zone of maximum stress with friction force may account for some of the differences observed in the origin of fracture cracks (refs. 58 and 59). Structure and orientation effects are not taken into account in these calculations.

Thermal fatigue. - The high temperatures that are generated at the contacting microjunctions can contribute to the generation of wear particles by fatigue. These temperatures may reach as high as 600° to 1000° C (873 to 1275 K) and last for very short times (ref. 4). These flash temperatures set up a thermal gradient in the microjunction that can result in differential stresses in the junction. The magnitude of these stresses will depend on many factors, some of which include heating rate, thermal properties of the material, density, shape of the microjunction, etc. Where the heating is very rapid, the expansion of the surface layers can create stresses in the material which exceed the breaking stress, and fracture in the junction can occur. Endurance with this method of fatigue is shorter in the presence of oxides on metal surfaces than it would be in their absence as

observed by Glenny and Taylor (ref. 60).

Still another area to be considered in the generation of wear particles by fatigue is one that develops when one or both surfaces in contact undergo plastic deformation in the microjunctions. The plastic deformation may occur to some depth in the junction. Because these junctions usually increase in cross-sectional area as the bulk material is approached, a zone will be reached where the deformation changes from plastic to elastic. The transition zone from the one type of deformation to the other will have differential stresses. The surface layer with repeated sliding or rubbing will develop a brittle nature due to work hardening, but, where deformation has been primarily elastic, the condition of the material will be what it was before the rubbing or sliding. This, then, is another zone vulnerable for fracture crack formation.

INFLUENCE OF REDUCING AMBIENT PRESSURES ON FRICTION

When the ambient pressure for two solid sliding surfaces in contact is reduced, one of the first effects is the removal of residual physically adsorbed films. The pressures at which the various adsorbed films will desorb will be a function of their heats of adsorption to the solid surfaces. Sliding or rubbing contact at reduced ambient pressures will in itself produce frictional heat at the interface between the two sliding surfaces. This frictional heat will help to promote the desorption of physically adsorbed species such as the atmospheric gases and water vapor.

EFFECT ON METAL OXIDES

With most of the transition metals, which form relatively stable metal oxides very rapidly, the simple reduction of pressure from atmospheric to about 10^{-6} torr will have very little influence on the removal of oxides from metal surfaces. The reduction of the ambient pressure, however, and the partial pressure of oxygen will influence the thermodynamic stability of

metal oxides. In general, as the concentration of oxygen in the
environment is reduced, the temperature for the thermodynamic
stability of the metal oxide is also reduced. Thus if we have a
metal reacting with oxygen, we can express it with the equation

$$M + \frac{1}{2} O_2 \rightarrow MO$$
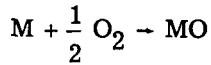
where M is any metal. The relation for the thermodynamic
stability of the oxide on the metal surface to the oxygen partial
pressure in the environment may be related by the equation

$$\Delta F = \Delta F^O + \frac{2.3 \ RT \ \log 1}{\sqrt{PO_2}}$$

where R is a constant, T is temperature, and P is pressure.

The relation of the thermodynamic stability or free-energy
formation of metal oxides as a function of oxygen partial pres-
sure is shown in figure 21. Examination of figure 21 indicates
that, as the oxygen partial pressure is reduced below 1 atmo-
sphere, the temperature for which the oxide is thermodynam-
ically stable is also reduced. In figure 21 the zero point on
the ordinate represents the threshold between thermodynamic
stability and instability. A positive free energy of formation
would indicate thermodynamic instability, and a negative free
energy of formation would indicate thermodynamic stability of
the metal oxide. When the oxygen partial pressure is greater
than 1 atmosphere, the oxide on the metal surface will have
greater thermodynamic stability than it does at an oxygen pres-
sure of 1 atmosphere or less.

Reducing the ambient pressure for materials in sliding or
rubbing contact has a tendency, then, to desorb adsorbed species
as well as to reduce the thermodynamic stability of the metal
oxides. It may be recalled from an earlier discussion that the
presence of the adsorbed films and metal oxides reduces the
tendency for metal surfaces to adhere one to another. For
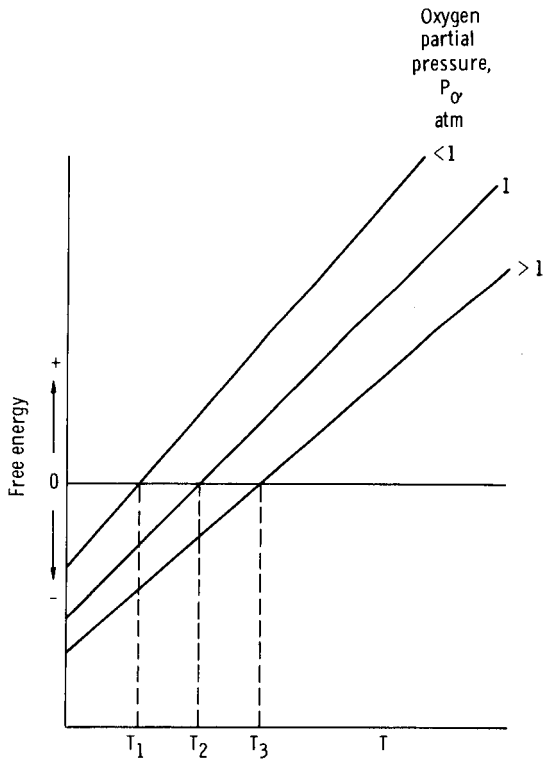
Figure 21. - Effect of oxygen pressure on free energy of formation of metal oxides.

metals that form a simple oxide (MO) and that have a relatively small free energy of dissociation, there is, on reduction of the ambient pressure, a point where the oxide may no longer be thermodynamically stable. We might anticipate that simple dissociation to oxygen and free metal could occur. This is, in fact, what is observed for such metals as silver. Simply reducing the ambient pressure for silver can render the AgO (silver oxide) thermodynamically unstable. With some metals, however, particularly those in the transition series, more than a single oxide may form by the reaction of the metal with oxygen. An example of such a metal is iron. Iron can form at least three stable oxides, FeO, Fe_3O_4, and Fe_2O_3. Normally at atmospheric pressure the oxide Fe_2O_3 is present on the outer surface of iron

and steels. If there are large concentrations of alloying ele-
ments in the steels, other oxides may be present as well. Re-
ducing the ambient pressure and the oxygen partial pressure
available for reaction with the iron or steel surface can result in
insufficient oxygen being available for the formation of the higher
oxide of iron, namely, Fe_2O_3, and the lower oxides will begin to
form at a sliding or rubbing surface.

EFFECT ON BEARING STEEL

In figure 22 friction data are presented as a function of am-
bient pressure for 52 100 bearing steel sliding on itself at a slid-
ing speed of 216 centimeters per second with a load of 1000
grams (1 kg) on a hemisphere contacting a flat at an ambient
temperature of 20° C (293 K). In reducing the ambient pressure
from 760 torr, a reduction in friction coefficient is observed.
When the pressure reaches 10^{-2} torr region, the friction has
achieved a minimum. A continuous reduction in the ambient
pressure results in an increase in friction coefficient. The shape
of this curve can be explained in terms of the amount of oxygen

Figure 22. - Coefficient of friction for 52100 sliding
on 52100 at various ambient pressures. Sliding
velocity, 216 centimeters per second; load,
1000 grams (9.8 N); ambient temperature, 20° C
(293 K).

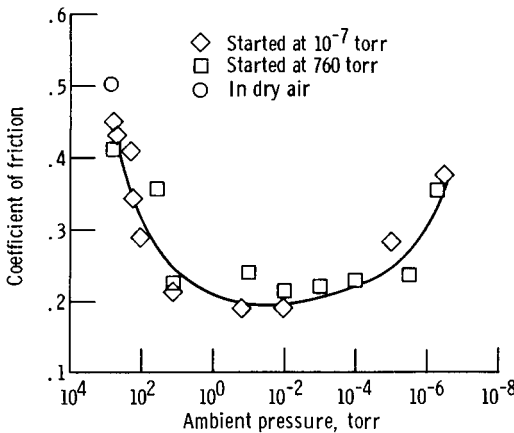available for the formation of the iron oxides on 52 1000 bearing steel surface. At 760 torr, the principal oxide on the surface is Fe_2O_3. As the ambient pressure is reduced, however, insufficient oxygen is available for reaction with the steel surface in the sliding process to form the higher oxide of iron. As a result, the lower oxides of iron, Fe_2O_3 and FeO, form on the iron surface. These oxides have lower frictional properties and provide better surface protection than the higher oxide of iron. As a consequence, a reduction in friction coefficient is observed. With continued reduction in the ambient pressure and the oxygen partial pressure, insufficient oxygen becomes available even for the formation of these lower oxides of iron. The friction at pressures below 10^{-4} torr begin to again increase. This gradual increase in friction is represented by contact at the interface which is the result of the increasing amount of metal contact. At the interface the surface is partially covered with the lower oxides of iron, and there is a degree of metal contact occurring as a result of insufficient oxygen available for the formation of a complete surface film of oxide.

In figure 22 a data point is plotted at 760 torr for experiments conducted in dry air. Note that even the presence of moisture or humidity in the air at 760 torr will have an influence on the friction coefficient. In dry air the friction coefficient for the 52100 bearing steel was approximately 0.50. In the presence of humidity or moisture in the air the friction coefficient was 0.45.

If, however, the experiment that gave rise to the friction results presented in figure 22 was repeated, if oxygen was completely excluded from the environment, and if all that was present on the 52100 bearing steel surfaces was the residual surface oxides, then the friction results are those presented in figure 23. In figure 23 the friction coefficient is plotted as a function of time. Initially, the friction coefficient is relatively low, approximately 0.45, as it was at 760 torr in figure 22. This relatively low friction coefficient is due to the presence of the iron oxide. But with continuous sliding as a function of time, the residual surface oxide present on the 52100 sliding steel surface
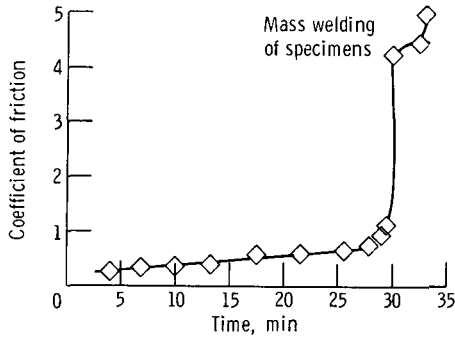
Figure 23. - Coefficient of friction for 52100 sliding on 52100 in vacuum. Sliding velocity, 216 centimeters per second; load, 1000 grams (9.8 N).

begins to wear away, and a greater and greater amount of metal contact begins to occur with an accompanying adhesion of the metal across the interface. Note that in figure 23 the friction coefficient is gradually increasing with time. After approximately 30 minutes of sliding, the surface is sufficiently devoid of oxide at the contacting interface, and there is a sufficiently large amount of metal-to-metal adhesion that the friction coefficient increases very rapidly and reaches a value of nearly five at which point mass welding of the specimens occur. This mass welding or gross seizure of the two solid surfaces in contact would have occurred when the surfaces were placed in contact, had both surfaces been clean and completely free of oxide and other contaminants.

The results presented in figures 22 and 23 indicate the marked influence that surface oxides have on the friction behavior of metals in sliding or rubbing contact. The oxide must be present to prevent complete seizure of the two parts in contact as indicated by figure 23, and the relative partial pressure of oxygen in the environment will have an influence on the friction results as shown in figure 22. Thus, not only is an oxide needed on the surface, but also the nature of the oxides on the surface have an influence on friction behavior.

Effect on Carbon

Metals and alloys are not the only materials that exhibit sensitivity in their friction properties to the effects of atmospheric pressure. In the case of some nonmetals, the sensitivity to the constituents of the atmosphere may be even greater than they are for metals. For example, graphite is a material which is widely used as a lubricant in a conventional atmospheric condition. When the ambient pressure, however, is reduced, graphite loses its lubricating properties as was shown by Savage (ref. 61). The graphite crystallites adsorbed oxygen and water vapor on the crystallite edges. The adsorption takes place primarily at the edges because the flats of the hexagonal crystallites are relatively low-energy surfaces. With a reduction in ambient pressure from atmospheric to approximately 1 torr, Savage (ref. 61) found that the lubricating properties of graphite were completely lost. This loss is due to an increase in the adhesion of the graphite to itself as a result of a loss of adsorbed moisture and hydrocarbons which prevents the adhesion of graphite to itself from occurring.

It is well known that the carbon-to-carbon bond is extremely strong and when the adsorbates are removed from the surface of graphite this strong bonding can develop between adjacent graphite crystals giving rise to relatively high friction coefficients for graphite. Although the friction coefficient of graphite under atmospheric conditions may be approximately 0.1, at reduced ambient pressures its friction coefficient may exceed 0.7.

Graphite and graphite-carbon materials are widely used in the field of lubrication in such applications as mechanical seals. These bodies are extremely sensitive to the presence of adsorbed species just as is the graphite. Figure 24 presents the coefficient of friction at various ambient pressures for a graphite-carbon body sliding on 440-C stainless steel at a sliding velocity of 216 centimeters per second under a contact load of a hemisphere on a flat of 1000 grams (10 N) and ambient temperature of 20° C (293 K).

In dry oxygen a reduction in ambient pressure from 760 torr
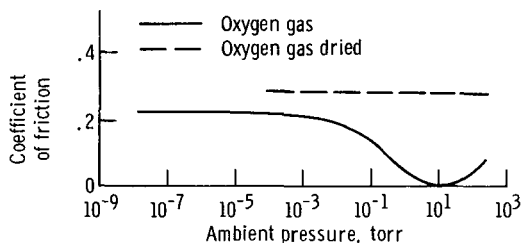
Figure 24. - Effect of various gases on coefficient of friction of graphite-carbon sliding on 440-C stainless steel at various ambient pressures. Sliding velocity, 216 centimeters per second; load, 1000 grams (9.8 N): ambient temperature, 20° C (293 K).

to approximately 10^{-4} torr has little or no effect on the friction coefficient of the graphite-carbon body sliding on the stainless-steel surface. If, however, the oxygen contains a small concentration of moisture, the friction coefficient is relatively low at 760 torr, and it remains low to a pressure of approximately 1 torr at which time the friction coefficient begins to increase. This increase in friction coefficient reflects the loss of the adsorbed moisture from the graphite-carbon body, which aids in the lubrication of the graphite body in sliding contact with the steel. When this adsorbed moisture is lost, however, the friction coefficient begins to increase; and, if the pressure is below 10^{-5} torr, it exceeds 0.2. The removal of the water from the graphite-carbon body by simply reducing the pressure to below 1 torr would indicate that the water is not very strongly adsorbed to the graphite-carbon surface because a simple reduction in pressure is sufficient to bring about its loss from the surface. In contrast, however, oxygen is very strongly bonded to carbon, and it requires extremely high temperatures in a vacuum environment to remove oxygen from a carbon body. As has been mentioned, chemisorbed oxygen on carbon surfaces may only be desorbed by the formation of carbon monoxide gas, which is then liberated from the solid surface. Smith, Pierce, and Joel (ref. 62) discuss the interaction of water with carbon, and Snow et al. (ref. 63) discuss the interaction of carbon bodies with

oxygen.

The increase in friction coefficient for carbon material (fig. 24), with a reduction in ambient pressure below 1 torr, is accompanied by a very marked increase in wear. The carbon body will wear at a very high rate at pressures below 10^{-5} torr. It is a combination of increase in friction and an excess of wear in the absence of moisture that give rise to graphite and graphite-carbon bodies being very poor materials for use in a vacuum environment.

In the development of high-altitude aircraft during the Second World War, this graphite and graphite-carbon property gave rise to dusting or the excessive wear of brush materials in generators.

When graphite or graphite-carbon bodies are in sliding contact with metal surfaces, as they are frequently in mechanical components of many lubrication devices, a transfer film of the graphite-carbon or carbon material to the metal surface will occur with repeated passes over the same surface. The metal surface in the sliding contact region will then, after a number of repeated passes over the same surface, become coated with a thin film of the graphite-carbon or carbon material. The result is that the graphite-carbon or carbon material is actually sliding on itself, and the friction behavior of the materials in contact may be influenced to a large extent by the frictional properties of the graphite-carbon or carbon material (see fig. 24).

When the experiment conducted in figure 24 was repeated with a graphite-carbon body sliding on silver instead of stainless steel, somewhat different results were obtained. The data of figure 25 present the coefficient of friction for graphite-carbon sliding on silver at various ambient pressures. Much as with graphite-carbon sliding on 440-C stainless steel in figure 24, the friction coefficient at 760 torr is relatively low and decreases to an even lower value at pressures to 1 torr much as it did in figure 24. At pressures below 1 torr, however, the friction coefficient begins to increase rather markedly. Unlike figure 24, however, the friction coefficient does not terminate at a value of approximately 0.2. In figure 25 the friction coefficient continues
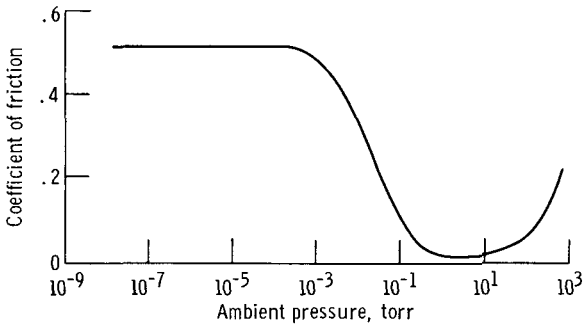
Figure 25. - Effect of ambient pressure on coefficient of friction for graphite carbon sliding on silver at various ambient pressures. Sliding velocity, 216 centimeters per second; load, 1000 grams (9.8 N); ambient temperature, 20° C (293 K).

to increase until a value of approximately 0.5. If both sliding experiments were stopped after a certain number of cycles of sliding over the same surface region at 760 torr and the specimens surfaces were examined, both the 440-C stainless steel and the silver would contain a transfer film of the graphite-carbon material. The presence of this film would indicate that the graphite-carbon material is basically sliding on itself and that the friction coefficients at 760 torr are largely due to the graphite-carbon material.

If these same surfaces are again tested and removed after operating at a pressure of 10^{-9} torr, the carbon transfer film in the case of the 440-C stainless steel, would still be present on the stainless-steel surface. Its presence indicates that the rise in friction coefficient to approximately 0.2 at the lower ambient pressures is simply due to a loss of moisture and other adsorbates in the graphite-carbon body. An examination of the electrolytic silver surface in the contact area after operation at 10^{-9} torr, however, revealed a complete absence of a carbon transfer film to the silver surface. The silver surface was completely devoid of carbon film. Examination of the graphite-carbon sliding body indicated that, in the contact region, silver (i.e., metallic silver) had transferred from the silver surface to the graphite-carbon body. Rather than the graphite-carbon sliding

on itself, as was the case for 440-C stainless steel at pressures below 10^{-5} torr, for silver (fig. 25) at pressures below 10^{-3} torr the carbon was basically removing silver from the silver surface such that silver was sliding on itself. Thus, the metallic silver was bonding to the carbon surface. This is extremely interesting because silver does not normally form thermodynamically stable carbides.

The difference in friction characteristics for carbon sliding on 440-C stainless steel and electrolytic silver at the lower ambient pressures (below 10^{-3} torr) may be attributed to the presence or absence of a transfer film of carbon. Figure 24 shows data for carbon sliding on carbon at low ambient pressures, and figure 25 for silver sliding on silver. In these experiments, the surfaces contained residual surface oxides before the start of the experiments. The carbon will bond to the oxygen of the metal oxide in both cases; that is, with the oxides on the stainless-steel and the silver surfaces. With the 440-C stainless-steel surface, the oxide is principally chromium oxide with some iron oxide present. These oxides are thermodynamically stable. As a consequence, the carbon can bond to the oxygen in these oxides and remain bonded to the 440-C stainless-steel surface at low ambient pressures of 10^{-9} torr.

With silver, however, the silver oxide is stable at 760 torr and a carbon transfer film is observed on the silver surface after sliding at 760 torr. When the ambient pressure is reduced below approximately 1 torr, the silver oxide becomes thermo-dynamically unstable and can, with the frictional heat generated at the sliding interface, dissociate. This dissociation of the silver oxide results in a loss of the presence of oxygen on the silver surface. The carbon can no longer bond to the oxygen on the silver, but now bonds directly to the silver. At these low pressures it appears that the bond strength in the graphite-carbon material is stronger than is the metallic silver bond, and as a consequence shear occurs in the metallic silver. The shear gives rise to the transfer of metallic silver to the carbon surface and accounts for the absence of a carbon transfer film

on the silver.

Thus with two dissimilar materials in contact (as in figs. 24 and 25) where graphite-carbon materials are sliding on metals, the effect of reducing the ambient pressure is extremely important in the friction behavior of the sliding couple. The influence of the partial pressure on the behavior of such mixed couples is a little more subtle than was observed with the bearing steel 52100 in sliding contact with itself. The results presented indicate that the environment can have a tremendous influence on the friction properties of various materials in sliding, rubbing, or rolling contact. The sensitivity of solid surfaces in sliding or rubbing contact to the presence of environmental pressure has also been observed with another crystalline form of carbon, namely, diamond.

EFFECT ON COVALENT AND IONIC SOLIDS

Bowden and Hanwell (ref. 64) conducted sliding friction experiments with diamond sliding on diamond (a (100) crystal stylus of diamond sliding on a (111) cleavage crystal face of diamond) and found that at atmospheric pressure in air the friction coefficient for diamond sliding on itself was slightly in excess of 0.1. The ambient pressure was reduced from atmospheric to 5×10^{-9} torr, and the specimens continued to slide with repeated passes over the same surface. After a definite number of cycles, the friction coefficient for diamond in contact with itself rose very rapidly to approximately 0.9. These results indicate that even a very brittle material such as diamond is extremely sensitive in its friction behavior to the presence of adsorbed surface species.

Reference 65 reports an experiment with sapphire sliding on sapphire. Decreasing the ambient pressure from 760 to 10^{-10} torr resulted in a fourfold increase in friction coefficient. These results further confirm the influence of adsorbed surface species on the friction of relatively brittle solids.

INFLUENCE OF ULTRAHIGH VACUUM ON FRICTION OF CLEAN METALS

In the previous discussion it has been shown that residual surface oxides on metallic surfaces can play a marked role in the friction behavior of metals even in vacuum. If the friction properties of metal surfaces are to be determined in a vacuum environment, it becomes necessary to carefully clean the surface in an ultrahigh vacuum environment and conduct friction experiments with clean surfaces in contact. Data obtained with such surfaces can then serve as a point of reference for determining the influence of various adsorbed and reacted surface films on friction and wear materials in contact. To eliminate the various surface films present on the metallic surface after the metal has been pumped down in a vacuum system to an ultrahigh vacuum pressure level, it becomes necessary to employ some cleaning technique. Various techniques have been devised for preparing clean surfaces in a vacuum environment. These include evaporation, sputtering, high temperature heating, ion bombardment and annealing, field dessorption, and cleavage. The advantages and disadvantages of these various cleaning techniques are discussed by Roberts (ref. 66).

MATCHED SINGLE CRYSTALS

It might be anticipated from preceding discussions that the situation which would give rise to the highest friction behavior for two metal surfaces in contact would be where two single crystals of like orientation are brought into contact. Two single crystals of the same material and of the same orientation, matched with their atomic planes at the interface as well as in their crystallographic directions, may be brought into contact such that atomic bonding would occur across the interface. Should the atomic matching be perfect, the interace between the two crystals would be lost, and the individual crystals would lose their individual identity. In actual practice, however, the achievement of such a condition is all but impossible. There is

always some mismatching in any attempt to bring like planes and crystallographic directions of the same materials into contact. Even so, the maximum in friction for two solid surfaces in contact would result because the least amount of imperfections would occur at the interface between two such surfaces.

Copper surfaces that have been cleaned by electron bombardment in a vacuum environment have been brought into contact with matched atomic planes and directions. Both the force of adhesion and the friction coefficient for the two surfaces in contact have been measured. The data of table VIII are for the adhesion and friction coefficients of three atomic planes of copper, (100), (110), and (111), in contact with themselves. Included are data on the adhesion and friction of polycrystalline copper. In addition to the adhesion and friction data, data for the modulus of elasticity and surface energies are also presented. Two copper surfaces were brought into contact to obtain the data of table VIII under a load of 50 grams with a hemispherical specimen contacting a flat. After contact under a 50-gram load was made, the applied load was removed, and the force required to fracture the atomic planes in contact was measured. The adhesion coefficients obtained are also presented in table VIII.

The adhesion coefficient is the force required to fracture the adhesive junction divided by the applied load (in this instance 50). Examination of table VIII indicates that the highest adhesion coefficient before sliding contact were obtained with the (100) and the polycrystalline copper surfaces. The lowest adhesion force was measured with the (111) surface of copper in contact with itself. A greater than threefold difference in adhesive force existed between the (111) and the (100) surfaces. As may be recalled, two properties related to adhesion are the modulus of elasticity, since it reflects the cohesive forces in the metal, and the surface energy, which is the energy required to generate a new surface from two surfaces that are cohered. The elastic modulus of the (111) surface indicates that it would have a greater resistance to deformation. As a consequence, the true contact area at the interface would be much less than, for example, for the (100) surface under the same applied load of 50 grams.

TABLE VIII. - VARIOUS PROPERTIES OF SINGLE-CRYSTAL AND POLYCRYSTALLINE COPPER (99.999 PERCENT)

Copper form and orientation	Young's modulus, dyne/cm² (or 10⁻¹ N/m²)	Surface energy, ergs/cm² (or 10⁻⁷ J/cm²)	Adhesion coefficient before sliding[a]	Coefficient of friction during sliding[b]	Adhesion coefficient after sliding[c]
Single-crystal (100) matched planes and directions	6.67×10^{11}	2900	1.02	>40.0	>130
Single-crystal (110) matched planes and directions	13.10×10^{11}	----	0.61	>40.0	50.0
Single-crystal (111) match planes and directions	19.4×10^{11}	2500	0.30	21.0	10.5
Polycrystal	12.0×10^{11}	----	1.00	>40.0	100

[a] Load 50 g (0.5 N); ambient pressure, 10^{-11} torr; ambient temperature, 20° C (293 K).

[b] Load 50 g (0.5 N); sliding velocity, 0.001 cm/sec; ambient pressure, 10^{-11} torr; ambient temperature, 20° C (293 K).

[c] Load 50 g (0.5 N); distance of slide in preferred slip directions, 0.735 cm; ambient pressure, 10^{-11} torr; ambient temperature, 20° C (293 K).

It might be anticipated that the true contact area for the (100) surface would be larger than that for the (111) surface based on the modulus of elasticity. The area of contact will obviously influence the measured adhesive forces. The surface energy or energy required to generate a new surface from the two surfaces in contact is lower on the (111) surface than on the (100) surface. This, means that it requires less energy to fracture (111) planes than (100) planes. The distance between the {111} planes is greater than that between {100} planes. The greater interplane distance indicates a weaker interplane bonding which correlates the difference in the surface energies.

Sliding was initiated between the surfaces in contact, and the friction coefficients measured during sliding. The friction results obtained are presented in table VIII. For the (100) and the (110) planes, the friction coefficients exceeded the value of 40, the limits of measuring of this apparatus. For the (111) surface the friction coefficient was 21. This friction coefficient of 21 for the (111) surface is approximately 20 times what is observed in air for the same copper crystals in contact. The friction coefficient for the polycrystalline copper also exceeded 40. The total sliding distance in the experiments was only 0.735 centimeter.

On the initiation of sliding, the friction coefficients were relatively low and increased continuously with tangential motion until such time that, within the (100) and the (110) surfaces, it exceeded a value of 40. This increase in friction coefficient with tangential motion is due to an increase in a true contact area due to plastic flow at the interface between the two contacting surfaces. As one surface slides over the other, the tangential motion causes an increase in the true contact area between the two solid surfaces giving rise to a greater amount of real area in contact and a continuous increasing in the friction force for the same applied load (ref. 67).

After sliding a distance of 0.735 centimeter, the experiments were stopped, and the force required to separate the surfaces or the adhesion coefficient was measured. In table VIII the

adhesion coefficient after sliding of the (100) surfaces in contact
exceed 103 or nearly 130 times the value obtained before sliding
commenced.   The value obtained for the (111) surface was 10.5,
a considerably lower value than was obtained for the (100) sur-
faces in contact.   The (110) surfaces exhibited an intermediate
adhesion coefficient of 50.   These large increases in adhesion
coefficient after sliding only a distance of 0.735 centimeter are
due to an increase in the contact area at the interface.   There is,
after sliding, a greater area over which atomic bonding has
occurred.   The forces necessary to separate the surfaces are
greater than in the initial adhesion experiments before sliding
had commenced.   The sliding process gives rise to growth of the
interfacial junctions with respect to their actual area, and this
marked increase in adhesion coefficient for the various orienta-
tions before and after sliding can be attributed to this junction
growth.   The results shown in table VIII indicate that for like
metals in contact the orientation of the surfaces has an influence
on the observed adhesion and friction behavior.

DISSIMILAR ATOMIC PLANES IN CONTACT

For the face-centered-cubic metal copper, the {111} or
highest atomic density planes and the preferred slip planes in the
face-centered-cubic system exhibited the lowest adhesion and
friction values; the {100} surfaces exhibited the highest.   The
next logical step in the measurement of friction properties for
metal surfaces in contact with respect to determining maxima in
friction to that of identically matched atomic planes across an in-
terface would be the situation where dissimilar atomic planes of
the same material are in contact across an interface.   With two
clean surfaces in contact this might be analogous to the formation
of a grain boundary since the interface between the two clean
crystal surfaces once contact is made would, in fact, be very
analogous to a grain boundary.

Adhesion and friction experiments have been conducted with
dissimilar planes of copper in contact.   Table IX presents the
adhesion and friction results for the (100) surface in contact with

TABLE IX. - COEFFICIENTS OF ADHESION AND

FRICTION FOR VARIOUS SINGLE-CRYSTAL

ORIENTATIONS OF COPPER

(99.999 PERCENT)

[Ambient pressure, 10^{-11} torr; load, 50 g (0.5 N).]

Matched planes	Adhesion co-efficient be-fore sliding	Coefficient of friction during slid-ing[a]	Adhesion co-efficient after sliding
(100) on (100)	1.02	~40.0	~130
(110) on (100)	.25	~40.0	32.5
(111) on (100)	.20	~40.0	40.0

[a]Sliding velocity 0.001 cm sec; (110) direction; sliding dis-
tance, 0.735 cm.

itself to serve as a point of reference for the (110) surface in
contact with (100) surface and the (111) surface in contact with
the (100) surface. The adhesive forces measured for the dis-
similar planes in contact were less than that obtained for the like
planes in contact, as might be anticipated. With dissimilar
atomic planes in contact, a greater concentration of imperfec-
tions would exist at the interface just as there are a greater
number of imperfections in a grain boundary than there are in the
bulk grain.

The initiation of sliding and the measurement of friction co-
efficients gave a continuous increase in friction with sliding as
was observed with reference to table VIII. The friction coeffi-
cient for all three couples in table IX exceeded 40 or the limits of
measurement of the device. Note that in table IX the friction co-
efficient for the (111) surface in sliding contact with the (100)
surface exceeded 40 or the limits of measurement of the appara-
tus, but in table VIII the friction coefficient for the (111) surface
sliding on itself achieved a value of only 21. It may be assumed
that the (100) surface is undergoing the greatest degree of defor-
mation at the interface, with sliding accounting for the greater

degree of true contact area between the two surfaces, and conse-
quently the higher friction coefficient in table IX than that ob-
served in table VIII.

Adhesion coefficients measured after the sliding experiment
ceased, indicated that the adhesion forces for the dissimilar
orientations in contact were lower than for the matched planes in
contact. These results agree with the initial adhesion coeffi-
cients obtained before sliding. The results of table VIII and IX
indicate that very high adhesion and friction forces can be meas-
ured between like metals in contact when the lattices and orienta-
tions are very nearly the same. With dissimilar orientations in
contact, analogous to the grain-boundary situations in bulk mate-
rials, the adhesion and friction forces are less than where the
atomic planes and directions are matched across the interface.
The farther one goes from the ideal matching of lattices, planes,
and directions across an interface, the greater might be the an-
ticipated dissimilarities at an interface of two solid surfaces in
contact, and the lower might be the anticipated adhesion and
friction forces. Thus, it might be expected that, for dissimilar
metals in contact, adhesion and the friction forces would be less
than like metal surfaces in contact.

DISSIMILAR METAL CRYSTALS IN CONTACT

In order to establish if, in fact, such is the case, experi-
ments have been conducted for copper in contact with other met-
als. Results obtained in such adhesion and friction experiments
are presented in table X where the high atomic density planes of
each metal under consideration was brought into contact with the
high atomic density (111) plane of copper. Adhesion and friction
forces were measured for copper in contact with nickel, with
cobalt, and with tungsten. Nickel is a face-centered-cubic metal
like copper, cobalt a hexagonal metal, and tungsten a body-
centered-cubic metal. The adhesion coefficients measured be-
fore the initiation of sliding for these various metal couples in
contact together with that for the copper (111) surface in contact
with itself are presented in table X.

TABLE X. - ADHESION AND FRICTION COEFFICIENTS FOR VARIOUS
SINGLE-CRYSTAL METAL COUPLES

[Load, 50 g (0.5 N); ambient pressure, 10^{-11} torr; sliding velocity, 0.001 cm/sec; sliding distance, 0.735 cm.]

Metal couples and orientations	Crystal structure	Adhesion coefficient before sliding	Friction coefficient during sliding	Adhesion coefficient after sliding	Solubility
Copper (111) on Copper (111)	Face-centered cubic on face-centered cubic	0.30	21.0	10.5	Complete
Copper (111)[110] on Nickel (111) [110]	Face-centered cubic on face-centered cubic	.25	4.0	2.0	Complete
Copper (111)[110] on Cobalt (0001)[1120]	Face-centered cubic on hexagonal	.10	2.00	.5	Partial
Copper (111)[110] on Tungsten (110)[111]	Face-centered cubic on body-centered cubic	$<.05$	1.40	.5	None

Table X shows that, for copper in contact with other metals, the adhesive forces are less than for the copper in contact with itself. The highest adhesive force for dissimilar metals in contact was measured for the copper in contact with nickel where the metals are completely soluble; that is, copper is completely soluble in nickel. The next highest adhesion coefficient was measured for copper in contact with cobalt where there is partial solubility of the metals one to another.

A number of investigators have indicated that solubility exhibits an influence on the adhesive behavior of solid surfaces in contact (e.g., ref. 68). These results would seem to indicate that solubility may have some influence on adhesive forces. The difficulty is that the crystal structure is also different in the data of table X. Cobalt is a hexagonal metal, but nickel is a face-centered cubic metal.

With copper in contact with tungsten, the lowest adhesion coefficient was measured. The adhesion coefficient was less than 0.05. The friction coefficients for the dissimilar metal couples in sliding contact were considerably lower than for copper (111) surface in sliding contact with itself or for dissimilar copper atomic planes in sliding contact (table IX). Note that the couple copper-tungsten, which exhibited the lowest adhesion coefficient, also exhibited the lowest friction coefficient during sliding. Sliding was terminated at a distance of 0.735 centimeter, and the forces of adhesion of the two surfaces in contact were measured. The adhesion coefficients are presented in table X.

For the dissimilar metals in contact, the adhesive force or the adhesion coefficient increased over the value observed before sliding began. This increase was due, as mentioned earlier, to an increase in the true contact area at the interface as a result of junctions growth which occurs during the sliding process. Figure 26 presents photographs of the nickel, cobalt, and tungsten surfaces after sliding in contact with the copper (111) plane. Examination of figure 26(a) for the copper sliding on nickel revealed that the transfer of copper to the nickel (111) surface as a result of adhesion. Shear occurred in the cohesively weaker of the two
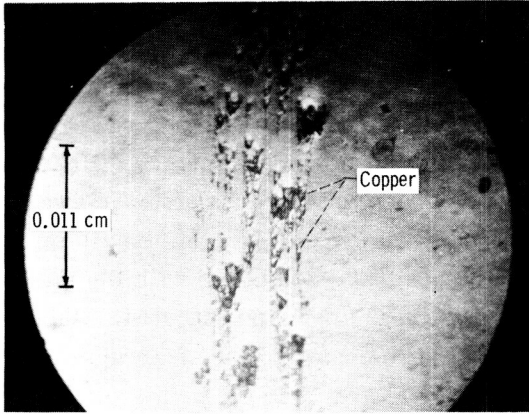
(a) Nickel, (111) plane.
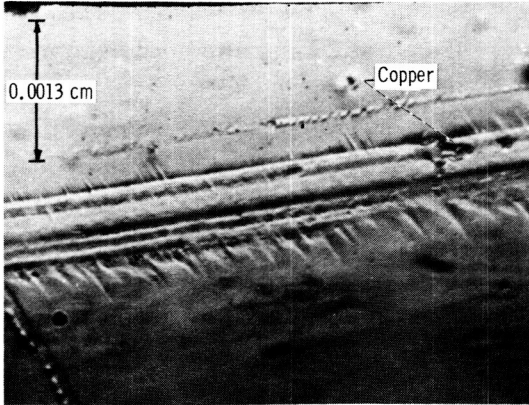
(b) Cobalt, (0001) plane.
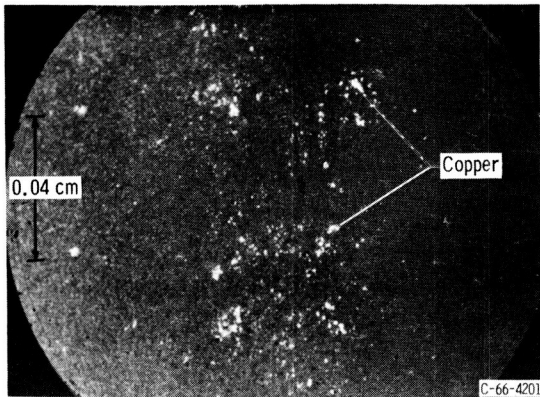
(c) Tungsten, (110) plane.

Figure 26. - Wear tracks for (111) plane of copper sliding in the
$[110]$ slip direction on various substrates in vacuum.

materials, in this case, copper. The adhesive junction between the copper and nickel was stronger than the cohesive junction in the copper. This mechanism of fracture was discussed earlier.

With the cobalt in sliding contact with copper, copper was also found to transfer to the cobalt surface. Here, however, the amount of copper present on the cobalt surface was relatively small as indicated by figure 26(b). This small amount of copper transferred to the cobalt as compared with the nickel indicates that the bonds between the copper and cobalt, which may have occurred on solid-state contact, were fracturing with sliding primarily at the interface. Note the relatively large area in contact by the width of the track and relatively small amount of copper transferred as indicated by the leader. The cobalt deformed along the track edges to form the slip bonds shown in the photograph.

Copper and tungsten are mutually insoluble. Despite this, copper transferred to the tungsten surface as indicated in figure 26(c). Again, shear appears with tangential sliding to have occurred in the cohesively weaker of the two materials, namely, copper. Note that the presence of copper on the tungsten surface indicates that the cohesive bonds in the copper were weaker where fracture occurred than the adhesive bonds of the copper to the tungsten surface. Taylor (ref. 69) has indicated in LEED studies the possibility of the formation of an intermetallic compound between copper and tungsten. The transfer of copper to the tungsten surface warns against using bulk materials properties such as solid solubility to predict surface behavior.

The surface of a metal can behave entirely differently from the material in the bulk. For example, the (111) surface in the face-centered-cubic system has an atomic coordination number of 9; whereas an atom in the bulk of the face-centered-cubic material has a coordination number of 12. The surface has a strong tendency to interact with other solids. Further, the surface itself, that is, the outermost atomic layer, because of a lower coordination number, is more prone to deformation than are atomic layers in the bulk lattice. Surface behavior, therefore, cannot be predicted on the behavior of bulk material properties.
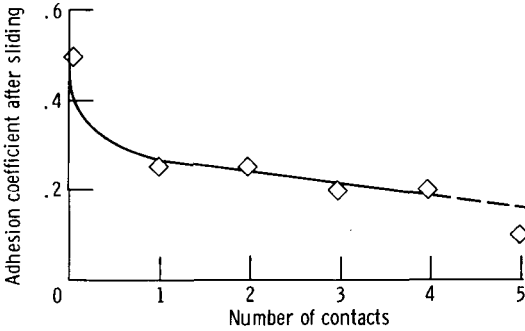
Figure 27. - Copper ((111) plane) sliding on single-crystal tungsten in vacuum (10^{-11} torr). Sliding velocity, 0.001 centimeter per second.

The force to fracture the adhesive junctions between two dis-
similar surfaces in contact is influenced by the amount of defor-
mation that has taken place in those surfaces. The data of fig-
ure 27 are a plot of the adhesion coefficient for copper sliding
in contact with tungsten. The contact was made in the same area
each time, and the adhesion coefficient is a function of the total
number of contacts. As the number of contacts increase, the
adhesion coefficient decreases. This results because with each
subsequent contact a greater amount of dislocations are intro-
duced into the surficial layer of copper. Increasing the number
of defects in the surficial layer of copper by repeated contacts
will promote the fracture of the adhesive junction between the
copper and the tungsten. The data of figure 27 reflect this effect.

INFLUENCE OF CRYSTAL STRUCTURE

Once atomically clean metal surfaces have been generated in
an ultrahigh vacuum environment, it is possible to measure the
influence of various physical properties on the adhesion and fric-
tion behavior of the metals in contact. The ability of surfaces to
deform plastically exhibits a marked influence on friction behav-
ior as well as adhesion since it influences the true contact area.
Further, friction is affected by the shear behavior of materials
in contact. It might therefore be anticipated that crystal struc-

ture would exhibit an influence on adhesion and friction. Crys-
tal structure is expected to have an influence on adhesion and
friction because the number of operable slip systems present in
the various crystal structures which characterize metals of the
periodic table vary. With face-centered-cubic metals there are
typically 12 operable slip systems. Body-centered-cubic metals
have 48. With hexagonal metals, however, there are only three
operable slip systems. Thus, hexagonal metals exhibit a mark-
edly smaller tendency to deform plastically than do the face-
centered-cubic and body-centered-cubic metals. For example,
hexagonal metals such as beryllium are relatively brittle and
they deform plastically only with difficulty. Further, hexagonal
metals are extremely prone to texturing. Their surface layers
can, with mechanical deformation of the surface by such opera-
tions as rolling or drawing, develop preferred surface orienta-
tions. There is no reason why similar texturing should not occur
for hexagonal metals during sliding or rubbing contact. With
such sliding and texturing, the basal or easy shear planes of the
hexagonal metals should be nearly parallel to the sliding inter-
face giving rise to relatively low forces of shear with the tangen-
tial motion of one surface over another.

The limited slip behavior in the hexagonal metals coupled
with this tendency to texture would, therefore, seem to indicate
that the hexagonal metals might well exhibit lower friction and
adhesion behavior than either body- or face-centered-cubic met-
als. Some adhesion and friction experiments have been con-
ducted with cobalt crystals of the basal orientation in contact with
themselves; these results can be compared with results obtained
for copper in contact with itself. The data of table XI indicate
that the adhesion coefficient for cobalt in contact with itself is
markedly less than that for copper in contact with itself. In both
cases the atomic planes in question are the lowest surface energy
planes of each of the respective crystal systems. The friction
force measured during sliding is markedly less for cobalt in con-
tact with cobalt than it is for copper in contact with copper. The
difference in adhesion coefficient before sliding under equivalent

TABLE XI. - COEFFICIENTS OF ADHESION AND FRICTION

FOR COPPER (99. 999 PERCENT) AND COBALT

(99. 99 PERCENT) SINGLE CRYSTALS

IN VACUUM (10^{-11} TORR)

[Load, 50 g (0. 5 N); ambient temperature, 20° C (293 K).]

Metal couples (matched poles)	Adhesion co-efficient be-fore sliding	Friction co-efficient dur-ing sliding	Adhesion co-efficient after sliding
Cu(111)[110] on Cu(111)[110]	0. 30	21. 00	10. 50
Co(0001)[11$\bar{2}$0] on Co(0001)[11$\bar{2}$0]	<.05	. 35	<. 05

loads as well as the difference in friction coefficient can be at-tributed to the differences in slip behavior for the hexagonal and cubic metals.

Cobalt. - It is interesting to note that the adhesion coeffi-cient after sliding ceased for cobalt in contact with itself was not greater than it was before sliding contact. The adhesion coeffi-cient in both instances was less than 0. 05. These results would indicate that the amount of junction growth for cobalt in sliding contact with cobalt is relatively nil and that the friction coeffi-cient as well as the adhesion coefficient for metals in contact may be dependent on crystal structure.

Cobalt is a hexagonal metal that exhibits a crystal transfor-mation. At approximately 420° C (693 K) cobalt will transform from the close-packed hexagonal to a face-centered-cubic struc-ture. It might be anticipated then, if in fact crystal structure does exhibit an influence on friction behavior, that, with crys-tal transformation, an increase in friction should occur. This should be expected because the number of operable slip systems will increase from three systems associated with the close-packed hexagonal form of cobalt to the 12 slip systems operable with the face-centered-cubic form.

Friction coefficients have been measured for cobalt at

various temperatures. The data of figure 28 were obtained for polycrystalline cobalt sliding on itself. In figure 28 the coefficient of friction for cobalt is plotted as a function of the slider temperature. At temperatures up to 300° C (573 K) the coefficient of friction for cobalt was approximately 0.35. At temperatures above 300° C (573 K), however, the friction coefficient began to increase, and it increased continuously with temperature until complete welding of the cobalt occurred, indicating very strong adhesion between the cobalt surfaces. If the bonds were broken (i.e., if the specimens were fractured), separated, and the specimens allowed to cool to room temperature such that the crystal transformation from the face-centered cubic to the close-packed hexagonal was again passed through, the cooling being accomplished in a vacuum, the friction force returned to the low value initially obtained with cobalt at room temperature in its hexagonal form.
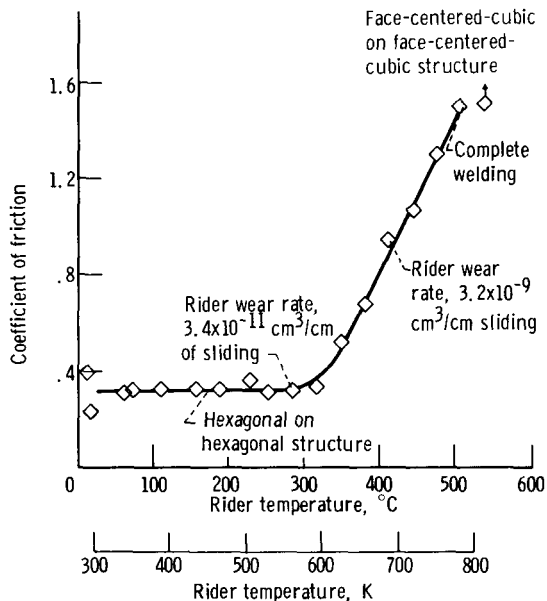

Figure 28. - Coefficient of friction at various ambient temperatures for cobalt sliding on cobalt in vacuum (10^{-9} to 10^{-7} torr). Sliding velocity, 197 centimeter per second; load, 1000 grams (9.8 N).

Not only did the friction increase markedly at temperatures above 300° C (573 K), but also the rate of adhesive wear. Wear measurements made at 300° C (573 K) indicated a wear rate of 3.4×10^{-11} cubic centimeter of wear material per centimeter in sliding; whereas, at 400° C (693 K) the wear rate was 3.2×10^{-9} cubic centimeter of wear material per centimeter of sliding. This is an approximately hundredfold increase in the rate of wear with the transformation of cobalt from close-packed hexagonal to the face-centered-cubic form.

It was mentioned earlier that the crystal transformation for cobalt from the close-packed hexagonal to the face-centered-cubic form occurs at a temperature of approximately 420° C (693 K). The data of figure 28 indicate an increase in friction coefficient at temperatures above 300° C (573 K). The difference in the temperature at which friction begins to increase in figure 28 and the actual transformation temperature of 420° C (693 K) is due to frictional heating at the interface. During the sliding process, considerable heat is generated at the sliding interface itself.

Thallium. - There are other hexagonal metals that exhibit crystal transformations. For example, thallium transforms from the close-packed hexagonal to the body-centered-cubic structure at 230° C (503 K). Sliding friction experiments conducted with thallium indicate that the friction coefficient increases markedly on crystal transformation from the close-packed hexagonal to the body-centered-cubic form.

Rare earth elements. - There are a number of the rare earth metals that exhibit a hexagonal crystal structure. Many of these undergo crystal transformations to other crystalline forms. Lanthanum, for example, transforms from the close-packed hexagonal to a face-centered-cubic form. Neodymium from a close-packed hexagonal to body-centered-cubic form. Praseodymium, cerium, samarium, and thulium all undergo, at some temperature, crystal transformations from a hexagonal to an either body- or face-centered-cubic structure (refs. 70 and 71). Bridgeman (ref. 72) has shown that the rare earth metal lanthanum can be induced to transform from the hexagonal to the

face-centered-cubic structure by means other than simply tem-
perature. High pressures, for example, can bring about the
crystal transformation from the hexagonal to the face-centered-
cubic form.

Sliding friction experiments have been conducted in vacuum
with lanthanum (ref. 73). In some experiments the specimen
temperatures were changed. It was observed that, as the crystal
transformation temperature (260° C or 533 K) was approached,
a marked increase in friction coefficient for lanthanum was noted.
Ultimately, at temperatures above 260° C (533 K) complete weld-
ing of the surfaces took place. This same crystal transforma-
tion could be brought about in a sliding process by holding the
ambient temperature constant and by simply increasing the load
on the specimens in contact or increasing the sliding speed for
surfaces in sliding contact. Both increasing the load and in-
creasing the sliding velocity will bring about an increase in in-
terfacial temperatures between the two surfaces in contact and
induce the crystal transformation to occur. In both types of slid-
ing friction experiments, in those where the load was changed
and in those where the sliding velocity was increased, the crystal
transformation was reflected by increase in friction just as it
was by changing temperature.

Not only are the friction properties of lanthanum markedly
influenced by the crystal transformation from the hexagonal to
the face-centered-cubic form, but also the wear behavior of
lanthanum is also strikingly different. Figure 29 shows two
440-C stainless-steel-disk surfaces which have been run in con-
tact with lanthanum sliders. The specimen in figure 29(a) shows
the transferred lanthanum when it was in the face-centered-cubic
form. Considerable adhesion and transfer of the lanthanum to
the 440-C surface occurred, with shear taking place in the lan-
thanum. In figure 29(b) the lanthanum was in the hexagonal form
when sliding on 440-C stainless steel, and the amount of trans-
fer of material from the lanthanum rider to the 440-C stainless-
steel-disk surface was appreciably less. In both instances ad-
hesion of the lanthanum in vacuum to the 440-C stainless-steel
surface occurs. With sliding in the cubic form, however, the
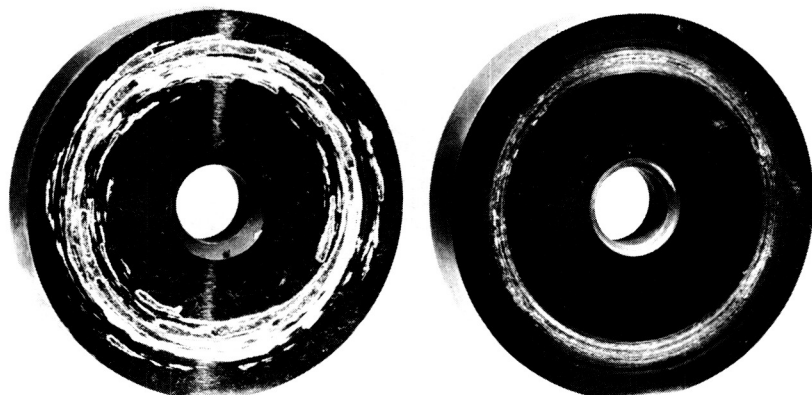
CS-33642

(a) Sliding with cubic form.   (b) Sliding with hexagonal form.

Figure 29. - 440-C stainless steel disk specimens. Rider specimen,, lanthanum; load, 100 grams (9.8 N); ambient pressure, 10^{-9} torr; ambient temperature, 20° C (293 K); duration of experiment, 1 hour.

multiple slip systems give rise to rapid generation of subsurface defects in the lanthanum, promoting subsurface fracture and the transfer of large particles of material to the 440-C stainless-steel surface.

With the hexagonal form of lanthanum sliding on 440-C stainless-steel, adhesion also occurred. But with repeated sliding over the same surface, preferred orientation or texturing of the hexagonal form occurred at the interface very rapidly. This results essentially from the tangential motion in the circumferential path on the disk surface in the shear taking place along basal planes. Since shear is restricted to the basal planes, repeated shear may occur in the same planes at the interface. With the face-centered-cubic form, however, dislocation interactions, as a result of the intersection of the multiple $\{111\}$ slip planes, give rise to the subsurface shear and fracture. With the hexagonal form, even though adhesion on an atomic basis of the lanthanum to the 440-C surface would occur, with the development of a thin transfer film of lanthanum to the 440-C, lanthanum will ultimately be sliding on lanthanum with shear taking place only in a thin film at the interface.

This situation is analogous to the behavior of placing a basal shearing solid lubricant at the surface. With very thin films of solid lubricant such as graphite or molybdenum disulfide, repeated shear can occur at the interface in the very thin film resulting in very little wear to the two mechanical components in contact. In figure 29(b) there is an analogous situation.

In table XII wear rates for various rider materials are presented. The sliders, lanthanum, samarium, and 440-C stainless steel, all contacted a 440-C stainless-steel flat surface. Sliding was on the flat surface in a circumferential path. An examination of table XII indicates that the rider wear rate for lanthanum in hexagonal form is considerably less than for lanthanum in the face-centered-cubic form. Comparing the data of table XII with the surfaces produced for the hexagonal and cubic forms of lanthanum sliding on 440-C stainless steel (fig. 29), the wear results are as one might anticipate.

Samarium is another hexagonal metal of the rare earth series. Its structure, however, is abnormal. In the normal hexagonal metal, the stacking sequence of atomic planes is A B A. In samarium the stacking sequence is A B A B C B C A C A. The C-axis lattice constant of this particular form of a hexagonal metal is $4\frac{1}{2}$ times that of the normal hexagonal structure and has been termed by some as a rhombohedral structure. Very little information is available on the slip behavior or deformation prop-

TABLE XII. - WEAR FOR VARIOUS RIDER MATERIALS

[Sliding against 440-C stainless steel; load, 1000 g
(9.8 N); ambient pressure, 10^{-9} torr; duration
of experiment, 1 hr.]

Rider material	Hardness (DPH)	Crystal structure	Rider wear rate, $cm^3/$ cm sliding
Lanthanum	40	Hexagonal	6.08×10^{-10}
		Face centered cubic	2.83×10^{-9}
Samarium	45	Hexagonal	2.62×10^{-10}
440-C stainless steel	600	Cubic	2.09×10^{-9}

erties of samarium.   The wear data of table XII indicate that
samarium exhibits a relatively low wear rate even when com-
pared with lanthanum in its hexagonal form.

The slider wear for 440-C stainless steel in contact with
the 440-C stainless-steel flat surface is also presented in ta-
ble XII to serve as a point of reference.   This steel is a com-
monly used bearing material in vacuum applications.   Table XII
shows that the wear rate for the hexagonal form of lanthanum is
appreciably less than the wear rate for the face-centered-cubic
form.   Further, both lanthanum and samarium in the hexagonal
forms exhibited lower wear rates than did the commonly used
bearing material 440-C stainless steel.

A rare earth metal that is relatively unusual with respect
to crystal transformation is cerium.   Cerium metal undergoes
three crystal transformations over the temperature range of
from -195° to 730° C (78 to 1003 K).   Below -195° C (78 K),
cerium is in a face-centered-cubic form.   At -195° C (78 K)
cerium transforms to a close-packed hexagonal structure.   At
a -73° C (200 K) cerium undergoes another crystal transforma-
tion from the close-packed hexagonal structure to a face-
centered-cubic structure.   At 730° C (1003 K) cerium transforms
from the face-centered-cubic structure to a body-centered-cubic
form (refs. 70 and 71).   Sliding friction experiments with cer-
ium at cryogenic temperatures indicated a relatively high fric-
tion coefficient for the low-temperature face-centered-cubic
form of cerium.   On transformation at -195° C (78 K) from the
face-centered-cubic to the close-packed hexagonal form, the
friction coefficient of cerium decreased and remained low to
temperatures near -70° C (203 K) at which time the cerium in-
creased in friction coefficient.   This increase occurred with the
crystal transformation to the face-centered-cubic structure.
Continuous heating of the surface resulted in continuous high-
friction measurements, and, at temperatures above 730° C
(1003 K) where the transformation of cerium from the face-
centered-cubic form to the body-centered-cubic form occurred,
no marked change in friction behavior was observed.

In general, at temperatures below and above 730° C (1003 K)

the friction coefficient for cerium was approximately $2\frac{1}{2}$ times
what it was when it existed in the close-packed hexagonal form
(between -195° and -73° C (78 and 200 K)). The cerium results
indicate further the marked influence of crystal structure on the
friction behavior of metals and also the sensitivity of friction
coefficient to crystal transformations.

  Lattice ratio. - The deformation characteristics of hexa-
gonal metals are somewhat related to their lattice parameters.
Hexagonal metals exhibiting near ideal atomic stacking, that is,
with c/a lattice ratios near 1.633, exhibit generally predom-
inantly basal slip in deformation at 20° C (293 K). One notable
exception is beryllium which exhibits basal slip and has a c/a
lattice ratio of only 1.57. Those hexagonal metals that have lat-
tice ratios less than 1.60 generally slip predominantly on non-
basal planes. Metals that exhibit primarily nonbasal slip be-
havior are titanium, zirconium, hafnium, erbium, and gado-
linium. These hexagonal metals generally slip primarily on
prismatic and pyramidal slip planes.

  With nonbasal slip predominating, a greater number of slip
systems can become operable in deformation. This can for two
surfaces in solid contact give rise to a greater true contact area
in deformation and, in sliding contact, to work hardening and a
resistance to shear because of intersection of slip plane disloca-
tions. With those hexagonal metals exhibiting predominately
basal slip behavior, this dislocation coalescence on slip planes
and its interaction is not readily achieved. The dislocations with
shear can simply pass out of the surface. It might be said that
those hexagonal metals that exhibit nonbasal slip behavior tend
to act more as cubic metals than as hexagonal metals in the sense
that they tend to deform more readily than those exhibiting pre-
dominantly basal slip mechanisms.

  From the foregoing discussion some relation between the
lattice parameters c/a lattice ratio for hexagonal metals, to
their friction properties might be expected to exist. Friction
measurements made of a number of hexagonal metals indicate
that it does. The friction data obtained for various hexagonal

metals sliding against 440-C surface in a vacuum environment
are presented in figure 30.   These data indicate that there is, in
fact, a relation between the lattice parameters of the hexagonal
metals and their friction coefficients.   Those hexagonal metals
exhibiting the near ideal stacking ratio of 1. 633 have lower fric-
tion coefficients than those exhibiting predominantly prismatic
and pyramidal slip, such as zirconium and hafnium.   Note in fig-
ure 30 that beryllium does not fall on the curve.   The friction co-
efficient is slightly above 0. 4.   As was mentioned earlier, beryl-
lium slips primarily on basal planes much like those hexagonal
metals that exhibit the near ideal stacking ratio.   As a conse-
quence, its friction properties are lower than other hexagonal
metals having a similar lattice ratio.   Titanium, which slips
predominantly on $\{10\bar{1}0\}$ slip planes, exhibits extremely high
friction coefficients in vacuum.   Similar high-friction results
are obtained for titanium in air in the presence of surface oxides.
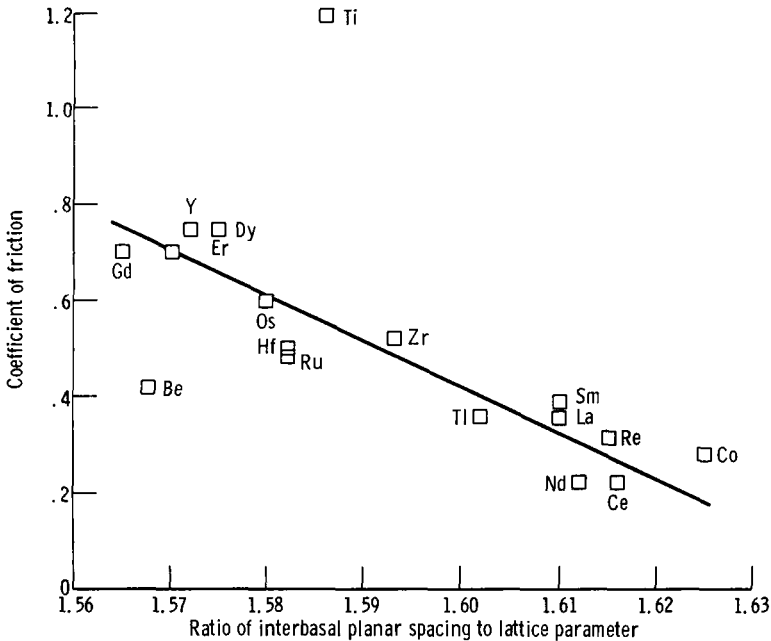
Figure 30. - Friction coefficients for various hexagonal metals sliding on 440-C in
vacuum (10^{-9} to 10^{-11} torr). Sliding velocity, 200 centimeters per second; load,
1000 grams (9. 8 N); no external heating.

If the lattice ratio has an influence on the friction behavior of hexagonal metals and their frictional properties, then it might be anticipated that the change in the c/a lattice ratio of hexagonal metals should result in a change in their friction behavior based on the data presented in figure 30. Titanium is a notoriously poor friction material in both an air environment and in vacuum. The poor friction properties of titanium in vacuum are demonstrated by the data of figure 30.

Titanium was alloyed with aluminum and tin. The additions of both aluminum and tin expanded the lattice ratio for titanium toward that of the ideal stacking ratio of 1.633 (see fig. 31). The additions of aluminum or tin to titanium expand the crystal lattice, and with this expansion in crystal lattice a decrease in friction coefficient is observed (fig. 31). These data coupled
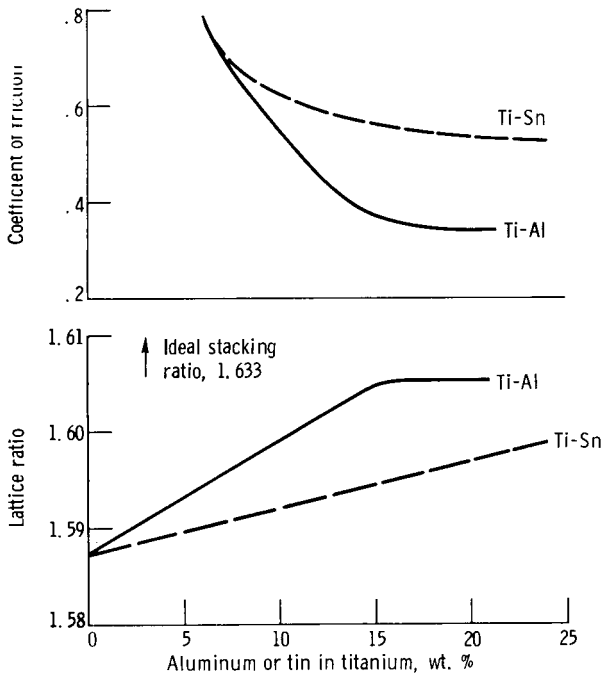
Figure 31. - Influence of aluminum and tin on friction and lattice ratio characteristics for titanium sliding on 440-C stainless steel in vacuum (10^{-9} torr). Sliding velocity, 197 centimeters per second; load, 1000 grams (9.8 N); no external heating.

with those of figure 30 indicate the dependence of the friction properties of hexagonal metals on lattice parameters and slip behavior.

Magnesium. - An interesting hexagonal metal with respect to slip behavior is magnesium. Magnesium exhibits primarily basal slip near and below room temperature. At temperatures above 20° C (293 K), however, magnesium deforms primarily by nonbasal slip mechanisms on the $\{1011\}$, $\{1012\}$, and $\{1010\}$ planes. Deformation experiments at temperatures from -195° to -200° C (78 to 73 K) indicate that ductility of magnesium is markedly dependent on its slip behavior. When primarily basal slip mechanisms operate, the ductility of magnesium is very low as indicated by the data presented in figure 32. The ductility of magnesium increases, however, with increase in temperature and an increase in the operation of nonbasal slip planes. The variation of slip behavior for magnesium has been described early in the literature (refs. 74 to 76). The low ductility of magnesium at temperatures below 20° C is attributed to the operation of only the three slip systems associated with basal slip in the magnesium.

Friction data obtained for magnesium at various temperatures in a vacuum environment are also presented in figure 32. It is interesting to compare the friction curve as a function of temperature with that of ductility of magnesium (fig. 32). Both friction and ductility increase with increasing temperatures and increase in the number of operating slip systems in the hexagonal metal magnesium. The friction coefficients presented in figure 32 for magnesium were obtained after a number of repeated passes were accomplished over the same surface (ref. 77). They represent an average friction coefficient at each of the temperatures after a steady state of friction was achieved.

Normally, the initial friction coefficients for metal surfaces in contact can be considerably different from the friction coefficients measured after sliding has occurred repeatedly over the same surface. There are many factors that can account for changes in friction coefficient with repeated sliding or passing over the same surface. A considerable amount of energy is put
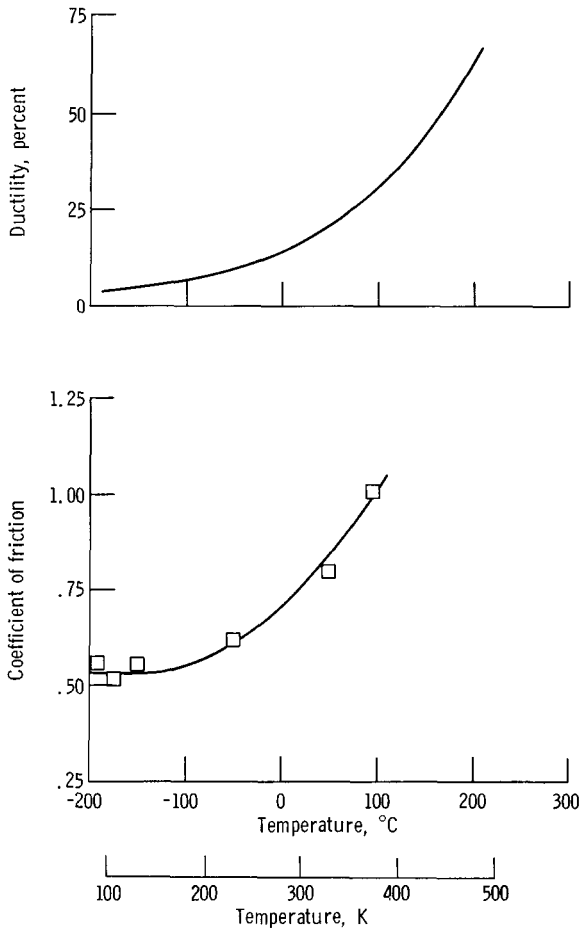
Figure 32. - Ductility and coefficient of friction for poly-
crystalline magnesium. Sliding velocity, 0.001 centi-
meter per second; ambient pressure, 10^{-10} torr; load,
50 grams (0.5 N).

into the surfaces in the process of sliding or rubbing contact.
This energy can be dissipated in the form of heat generated at
the interface, with the heat being transferred into the surficial
layers of the two solid surfaces.   If the heating is sufficiently
high at the interface, it can produce localized recrystallization
of the surface where the recrystallization temperatures of the
metal surfaces in contact are relatively low.   Further, the ex-
treme pressures at the real points of contact, or in the real con-

tact area, for the metals in solid contact can give rise with slid-
ing to development of surface texturing much as occurs in rolling
or drawing of metal surfaces.

Magnesium has a relatively low recrystallization tempera-
ture. It might, therefore, be anticipated that recrystallization
in magnesium could occur at relatively low temperatures in a
sliding process, temperatures considerably below the ambient
temperature. It will be recalled that very high interface temper-
atures can be generated as a result of the sliding process. Fric-
tion data are presented for polycrystalline magnesium sliding on
itself in a vacuum environment (10^{-10} torr) at various tempera-
tures (see fig. 33). The sliding velocity was extremely low,
only 0.001 centimeter per second. The load for a hemisphere
contacting a flat was only 50 grams (0.49 N). And the friction
coefficient is plotted in figure 33 as a function of the number of
passes over the same surface. There are three sets of data

Figure 33. - Coefficient of friction for polycrystalline magnesium sliding on polycrystalline
magnesium in vacuum at various temperatures. Sliding velocity, 0.001 centimeter per
second; load, 50 gram (0.5 N); ambient pressure, 10^{-10} torr.

presented in figure 33: one set of data obtained at -190° C (83 K),
a set at 25° C (298 K), and a set at 90° (363 K).

At -195° C (78 K) the friction coefficient in figure 33 does
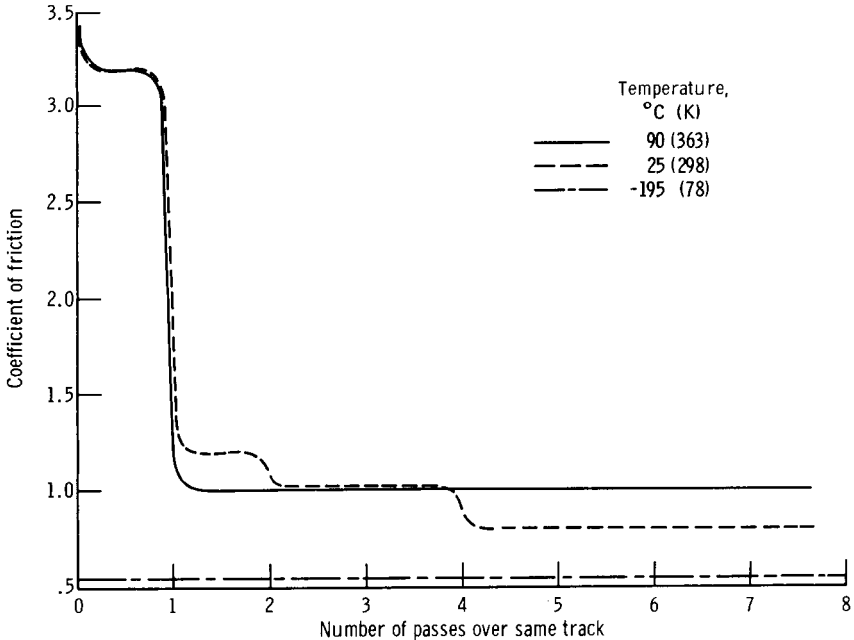not change with repeated passes (eight passes) over the same
surface. But when the specimen surfaces are allowed to heat
to 25° C, the friction coefficient in the first pass is extremely
high, in excess of 3.0. In the second pass over the same sur-
face the friction coefficient decreased to a value of approximately
1.30. With a completion of four passes over the same surface
the friction coefficient decreased to a value of less than 1.0.
This stepwise decrease in friction coefficient with repeated num-
ber of passes over the same surface reflects an effect of re-
crystallization and texturing of the magnesium surface with
sliding. If the temperature is increased further from 25° to
90° C (298 to 363 K), the friction coefficient starts out at the
same initial high value as at 25° C (298 K) because of the random
orientation of the polycrystalline surface and a random distribu-
tion of the crystal orientations on the surface with the first pass.
However, during the first pass across the surface, recrystalli-
zation and texturing of the surface takes place so that on the
second pass the friction coefficient has decreased from a value
of in excess of 3.0 to approximately 1.0. The friction remained
at that value for the rest of the passes over the same surface.
Note in figure 33 that this recrystallization and texturing oc-
curred in only a single pass at 90° C (363 K) but at 25° C (298 K),
four passes were necessary before an equilibrium friction value
was achieved.

At -195° C (78 K) the friction coefficient was relatively low,
0.5. At this temperature, magnesium exhibits predominantly
the basal slip mechanism. No change was observed in friction
coefficient with repeated passes on the surface. The surface
examined at -195° C (78 K) was run at 25° C (298 K) for a per-
iod of time before the reduction of temperature to develop a
surface texture. Thus, the friction coefficients obtained at
-195° C (78 K) reflect the friction associated with the basal slip
mechanism. At 25° and 90° C (298 and 363 K) the surfaces were
electropolished, randomly oriented surfaces.

The high friction coefficients obtained in the initial pass are associated with the randomness of the orientation of the surface. With repeated passes, recrystallization and a development of a textured surface caused the friction coefficients to decrease. The friction coefficient at 90° C (363 K) was approximately twice that at -195° C (78 K). This difference in friction coefficient is attributed (as was pointed out in ref. 32) to a difference in the slip behavior of the hexagonal metal magnesium with temperature. At 90° C (363 K) prismatic and pyramidal slip systems are operating with the deformation of magnesium accounting for the higher friction coefficient observed at this temperature.

RECRYSTALLIZATION AND TEXTURING

Recrystallization and texturing at a sliding or rubbing interface has been observed for a number of materials in contact. The combination of load applied to the two surfaces in contact, the sliding speed of the surfaces with respect to each other, and the frictional heat generated at the interface are sufficient to bring about recrystallization readily for a number of materials. Titanium, for example, normally has a recrystallization temperature of 900° C (1173 K). With deformation, however, this recrystallization temperature can be reduced to as low as 400° C (673 K). Sliding friction experiments indicate that recrystallization can occur for titanium in sliding contact with itself by simply varying the load applied to the two solid surfaces in contact.

In single-crystal titanium sliding friction experiments with the basal orientation parallel to the sliding interface in one set of experiments and with the prismatic orientation parallel to the sliding interface in a second set of experiments, differences in friction coefficients for the two orientations were observed. These differences are shown by the data of figure 34. The friction coefficient for the basal orientation was considerably higher than that for the prismatic orientation. With repeated cycling over the same surface, the friction coefficient increased and then reached some equilibrium value after approximately 10 minutes
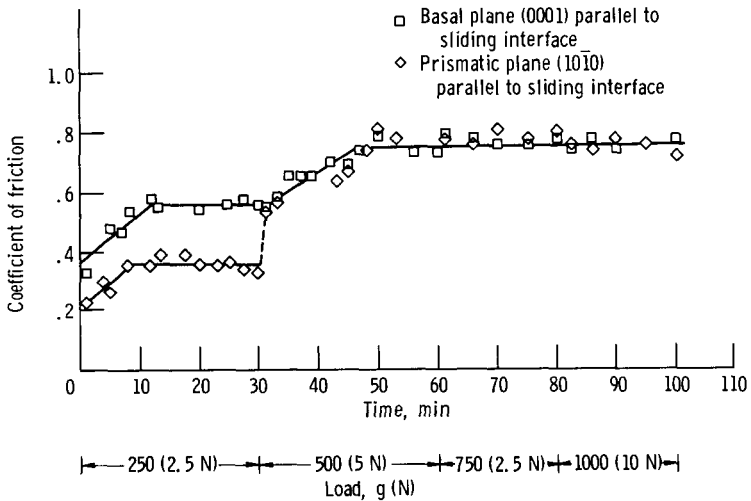
Figure 34. - Coefficient of friction for titanium single crystals (99. 99 percent pure) sliding on polycrystalline titanium. Sliding velocity, 2. 28 centimeters per second; ambient pressure, 10^{-9} torr; no external heating.

of sliding. After the 10 minutes of sliding, very little change in friction coefficient was observed. The load for this sliding experiment was 250 grams (2. 5 N) with a hemispherical rider in contact with a flat surface. If, however, after 30 minutes of sliding the load was increased from 250 to 500 grams (2. 5 to 5. 0 N), the friction coefficient for both orientations increased. The friction coefficients continued to increase with continued sliding for approximately 15 minutes of sliding. This increase in friction coefficient for the two orientations and the sameness in the friction coefficients for the two orientations at the 500-gram (5. 0-N) load were believed to be due to recrystallization and texturing of the surface.

After approximately 50 minutes of sliding, the friction coefficients remained relatively unchanged under the 500-gram (5. 0-N) load. Further increases in load to 750 and 1000 grams (7. 5 and 10 N) did not result in any further increase in friction coefficients at total sliding times to 100 minutes at a sliding velocity of 2. 28 centimeters per second. The equilibrium friction coefficient achieved after approximately 50 minutes of sliding represents the friction coefficient for a recrystallized, textured

titanium surface in sliding contact with itself. X-ray examina-
tion of the sliding surfaces after the completion of the sliding ex-
periments indicated, in fact, that the surfaces were textures and
had undergone recrystallization. The recrystallization process
introduced grain boundaries in the titanium surfaces which may
account for observed increase in friction coefficient (see fig. 34).
The friction values in figure 34 are much higher for the recrys-
tallized surface than they were for the single crystals of the
basal and prismatic orientation.

These results are somewhat different from those obtained
with magnesium in sliding contact with itself (fig. 33). In fig-
ure 33, however, experiments were started with a polycrys-
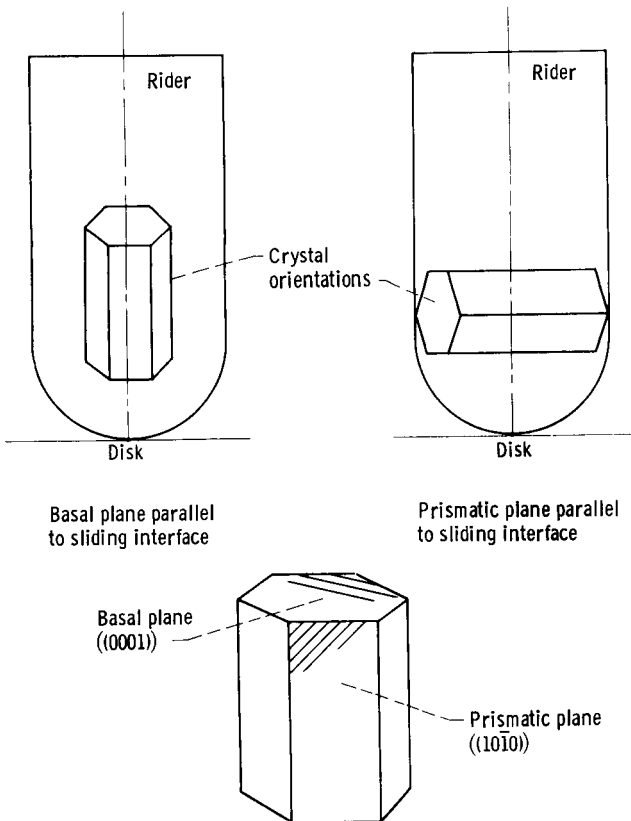
Figure 35. - Orientation of titanium single crystals for sliding in vacuum.

talline surface so the grain boundaries were already present before the recrystallization and texturing. There, a reduction in friction coefficient might be anticipated with texturing. In figure 34 the introduction of grain boundaries would be expected to result in an increase in the friction behavior of the materials in contact as observed. Because of the lattice stacking ratio for titanium, the prismatic planes in titanium are atomically denser than the basal planes. As a consequence, the titanium prismatic planes, namely, the $\{10\bar{1}0\}$ planes, are more resistant to deformation and exhibit higher hardnesses and lower friction coefficients than do the basal plane. As will be shown, this is the opposite of the result normally observed for more typical hexagonal metals.

The orientation of the titanium single crystals for the experimental resulted presented in figure 34 are shown in figure 35. For the basal orientation at the sliding interface, the basal plane of the rider specimen was oriented such that it was parallel to the sliding interface. For the prismatic orientation, the hexagonal crystal of titanium was oriented as indicated in the upper righthand drawing of figure 35.

ANISOTROPY

Hexagonal metals. - It is well known that hexagonal metals exhibit anisotropic deformation behavior (ref. 78). It is reasonable to assume, therefore, that friction properties of hexagonal metals would also be anisotropic. Friction experiments have been conducted with various hexagonal metals to determine the influence of orientation on the friction behavior. Some results on the influence of orientation on the friction properties of various hexagonal metals are presented in table XIII. Although these hexagonal metals, with the exception of titanium, exhibit primarily a basal slip mechanism at room temperature, the preferred slip direction is in the $\langle 11\bar{2}0 \rangle$ direction. Each of these metals has three operable slip systems. Titanium, however, slips predominantly on the $\{10\bar{1}0\}$ and $\{10\bar{1}1\}$ planes and in $\langle 11\bar{2}0 \rangle$ directions. As a consequence, titanium has nine pos-

TABLE XIII. - PROPERTIES OF VARIOUS HEXAGONAL METALS

Metal	Lattice ratio, c/a	Primary slip plane at 20° C (293 K)	Slip direction	Number of slip systems	Knoop hardness {0001}⟨11$\bar{2}$0⟩	Knoop hardness (10$\bar{1}$0)⟨11$\bar{2}$0⟩	Coefficient of friction[a] (0001) plane ⟨11$\bar{2}$0⟩	(0001) plane ⟨10$\bar{1}$0⟩	(10$\bar{1}$0) plane ⟨11$\bar{2}$0⟩	(10$\bar{1}$0) plane [0001]
Magnesium	1.624	(0001)	⟨11$\bar{2}$0⟩	3	23	13	0.40	----	0.90	----
Cobalt	1.624	→	→	→	---	180	.38	----	.80	---
Rhenium	1.615	→	→	→	250	50	.29	0.38	.50	0.80
Beryllium	1.568	{10$\bar{1}$0} {10$\bar{1}$1}	→	→	220	80	.48	.51	---	.70
Titanium	1.587		------	6	115	132	.56	----	.36	----

[a]Friction coefficients measured in vacuum (10^{-9} to 10^{-11} torr) with single-crystal rider sliding on polycrystalline disk of the same material.

sible operable slip systems.

Hardness measurements on the hexagonal metals exhibiting primarily the basal slip mechanism indicate that the hardness is greater on the basal planes than on the prismatic planes (see table XIII). With titanium, however, where the atomic packing is greater on the prismatic plane, the hardness also is greater on the prismatic plane.

Friction coefficients measured for the various hexagonal metals in sliding in a vacuum of 10^{-9} to 10^{-11} torr are presented in table XIII for the (0001) and $\{10\bar{1}0\}$ planes of the hexagonal metals. In the $\langle 11\bar{2}0 \rangle$ direction, where sliding is restricted to a particular crystallographic direction (i.e., $\langle 11\bar{2}0 \rangle$), the friction coefficient for those metals exhibiting predominantly basal slip was lower on the (0001) plane than on the $\{10\bar{1}0\}$ planes. With titanium, the friction coefficient, however, was lower on the prismatic $\{10\bar{1}0\}$ planes than it was on the basal (0001) plane. The friction results seem to agree with the hardness measurements, namely, that the friction coefficient and the hardness are highest on the highest atomic density plane for the hexagonal metals. With titanium, however, because of the short distance in spacing between the basal planes, the prismatic plane becomes fairly atomically dense, and as a consequence it exhibits a lower friction coefficient and a higher hardness than on its basal plane. The preferred crystallographic slip direction or the direction of shear for the basal plane is the $\langle 11\bar{2}0 \rangle$ direction. Examination of the friction coefficient on the (0001) plane in table XIII indicate that the friction coefficient was lower in the $\langle 11\bar{2}0 \rangle$ direction than it was in the $\langle 10\bar{1}0 \rangle$ direction. The friction coefficient is reflecting the necessary force required to shear at the interface with the basal planes of the hexagonal metals parallel to the interface. The results of table XIII indicate that it is easier to shear in the preferred crystallographic direction than it is to shear in the $\langle 10\bar{1}0 \rangle$ direction.

The data of table XIII indicate that, just as with other properties of the hexagonal metals, the friction behavior of hexagonal metals are highly anisotropic. Friction coefficients are sensitive not only to the atomic plane but also to crystallographic di-

rection.   The anisotropic friction behavior of face-centered-cubic metals was discussed earlier in reference to table VIII. Thus, the face-centered-cubic metals and the close-packed hexagonal metals exhibit a high degree of frictional anisotropy.

The three principal crystal structures for metals, are the face-centered cubic, the close-packed hexagonal, and the body-centered cubic.   The least anisotropic of these crystalline forms is the body-centered-cubic structure.   Further, of these, the body-centered-cubic metal that might be expected to exhibit the least degree of anisotropic behavior is tungsten (ref. 79).

Body-centered-cubic metals. - Friction experiments have been conducted to determine the influence of atomic orientation on the friction behavior of the body centered cubic metal tungsten in vacuum.   Friction results obtained for sapphire sliding on the (100) plane of tungsten in various crystallographic directions are presented in table XIV.   These data indicate both Knoop hardness and friction coefficients for three atomic directions on the (100) plane: $\langle 100 \rangle$, $\langle 120 \rangle$, and the $\langle 110 \rangle$.   The Knoop hardness was the greatest in the $\langle 100 \rangle$ direction, and the friction coefficient was least in this particular crystallographic direction with sliding.   In the $\langle 110 \rangle$ direction the Knoop hardness was least and friction greatest.   In the $\langle 100 \rangle$ direction, where the hardness is

TABLE XIV. - PROPERTIES OF BODY-

CENTERED-CUBIC METAL ATOMIC

PLANE (100) OF TUNGSTEN

[Sapphire rider; load, 500 g (0.5 N);
sliding velocity, 0.013 cm/sec;
ambient temperature, 20° C (293 K);
ambient pressure, 10^{-10} torr.]

Direction	Knoop hardness	Coefficient of friction
$\langle 100 \rangle$	420	0.70
$\langle 120 \rangle$	395	.98
$\langle 110 \rangle$	370	1.23

the greatest, the amount of deformation under load and the true
contact area would be expected to be less than in the $\langle 110 \rangle$ direc-
tion where the Knoop hardness is lower. As a consequence, the
true contact area would be greater as well as the friction coeffi-
cient being higher because of the increase in true contact area
with initial contact and with sliding.

The results given in table XIV indicate that even the least
anisotropic of the metal crystal systems, namely, the body-
centered-cubic system, exhibits anisotropic friction behavior
when the surfaces are examined in the absence of oxides and
other surface contaminants. These experiments were conducted
in a vacuum environment.

The discussion on frictional anisotropy thus far has covered
primarily single crystals in the face-centered-cubic, close-
packed hexagonal, and body-centered-cubic forms. What effect
does orientation have on the friction behavior of polycrystalline
metals? In most practical devices involving friction and wear,
the surfaces in contact are usually polycrystalline materials
rather than single crystals. Do polycrystals exhibit anisotropic
friction behavior just as do the single crystals? Friction experi-
ments have been conducted on the least anisotropic of the metal
systems, the body-centered-cubic metal tungsten, in the poly-
crystalline form to determine whether they do exhibit these same
properties.

A tungsten disk specimen was used in the friction experi-
ments. The tungsten disk had relatively large grains as shown
by figure 36, and contained only a total number of nine grains.
The orientations of each of the grains was determined by X-ray
diffraction, and the orientations are indicated in the unit triangle
in figure 36. A sapphire sphere with the $(10\overline{1}0)$ plane sliding in
contact with the tungsten surface did so near the circumferential
of the tungsten disk (fig. 36). The dashed line in figure 36 indi-
cates the orientations of each of the grains. The friction force
with sliding was continuously monitored. The sliding experiment
was conducted at low speeds so that the friction coefficient could
be monitored in each grain and with the change in crystallo-
graphic direction within the grain. Friction results obtained in

making one complete revolution around the disk surface with this
sapphire ball in both vacuum, with surfaces that had been
cleaned, and in air are presented in figure 36.   An examination
of figure 36(c) indicates that a simple change in crystallographic
direction within any one grain resulted in a change in friction
character observed with sliding.   These results are as might be
anticipated in light of the results obtained in table XIV.

The second observation to be made from figure 36(c) with
the sapphire sliding on the tungsten polycrystalline surface is
that, as grain boundaries were passed over and the slider moved
from one crystallographic slip system to another, the friction
coefficient changed considerably.   The relatively rapid changes
in friction coefficient (fig. 36) occurred as grain boundaries were
approached.   The grain boundaries are indicated in figure 36(c)
as the dashed lines running parallel to the ordinate.

When figure 36(c) is compared with figure 36(d) marked dif-
ferences in friction behavior are observed for sapphire sliding
on tungsten in vacuum at 10^{-10} torr and in air at 760 torr.   In
general, for nearly all orientations the friction level was lower
in air than it was in vacuum.   Thus, the first effect observed
is that the friction coefficient is appreciably reduced for the
various orientations.   The second observation is that the friction
behavior with oxides present may be entirely different from that
in the absence of the surface oxides.

The difference in friction behavior in any one grain in fig-
ure 36(d) from that in figure 36(c) is not simply one of lowering
the overall friction level but a difference in the character of the
friction trace with change in crystallographic direction.   In no
one grain is the shape of the friction trace the same in vacuum
and in air.   Thus, the effect of surface oxides is more than sim-
ply reducing the amount of adhesion that occurs at the interface
and the overall friction force level.   As has already been dis-
cussed in reference to table I, the kinetics of oxidation is a func-
tion of the orientations exposed.   The higher surface energy
planes may be expected to react more readily with oxygen to
form oxides than the less active lower surface energy atomic
planes in tungsten.   Not only will the atomic plane itself influ-

(a) Tungsten disk.

CD-8131

(b) Unit triangle.

Figure 36. - Coefficient of friction of sapphire (10$\bar{1}$0) plane sliding in 0001 direction on polycrystalline tungsten. Sliding velocity, 0.013 centimeter per second; load, 500 grams (4.9 N); ambient temperature, 20° C (293 K).
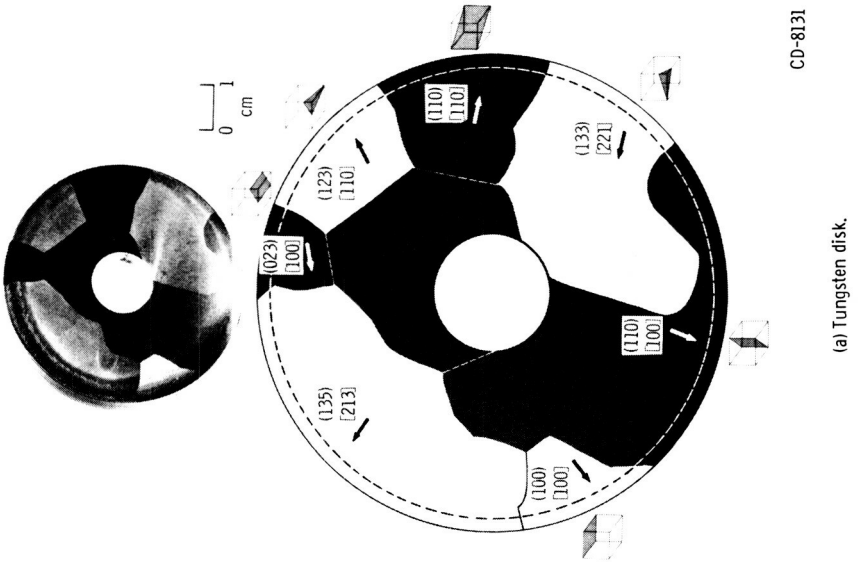
ence the amount and the nature of the oxide formed, but also on any particular plane the energy distribution on the plane will vary (ref. 80), and this certainly can be expected to influence the nature of the oxide on a particular atomic surface as well as friction.

In most practical engineering applications relatively small grain size metals and alloys are used. As a consequence, the difference in friction behavior observed with orientation may be much more subtle than was observed in the data of figure 36. None the less, even when the grain size is relatively small, if the relative motion between the two surfaces in contact is very slow, it is quite possible that in engineering applications differences in friction behavior may simply be due to a change in crystallographic orientation on the surface. Where the loads and surface speed are sufficiently high so that, after repeated passes over the same surface, a texturing or recrystallization followed by texturing of the surface has occurred, the effect of crystallographic orientation may be less pronounced. If however, an engineering application where experiments are conducted at relatively slow speeds and under light loads and where recrystallization or texturing does not occur, these effects may be observed.

Although orientation will influence the friction behavior of metals in a vacuum environment pronouncedly (see fig. 36(c)), friction is still influenced by orientation even in the presence of the normal surface films encountered in an air atmosphere as indicated by the data in figure 36(d).

Ionic solids. - Although metals are most frequently used in mechanical devices involving friction and wear, anisotropic friction behavior is not restricted to metals alone. Ionic solids such as aluminum oxide and covalent materials such as diamond also exhibit anisotropic friction behavior. Sapphire (single-crystal aluminum oxide) has a rhombohedral type of crystal structure. Its slip behavior with plastic deformation is very analogous to the hexagonal metals. Friction studies with the ionic solid aluminum oxide indicate that the friction coefficient is lower on the preferred slip or high atomic density plane, namely, the (0001)

plane. This plane is analogous to the basal plane in the hexagonal metals. Friction has been observed to be lower on (0001) plane than on the prismatic (10$\bar{1}$0) plane when sliding in the preferred $\langle 11\bar{2}0 \rangle$ crystallographic direction. Further simple changes in crystallographic direction on either of these two planes resulted in marked changes in friction behavior.

Bowden and Hanwell (refs. 81 and 82) have measured the friction of diamond in a vacuum environment. Diamond, the cohesively strongest material, exhibits an extreme sensitivity to the presence of the environment on its friction behavior. Bowden and Hanwell found that the friction coefficient for a {111} natural cleavage surface of diamond increased from 0.05 in air to 0.9 in a vacuum environment. The marked changes in friction coefficients were due to the removal of surface adsorbates from the diamond surface. As was discussed earlier, carbon might be anticipated to exhibit high adhesion forces and relatively high friction where the surfaces are clean and where carbon-to-carbon bonds can form across the interface. The earlier discussion in reference to diamond indicates that this is true for the diamond structure of carbon as well as for the graphitic form of carbon. Thus, adhesion is an important factor determining the friction of covalently bonded solids such as carbon whether in diamond or in graphite form. Both graphite and diamond exhibit this marked increase in friction behavior on removal of adsorbates from their surfaces.

Metal Alloys

The addition of alloying elements to metals can markedly alter their adhesion behavior. With clean elemental metals in sliding or rubbing contact, high friction coefficients and complete seizure has been observed by the authors of references 83 and 84 as well as the present author. When, however, complex alloys are examined in a sliding friction experiment in a vacuum environment, markedly varying results may be achieved. Some bearing alloys such as 52100 bearing steel when operated in a vacuum environment will undergo complete seizure as was

discussed in reference to figure 23. Other bearing alloys such
as 440-C stainless steel, however, do not cold weld as readily
in a vacuum environment. When the friction experiments are
conducted at the same environmental pressure level and the
cleaning procedures are the same for both surfaces, the question
may be posed as to what accounts for the fact that a 52100 bear-
ing steel will undergo a complete seizure in a vacuum environ-
ment while a 440-C bearing steel is much more resistant to such
seizure.

Equilibrium Segregation

The difference in the friction behavior for the two alloys in
the vacuum environment is not attributable to the environment
itself but rather to the nature or the composition of the alloy.
Alloying constituents can undergo equilibrium segregation of the
surface resulting in a concentration of an alloying element on the
surface far in excess of its concentration in the bulk. In steels,
for example, alloying elements such as carbon and sulphur have
been shown with the use of the Auger emission spectrometer to
concentrate on the surface (refs. 85 to 87).

This segregation of nonmetallic alloying elements on the
surface can reduce appreciably the adhesion between two metal-
lic surfaces and thereby reduce the friction in sliding or rubbing
contact. Figure 37 is an Auger emission spectrometer trace of
the electron energy distribution plotted as a function of electron
energy. The data of figure 37 indicate the presence of various
elements on an iron (001) surface after simple heating in a vac-
uum environment. The Auger trace shows the presence on the
surface of the elements sulphur, carbon, oxygen, and iron.
The iron sample was simply heated in a vacuum environment of
500° C (793 K) for a relatively short period of time before tak-
ing the sample. Thus the presence of oxygen on the iron surface
would be expected because the iron oxides had not been disso-
ciated. The iron surface, however, contains also carbon and
sulphur.

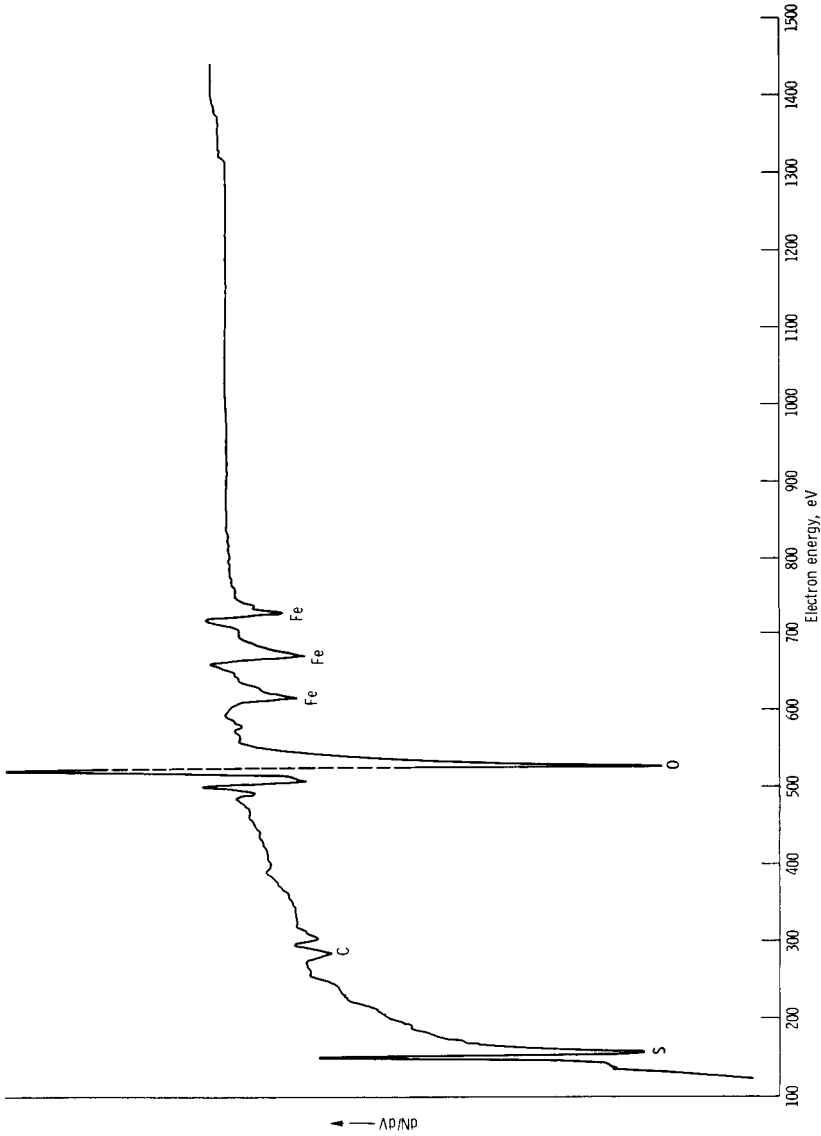Carbon and sulphur are present on the surface as a result of

Figure 37. - Auger emission spectrometric analysis of iron (001) surface after simple heating in vacuum.

the diffusion of these two elements to the iron surface with heating. Initial concentration of sulphur in the iron sample, which was electron beamed and zone refined, was less than 18 ppm, and the concentration of carbon in the iron sample was less than 8 ppm. Even with these relatively small concentrations of sulphur and carbon, heating of the iron in the vacuum environment produced diffusion of the sulphur and carbon to the surface of the iron.

This segregation of materials on the surface was originally discussed from a thermodynamic point of view by Gibbs (ref. 88). In this treatment of the subject, Gibbs considered two liquids, a solute and a solvent. He indicated that, if the solute, by being present on the surface, would reduce the surface energy of the system, then it in fact would migrate to the surface thereby accomplishing a reduction in the surface energy of the system. If, however, an alloying element or solute element increased the energy of the surface, it would not migrate and segregate at the surface. Those elements that tend to diffuse and segregate at the surface have been termed holiophylic elements, and those that tend to avoid the surface, holiophobic elements. Thus alloying constituents present in the metal may markedly alter adhesion and friction behavior.

During the sliding process frictional heat is generated at the interface, as has already been discussed. This frictional heat could bring about the diffusion of alloying elements that are holiophobic resulting in their segregation at the surface and altering adhesion and friction behavior of the two bearing steels 52100 and 440-C stainless-steel. The carbon content in the 440-C stainless-steel is considerably higher than it is in the 52100 bearing steel. Figure 37 shows that carbon will undergo equilibrium segregation to an iron surface.

The presence of the alloying elements that undergo segregation to a metal surface make achieving atomically clean metal surfaces extremely difficult, if not in some cases impossible, where the alloying concentration is high. This concept, however, can be used to advantage where a reduction in the friction and wear behavior of materials in solid contact is desired. For ex-

ample, alloys have been prepared in which the sulphur concentration in ferrous base materials was deliberately increased, so that equilibrium segregation would take place and thus prevent adhesion and minimize friction during rubbing contact in a vacuum environment. The addition, for example, of 0.1 percent of sulphur to 52100 bearing steel reduces the friction from a condition of complete seizure of the bearing material in contact with itself to a friction coefficient of 0.8 in a vacuum environment. The segregation of such alloying elements as sulphur and carbon to a metal surface are ideal in achieving a reduction in friction and adhesion because of their nonmetallic nature.

Where the alloying element, however, is metallic in nature, it segregates to a solvent metal surface adhesion, and friction may not be reduced. In some instances the alloying element, on segregation to the surface, may actually increase adhesion and friction behavior. The data of figure 38 are the adhesion forces for copper, copper and aluminum, and aluminum single crystals with a (111) orientation contacting a gold surface also having a (111) orientation. With copper in contact with the gold, the adhe-
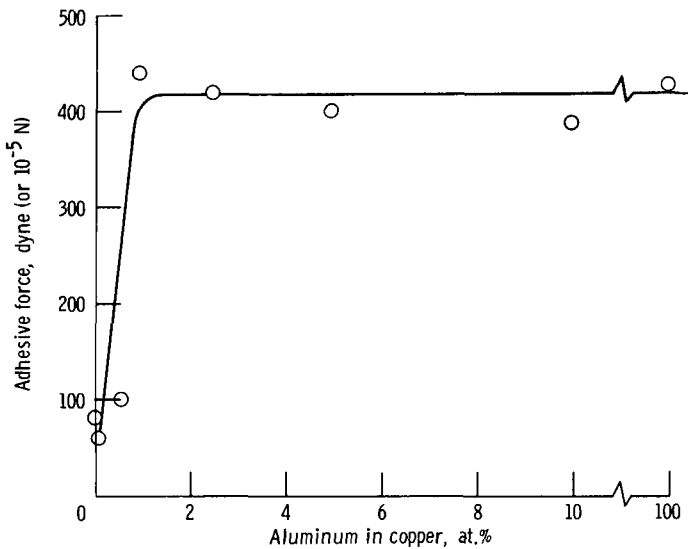

Figure 38. - Adhesive force of (111) gold to (111) surface of copper, aluminum, and various aluminum-copper alloys. Initial applied load, 20 dynes (20×10^{-5} N); contact time, 10 seconds.

sive force between the copper and the gold surface was relatively low, approximately 80 dynes (80×10^{-5} N). With the addition of as little as 1 atomic percent aluminum in the copper, the adhesion force of the copper-aluminum alloy to the gold increased to over 400 dynes (4.00×10^{-5} N). Further increases in the aluminum content beyond 1 atomic percent did not result in any further increase in the adhesive force of the copper-aluminum alloy to the gold.

The adhesive force was approximately 400 dynes with pure aluminum in contact with the gold. Thus the adhesive force of the copper containing 1.0 atomic percent aluminum was the same as the adhesive force of the gold to aluminum. This force was five times greater than what it was for the adhesion of copper and gold. The increase in adhesive force of copper to gold with the addition of as little as 1 atomic percent of aluminum to the copper is due to equilibrium segregation of the aluminum on the copper surface such that the concentration of aluminum on the copper surface far exceeds the concentration of the aluminum in the bulk copper. The concentration of aluminum on the copper surface with as little as 1 atomic percent aluminum in the copper was determined with Auger emission spectrometry analysis to be as much as 0.6 monolayer.

The presence of a very small concentration of aluminum brought about a change in the adhesion properties of copper such that the alloy behaved more like aluminum in adhesive contact with gold than it did like copper. There are conceivably other alloying elements that can be added to a solvent metal such as copper which will bring about an equilibrium segregation and a reduction in the adhesive force. The data of figure 38 do indicate the extremely potent force small concentrations of alloying elements can have on the adhesion behavior of metals in contact.

Friction experiments with the same surfaces as shown in figure 38 indicated a similar behavior in sliding friction. The foregoing discussion indicates that future considerations in bearing gear and seal materials for mechanical systems ought to take into consideration the influence of alloying elements on adhesion

and friction behavior where the mechanical components are to be used in a vacuum environment.

OTHER METAL PROPERTIES RELATED TO FRICTION AND VACUUM

ELASTIC PROPERTIES

The elastic properties of metals are related to their cohesive energy. Usually, the stronger the cohesive bonds in the metal, the higher the elastic modulus. With increasing cohesive energy and modulus of elasticity, metals tend to become less and less ductile. For example, in the body-centered-cubic system iron is fairly ductile. Tungsten, on the other hand, which has a markedly higher cohesive energy and elastic modulus, is relatively brittle and fractures very readily. With clean iron surfaces in contact, strong adhesion occurs across the interface. With sliding, a continuous increase in true contact area occurs resulting in junction growth, and friction coefficients continue to increase until complete seizure of the iron surfaces occurs (refs. 4 and 89).

When two tungsten surfaces are brought into contact, deformation will occur at the interface of the two tungsten surfaces, and a true contact area will be established just as with iron. On sliding with tungsten, however, the junction growth, which is normally observed with iron, will not be observed because of the relatively brittle nature of the tungsten junction formed. The junctions will fracture in a relatively brittle manner, and the increase in true contact area observed with tangential motion for relatively ductile body-centered-cubic metals such as iron will not be observed. Sliding friction experiments with tungsten in a vacuum environment indicate that, although the adhesion of tungsten to itself will occur very readily, the tungsten will exhibit a stick-slip type of sliding motion. The stick part associated with the adhesion of the tungsten to itself; the slip associated with the fracture of the adhesive junction and a corre-

sponding rapid decrease in friction. The stick-slip type of friction will occur for prolonged periods of time for tungsten in contact with itself with no notable increase in friction coefficient occurring. The friction coefficient for tungsten during this stick-slip sliding will be relatively high, approximately 3.0 with friction coefficients reaching as high as 5.0 during the stick portion of the stick-slip curve. At no point, however, is complete seizure of the tungsten to itself observed (ref. 90).

This type of behavior for metals such as tungsten is extremely analogous to the friction behavior observed in references 81 and 82 with diamond in contact with itself. With very high cohesive strength covalent and ionic crystals, the brittle nature of the junctions formed at the interface will fracture very readily, and the friction force, although high, will never be high enough to effect a complete seizure because the growth in the junction at the interface that normally occurs in the more ductile metals does not occur in the covalent or ionic metals.

Other metals with extremely high moduli of elasticity such as osmium exhibit a behavior similar to tungsten. With osmium, however, there is an added consideration of crystal structure since osmium possesses a hexagonal structure, and the structure itself will in part lower the friction properties of osmium. Extremely low friction coefficients are observed with osmium in sliding contact with itself in a vacuum environment.

From the foregoing discussion it might be anticipated that the ductile-brittle transition in body-centered-cubic metals such as iron and molybdenum would have an influence on their friction behavior.

DUCTILE TO BRITTLE TRANSITIONS

Friction measurements have been made in a vacuum environment with iron, molybdenum, and tantalum at temperatures below 300 K. At sufficiently low temperatures, decreases in friction coefficients for iron and molybdenum have been observed. These decreases are attributed to a transformation from the ductile to the brittle state in these metals. Figure 39 presents re-
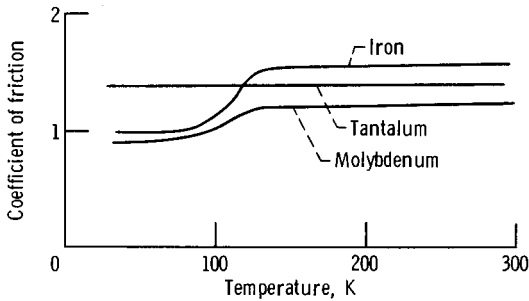
Figure 39. - Effect of temperature on the coefficient of friction of tantalum, iron, and molybdenum. Iron and molybdenum show a decrease in friction at low temperatures; tantalum does not (ref. 90).

sults obtained by the authors of reference 91. The decrease in friction coefficient for iron and molybdenum at low temperatures in vacuum is readily apparent from the figure. Note that tantalum, however, does not change in friction coefficient over the temperature range of from 20 to 300 K. The reason for the iron and molybdenum decreasing in friction in the region of approximately 120 K is believed to be due to the transformation of the iron and the molybdenum from the ductile to the brittle state. It appears, therefore, that ductile-brittle transitions exert influence on the friction behavior of metals in contact.

The present author has observed similar results in sliding friction experiments with iron-silicon crystals in a vacuum at 10^{-10} torr. In the region of transformation of the iron-silicon crystals from ductile to brittle behavior (temperature of approximately -80° to -100° C or 193 to 173 K) a decrease in friction coefficient was observed for the iron-silicon with transformation from the ductile to the brittle state. In addition, as might be expected, the wear track width decreased appreciably in size as shown in figure 40 for these experiments. In figure 40 both the microhardness in the wear track and the wear track width are plotted as functions of temperature for the iron-silicon crystals. In the region of transformation from ductile to brittle behavior a marked increase in the microhardness in the wear track occurred, and a decrease in the wear track width took place. The
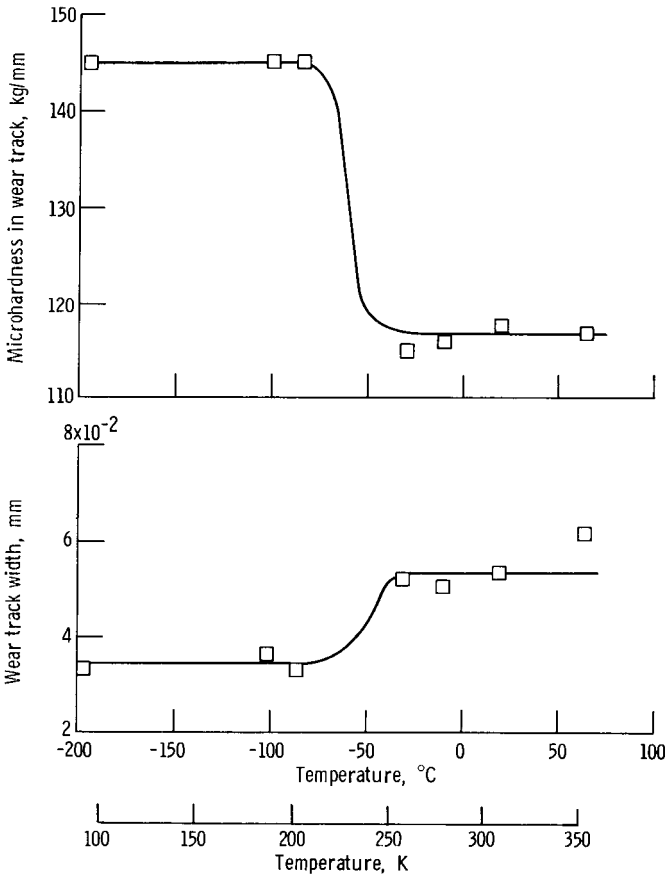
Figure 40. - Deformation and work hardening measurements in sliding friction studies with iron - $3\frac{1}{2}$ percent silicon in vacuum. Experiments on (001) face of crystal; Al_2O_3 rider specimen; sliding velocity, 0.001 centimeter per second; load, 60 grams (0.6 N); ambient pressure, 10^{-10} torr.

results of figure 40 indicate that, with sliding and transformation from the ductile to brittle state, the amount of metal undergoing deformation at the sliding interface decreased appreciably. The amount of metal being deformed plastically was appreciably less. The hardness measurements, however, indicate that the degree of work hardening in the sliding-contact region increased appreciably in the brittle region. The total volume of material being worked at the interface is markedly less in the case of the sliding experiments conducted below the ductile-brittle transi-

tion temperature. But above that temperature a greater volume
of metal is involved in the deformation process. The results of
figure 40 authenticate the earlier comment that the true contact
area in the brittle region would be markedly less than the con-
tact area when the metal is flowing plastically.

ORDER-DISORDER REACTIONS

Another property of metals, which is known to effect defor-
mation behavior, is order-disorder reactions in alloys. In many
alloy systems selective heat treatments can bring about the or-
dering of atoms in the structure. Typical metal alloys that ex-
hibit ordering are the copper-gold alloys Cu_3Au and $CuAu$. On
selective heat treating, these particular alloys can undergo
atomic ordering whereby the copper atoms will take up regular
lattice sites with respect to the gold in the matrix. The order-
ing of the atoms is shown schematically in figure 41. The order
structure is sometimes called a superlattice structure. The
copper-gold ordered alloys Cu_3Au and $CuAu$ are somewhat
classic in that they have been very thoroughly examined in the
literature and represent what might be considered ideal ordered
systems. Many mechanical properties have therefore been de-
termined for the Cu_3Au and $CuAu$ structures in both the ordered
and disordered state.

Figure 42 shows hot hardness, modulus elasticity, and fric-
tion coefficient as functions of temperature for the Cu_3Au super-
lattice structure. In the ordered state the modulus elasticity and
the hot hardness of the materials were relatively high. As the
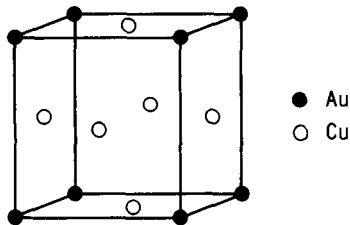
Figure 41. - The Cu_3Au super lattice
structure.
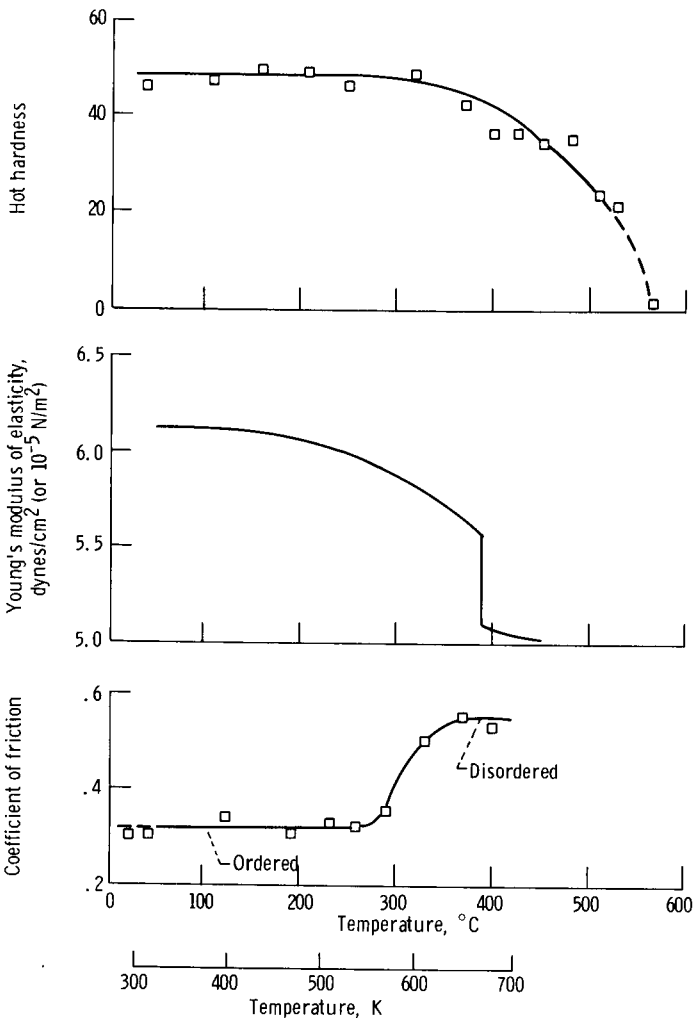
Figure 42. - Hardness, Young's modulus, and coefficient of friction for Cu_3Au (75 at.% copper - 25 at.% gold) sliding on 440-C stainless steel at various temperatures. Load, 1000 grams (9.8 N); ambient pressure, 10^{-9} torr.

temperature was increased from room temperature to near the transformation from the ordered to disordered state, the hot hardness and the modulus elasticity began to decrease. The change in mechanical behavior with transformation is relatively abrupt as indicated in figure 42 in the modulus of elasticity data. From foregoing discussions it is well known that modulus of

elasticity and the change in hardness are going to influence the friction behavior for the Cu_3Au alloy, and the friction coefficients plotted as a function of temperature in figure 42 indicate that they, in fact, do. In the ordered state, the friction coefficient was relatively low, slightly in excess of 0.3. As the transformation temperature was approached, however, the friction coefficient began to increase, and in the disordered state the friction coefficient achieved a value of about 0.55.

The friction experiments in figure 42 were conducted with the alloy Cu_3Au in the ordered state. With the alloy sliding on 440-C stainless steel, a transfer film of the copper-gold alloy to the 440-C stainless steel was achieved in sliding such that the alloy was essentially sliding on a thin film of itself. Similar experiments were conducted with Cu_3Au sliding on itself. The friction levels were generally higher than those observed in figure 42; still, the friction coefficient underwent a marked increase with transformation from the ordered to the disordered state. The change was much more drastic than that seen in figure 42. Friction experiments have also been conducted with the CuAu structure in the ordered and disordered state. Again, friction coefficients were found to be lower in the ordered than the disordered state.

Another alloy that exhibits ordering is the iron-cobalt alloy FeCo in which there is 50-atomic-percent iron and 50-atomic-percent cobalt. This particular alloy orders and retains its ordering to a relatively high temperature, approximately 700° C (973 K). Friction and wear experiments conducted in vacuum environment with FeCo sliding on itself indicate friction coefficients of approximately 0.6 in the ordered state. As the transformation temperature is approached, friction begins to increase. After transformation is completed, the friction coefficient reaches values in excess of 15. Wear measurements made of FeCo in both the ordered and disordered states indicate that, in the ordered state, the wear was only one tenth of what it was in the disordered state for the alloy.

From the foregoing discussions on the influence of crystal structure, elastic properties, ductile-brittle transitions, and

order-disorder transformations it can be seen that those proper-
ties of metals and alloys that influence their ductile behavior will
influence the friction and wear of the materials in a vacuum envi-
ronment. Those metals that exhibited a relatively limited num-
ber of slip systems, and therefore limited ductility, exhibited
lower friction. Those metals that have high moduli of elasticity,
reflecting a high cohesive strength, tended to be somewhat more
brittle than metals with lower moduli of elasticity and as a con-
sequence exhibited lower friction than their counterparts with the
same crystal structure but markedly lower elastic moduli. Like-
wise, transformations from ductile to brittle behavior influence
friction and wear. When the materials are in the brittle state
they exhibit lower friction than in the ductile state. Large in-
creases in friction coefficient are inhibited because of the lack of
junction growth associated with the materials in the brittle state.
Last, order-disorder transformations also influence the ductile
behavior of metals and influence both friction and wear when slid-
ing in vacuum. Note that many of these properties, which have
been related to friction and wear, are the result of experiments
conducted in a vacuum environment. The data may, however, in
many instances be applicable to other environments where metal-
to-metal contact can occur through the films present on the
surfaces (ref. 92).

FRICTION BEHAVIOR OF NONMETALS

IN A VACUUM ENVIRONMENT

The influence of vacuum on the friction behavior of the co-
valent structure of diamond has already been discussed. The
friction coefficient for diamond on the natural (111) cleavage
plane increases from a value of 0.05 in air at 760 torr to 0.9 in
a vacuum of 10^{-10} torr (see refs. 81 and 82). The marked in-
crease is due to the desorption of adsorbed surface species,
which promotes the adhesion of diamond to itself across the in-
terface. With carbon-to-carbon bond formation across the in-
terface, even though the true contact area may be extremely

small because of the high cohesive strength of diamond, the co-
hesive strength of the junction will give rise to the requirement
of relatively high forces to fracture these junctions. Thus, a
relatively high friction coefficient of 0. 9 is observed for diamond
in a vacuum environment. It is of interest to note that graphite,
in the absence of adsorbed species, will exhibit friction coeffi-
cients very similar to those of diamond in a vacuum environment.
Since, for both species, carbon-to-carbon bonding occurs across
the interface, the relative similarity in the friction properties of
graphite and diamond in a vacuum environment are not too sur-
prising.

Ionic solids as well as covalent materials will exhibit strong
bonds of adhesion in a vacuum environment in the absence of re-
sidual surface films. Aluminum oxide in both its single and
polycrystalline forms exhibit marked increases in friction coef-
ficients when sliding is conducted in a vacuum (ref. 65). Thus,
adhesion not only plays an important part in the determination of
friction behavior of metals but also in determining the frictional
properties of covalent and ionic solids as well. Frequently in
sliding, rolling, or rubbing contact, dissimilar materials are
in contact across the interface. A metal surface may contact a
nonmetal such as a covalent or ionic solid. The friction and
wear behavior of such couples in a vacuum environment will be
determined to a great extent by the nature of the interaction of
the surfaces when the residual surface films are worn away or
deliberately removed. It may be well to consider the nature of
the interaction of metal with nonmetal and the influence of that
interaction on friction in vacuum by use of a specific example.

ALUMINUM OXIDE

Aluminum oxide has been considered for use in contact with
metals in a number of practical devices. It can also be used to
help us understand the nature of the interactions of metals with a
nonmetal. One of the first considerations of such dissimilar
couples in contact is the differences in the behavior of the two
materials. For example, aluminum oxide has a much higher

strength in compression than metals, but it is relatively brittle and fractures readily. The metal in contact, however, is relatively ductile and will deform in sliding, rubbing, or rolling contact quite readily. The ease with which a metal will deform plastically under a load when in contact with aluminum oxide may give rise to situations where the shear term in the friction equation $f = s + p$ may become of secondary importance and the plowing term may take on predominance in determining friction coefficients. For example, if a sliding experiment is conducted in a vacuum environment with single-crystal aluminum oxide (sapphire) sliding on copper, considerable plowing of the copper surface would occur by the sapphire. If the sapphire is in a spherical or hemispherical form, the copper will deform plastically under an applied load on the sapphire giving rise to a plowing component in the friction force measured. This in turn can give rise to a relatively high friction coefficient as shown in figure 43.

In figure 43 the left bar is the friction coefficient for the sapphire sliding on copper. When both the copper and aluminum oxide surfaces are clean, adhesion of the copper to the oxygen of the aluminum oxide will occur with sliding, and fracture can occur in the sapphire as shown by the pits in the photomicrograph above the left hand bar in figure 43. The friction coefficient is relatively high for the sapphire in contact with the copper, 1.5. If the specimen couples are reversed so that a copper sphere is sliding on a sapphire flat, an entirely different friction result is obtained. The bar at the right indicates a friction coefficient for the copper sliding on the sapphire of only 0.2. The photomicrograph above the bar on the right hand side indicates that adhesion of the copper to the sapphire also occurred in this particular experiment with fracture occurring in the sapphire just as it had done in the experiment in which the sapphire slid on the copper. Thus, the shear or fracture component contributed to the friction coefficient is essentially the same in both experiments.

The marked difference in friction behavior in the two experiments may be attributed to plowing. With the extremely hard
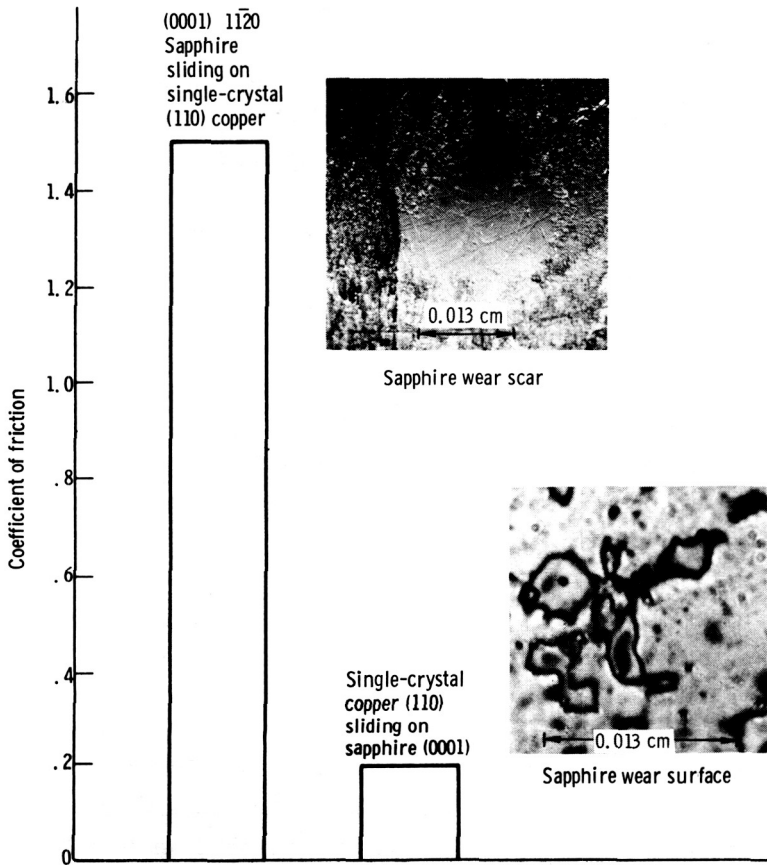
Figure 43. - Coefficient of friction for copper in sliding contact with sapphire in vacuum (10^{-10} torr). Sliding velocity, 0.013 centimeter per second; load, 100 grams (0.98 N).

high modulus sapphire in sliding contact with the soft and ductile copper, the copper will deform plastically ahead of the sapphire slider, and a large component of the friction force will be determined by the force required to plow copper ahead of the rider specimen. With the copper sliding on the sapphire surface, the copper deforms until the load is supported and the true contact area is developed at the interface. With sliding there is relatively little if any plowing components in the friction force because the sapphire is extremely resistance to deformation. Thus, a greater than sevenfold difference in friction behavior can be obtained simply from a choice of the particular arrange-

ment of the materials in contact. The friction force in figure 43
for the copper sliding on the sapphire is determined primarily
by the force to fracture the sapphire subsurface along the cleav-
age plane of sapphire, namely, the (0001) plane. The photomi-
crograph in figure 43 indicates that adhesion of the sapphire to
the copper had occurred and that fracture had taken place in the
sapphire subsurface resulting in the plucking out or removal of
sapphire from the surface.

If the fracture strength of the sapphire along the cleavage
plane is determining the friction force shown in figure 43, the
nature of the metal in contact with the sapphire should have very
little influence on the friction force. The friction force should
be the same for various metals as long as adhesion of the metal
to the sapphire will occur. Friction experiments with various
metals in contact with the (0001) surface of sapphire indicate that
this is in fact the case.

Friction data are presented in figure 44 for copper, nickel,
rhenium, cobalt, and beryllium in contact with sapphire. The
friction coefficients were all approximately 0. 2 as they were for
copper in figure 43. The mechanism accounting for the friction
force for the surfaces in sliding contact are essentially the same:
The metal had taken on fractured sapphire, and the sapphire sur-
face showed evidence of plucking out or removal of material.
The photomicrograph in figure 44 indicates the cleavage of the
sapphire subsurface after having been contacted by beryllium.
The nature of the surface was essentially similar to that obtained
in figure 43 for copper in contact with sapphire. A prerequisite
for this sameness in friction coefficient is that the metal form a
stable metal oxide. If the metal did not form a stable metal
oxide these friction coefficients were not obtained.

Similar friction experiments conducted with both silver and
gold in contact with sapphire in a vacuum of 10^{-10} torr resulted
in friction coefficients one half of the values presented in fig-
ure 44 for the other metals. Gold does not form a stable oxide
even in air at 760 torr. Thus, the gold did not adhere to the sap-
phire, and the friction forces were small. With silver as was
mentioned earlier in a discussion on silver-carbon interactions,
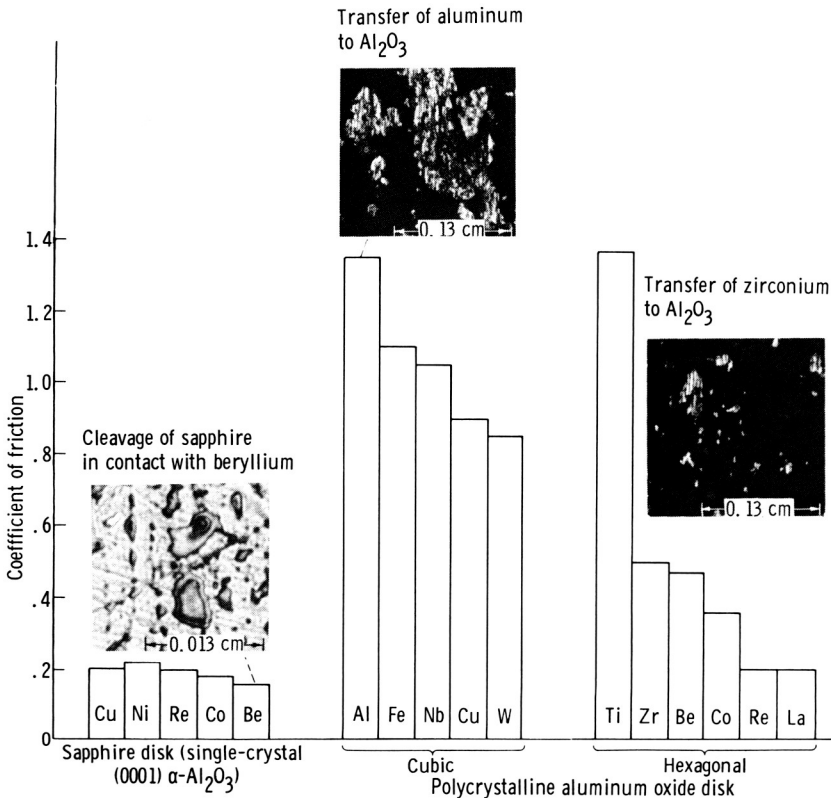
Figure 44. – Coefficient of friction for various metals sliding on aluminum oxide in vacuum (10^{-10} torr). Sliding velocity, 0.013 centimeter per second; load, 1000 grams (9.8 N); experiment duration, 1 hour.

the silver oxide will dissociate on the reduction of the ambient pressure and becomes unstable in a vacuum of 10^{-10} torr. As a consequence, similar friction coefficients of 0.1 was obtained for the silver in contact with the sapphire. Examination of the sapphire surface after sliding contact with silver and with gold revealed no cleavage or fracture of the sapphire. Thus, where the metal oxide was thermodynamically unstable, adhesion of the metal to the sapphire surface did not occur, and very low friction coefficients were obtained. These results indicate that chemical interaction may play an important role in the friction of solid surfaces. Entirely different experimental results were obtained when metals were in sliding contact with polycrystalline aluminum oxide.

With the various metals in contact with polycrystalline alum-
inum oxide, the friction forces measured were generally much
higher than those obtained on sapphire, and friction was a func-
tion of the structure of the metal as shown by the data of fig-
ure 44.   Adhesion of the metals to the aluminum oxide still oc-
curred as it had in contact with the single-crystal aluminum
oxide.   With the metals in contact with polycrystalline aluminum
oxide, however, a number of different random orientations are
present at the interface.   And with tangential motion the alumi-
num oxide is more resistant to shear than it was where metals
were sliding on single-crystal aluminum oxide with a cleavage
plane parallel to the interface.   With random orientations in the
aluminum oxide present at the interface, it is very unlikely that
many of the grains in the polycrystalline aluminum oxide had a
favorable orientation for fracture along the (0001) cleavage
plane.   As a consequence, shear took place in the metal rather
than fracture in the aluminum oxide.   This was evidenced by the
presence of metal on the polycrystalline aluminum oxide sur-
face.   Thus, the aluminum oxide was more resistant to brittle
fracture, and the weaker of the two materials at the interface
was the metal rather than the aluminum oxide.

The presence of the metal on the polycrystalline aluminum
oxide surface is shown for two metals, aluminum and zirconium,
in the photographic inserts in figure 44.   The results obtained
with the single-crystal as well as the polycrystalline aluminum
oxide in contact with various metals indicate that the chemical
bond of adhesion of the metal to the aluminum oxide was stronger
than the cohesive bond in the weaker of the two materials.   In
the case of the metal sliding on sapphire, the weakest region was
the cohesive bonds along the cleavage plane in the sapphire.   With
tangential motion, cleavage occurred in the sapphire.   With the
metals in contact with the polycrystalline aluminum oxide, the
weakest region was the cohesive bonds in the metal, and shear oc-
curred in the metal.   The shear properties of the metal will then
determine to a great extent the friction coefficients measured.   In
figure 44 it will be noted that the friction coefficients for the
cubic metals in general were higher in sliding contact with the

polycrystalline aluminum oxide than were the friction coefficients
for the hexagonal metals. This observation is in keeping with the
earlier discussion relating crystal structure to the friction be-
havior of metals. The notable exception in figure 44 is titanium.
Its behavior was discussed earlier in reference to the friction
properties of hexagonal metals.

The data of figure 44 indicate that not only the geometry of
the material surfaces in contact is important (see fig. 43) but
also the state of the materials, that is, whether they are in the
single or polycrystalline form. Where metals are in contact with
nonmetals, the friction coefficient will be determined to a large
extent by the properties of the region where fracture predomi-
nates. If adhesion of metal to nonmetal surface does not occur
as in the case of silver and gold to the sapphire, very low fric-
tion coefficients will be achieved. When adhesion of the metal to
the nonmetal does occur, as was observed with metals that form
stable oxides, the friction force may be determined by the loca-
tion where fracture occurs. If fracture occurs in the nonmetal,
as in the case of sapphire, the cleavage or fracture strength in
the sapphire may determine the friction force. When the non-
metal such as the aluminum oxide is stronger than the cohesive
bonds in the metal as was observed with polycrystalline alum-
inum oxide, shear in the metal may determine the friction forces
measured.

The nature of the bonding of metals to the oxygen of alum-
inum oxide is shown diagramatically in figure 45. If a (0001)
plane of sapphire is considered, for example, the surface of the
sapphire is covered by a layer of oxygen ions. In the first sub-
surface layer the aluminum positive ions (Al^3) are arranged in
octahedral array. On the surface of the sapphire that is to be
bonded to the oxygen ions, various sites exist for the possible
chemical bonding of metals when they contact the oxygen of the
sapphire. There are other sites on the surface that are not fa-
vored for chemical bonding and only van der Waals interactions
can occur. These sites are indicated in figure 45. Where the
metals do not form stable oxides as is the case with gold and
silver, no chemical bonding to the available oxygen sites on the

◯ Al^{+3} in first subsurface layer and arranged in
    octahedral array

◯ Surface covered by layer of O^{-2}

◯ Sites for chemical bonding of metals with oxygen when in contact
    with surface

◉ Sites for van der Waals interaction with metals sliding on surface

(0001) Plane of sapphire   CD-8498-15

Rider — — — — — — — — — Metal — — — Metal-to-metal bonding

Interface — — — — — — — — — Metal - oxygen chemical
                                                    and van der Waals forces
Disk — — — — — Al_2O_3 — — — Al_2O_3 chemical bonding
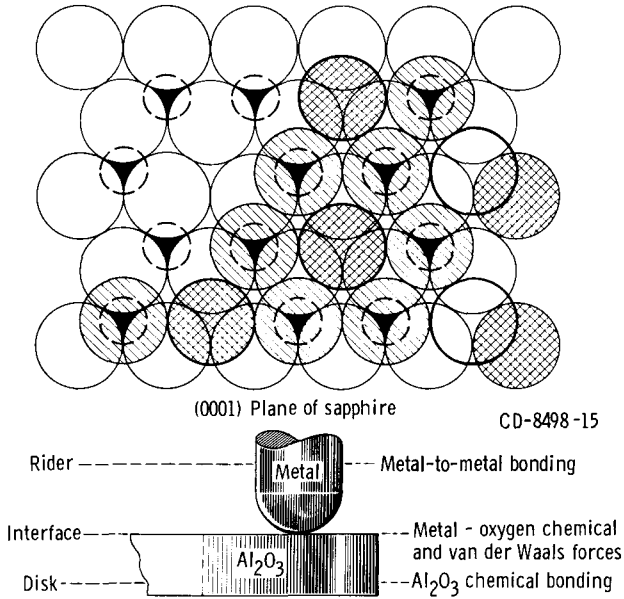
Figure 45. - Nature of surface interaction and bonding of metal to
aluminum oxide.

sapphire surface occurs. At best, weak van der Waals interac-
tions between the metals and the oxygen will take place. When,
however, the metals do form stable oxides, chemical interaction
of the metal with the oxygen ions on the sapphire surface can
occur as indicated in figure 45.

With the tangential motion of the metal rider on the alumi-
num oxide, the friction force will be determined, as already dis-
cussed, by the zone or region in which shear or fracture will
occur. When metal transfer to the nonmetal takes place, as was
observed for the metals in sliding contact with polycrystalline
aluminum oxide, the metals will ultimately be sliding on them-
selves. Those factors that determine the friction behavior of

the metals may in fact determine the friction properties of the couple.

CARBONS

Metals may not only transfer to nonmetal; in some instances the nonmetal will transfer to the metal surface. With carbons in contact with metal surfaces, as long as a residual surface oxide is present on the metal surface, the carbon will bond to the oxygen of the metal oxide and a transfer film of carbon will develop on the metal surface with sliding or rubbing contact. Thus, for carbons in contact with metals in a normal atmospheric environment or in vacuum with residual surface oxides present, the carbon will actually be sliding on a transfer film of carbon rather than sliding on the metal. Where the metal oxides are, however, thermodynamically unstable and dissociate, the carbon will, in fact, be sliding on the metal. Under such conditions the metal can transfer to the carbon surface and ultimately metal will slide on metal.

ADSORBED FILMS AND THEIR EFFECT ON METALLIC FRICTION

Clean metallic surfaces in a vacuum environment possess a certain degree of unsaturation on the surface. When gases are admitted into the vacuum system, they tend to accumulate on the surface. This process is referred to as adsorption. Adsorption on metallic surfaces takes place with a decrease in the overall surface energy ΔG. This decrease is normally accompanied by a decrease in entropy ΔS. Confining an adsorbed molecule or atom to the surface layer resulted in the loss of certain degrees of freedom.

The equation

$$\Delta G = \Delta H - T \Delta S$$

indicates with the adsorption of gases that ΔH is negative and

that the adsorption process takes place in an exothermic manner. The degrees of surface unsaturation can vary widely for materials, and the surfaces of many substances are inert to certain gaseous species. When these gaseous species adsorb on the surface, the only forces of attraction between the adsorbing species and the surface are forces of physical attraction similar to those encountered in the liquification of gases. This kind of adsorption is frequently called physical or van der Waals adsorption. It is very similar in nature of the simple condensation of a vapor on a surface from its own liquid.

When a high degree of unsaturation exists on a surface, the valency requirements of the atoms may not be satisfied by bonding to adjacent like atoms. In such situations certain adsorbed species will tend to chemically bond to the surface, and this process of the chemical bonding of the adsorbing species to the metal surface is called chemisorption. The major difference between the two types of adsorption, physical and chemical, is that electron transfer takes place between the adsorbing species and the adsorbant in chemisorption but this does not occur in the case of physical adsorption. It should be mentioned that these are the only two types of adsorption that have been encountered.

Differences in the Types of Adsorption

There are some basic criteria that can be used to distinguish between the two types of adsorption. The best single criterion for determining the differences between physical and chemical adsorption is the magnitude of the heats of adsorption. Chemical bonds are normally much stronger than the physical forces of attraction, and one might anticipate that chemisorption would involve greater heats of adsorption than would physical adsorption. This, in general, has been found to be the case. The heats of physical adsorption are generally low, approximately 10 kilocalories per mole (4.18×10^4 J/mole) or less as is indicated in table XV. One exception in table XV is water. Water can physically adsorb to surfaces with energies as high as

TABLE XV. - MAXIMUM

HEATS OF PHYSICAL

ADSORPTION

(REF. 6)

Gas	Maximum heat of physical adsorption	
	kcal/mole	J/mole
H_2	2.0	8.4×10^3
O_2	5.0	21.0
N_2	5.0	21.0
CO	6.0	25.2
CO_2	9.0	37.8
CH_4	5.0	21.0
C_2H_4	8.0	33.6
C_2H_2	9.0	37.8
NH_3	9.0	37.8
H_2O	14.0	58.8
Cl_2	8.5	35.7

14 kilocalories per mole (5.9×10^4 J/mole). Likewise heats of chemical adsorption as low as 3 kilocalories per mole (1.26×10^4 J/mole) have been observed with hydrogen adsorption (refs. 93 and 94). Ten kilocalories per mole (4.18×10^4 J/mole) is simply an arbitrary rule of thumb, but it does indicate that one in general may anticipate lower heats of adsorption for physical adsorption than for chemical adsorption.

Table XVI presents some heats of chemisorption of various gases to different metal surfaces. An examination of the heats of chemisorption indicates that the heats of chemisorption are higher than the heats of physical adsorption observed in table XV. For example, oxygen can physically adsorb to a surface with a maximum energy of physical adsorption of 5 kilocalories per mole (2.09×10^4 J/mole), but with the chemisorption of oxygen on tungsten, for example, the energy involved is 194 kilocalories per mole (8.15×10^6 J/mole).

TABLE XVI. - HEATS OF CHEMISORPTION AT LOW

COVERAGE (REF. 6)

Gas chemisorbed on metal	Heat of chemisorption, $-\Delta H$, kcal/mole	Gas chemisorbed on metal	Heat of chemisorption, $-\Delta H$, kcal/mole
O_2 on W	194	H_2 on Ni	30
N_2 on W	85	NH_3 on Ni	36
H_2 on W	46	CO on Ni	35
NH_3 on W	70	H_2 on Rh	26
CO_2 on W	125	H_2 on Co	24
H_2 on Ta	46	H_2 on Fe	32
O_2 on Ni	115	H_2 on Cu	8

A second criterion that can be used to distinguish between the two types of adsorption is the temperature range over which the adsorption process proceeds. Since physical adsorption is somewhat related to liquification, the physical adsorption process tends to occur at temperatures near or below the boiling point of the adsorbate at the pressures considered. Chemisorption, on the other hand, usually takes place at temperatures far above the boiling point.

A third guide for distinguishing between the types of adsorption is that chemisorption is a chemical reaction and therefore may require an activation energy. In contrast, physical adsorption requires no activation energy just as the condensation of liquids from their vapor requires none.

A fourth and very important criterion for distinguishing between the two types of adsorption is that of specificity. A chemical adsorption has a certain specificity, while a physical one does not. This is demonstrated by the data of table XVII, which provides the activities of various gases toward metal films. It can be seen from table XVII that, while certain gases will chemisorb to a particular group of metals, others will not. Some metal surfaces are extremely reactive, and a large number of gases will chemisorb to their surfaces. Tungsten, tan-

TABLE XVII. - ACTIVITIES OF METAL FILMS IN

CHEMISORPTION (REF. 6)

Metals	Gases[a]					
	N_2	H_2	CO	C_2H_4	C_2H_2	O_2
W, Ta, Mo, Ti, Zr, Fe, Ca, Ba	+	+	+	+	+	+
Ni, Pt, Rh, Pd	-	+	+	+	+	+
Cu, Al	-	-	+	+	+	+
K	-	-	-	-	+	+
Zn, Cd, In, Sn, Pb, Ag	-	-	-	-	-	+
Au	-	-	+	+	+	-

[a]Gas chemisorbed, +; not chemisorbed, -.

talum, molybdenum, and iron are typical of metals that are ex-
tremely reactive and with which many gases can interact by
chemisorption. In contrast, a metal such as gold is relatively
inactive with respect to its interaction with gaseous species ad-
mitted to a vacuum environment. While carbon monoxide,
ethylene, and acetylene will chemisorb to gold, gases such as
nitrogen, hydrogen, and oxygen will not.

A fifth factor to be considered in distinguishing between
chemical and physical adsorption is that chemical adsorption is
a single-layer process. Once the surface is covered with a
monolayer of the adsorbed species, chemisorption ceases. The
addition of further gas to the surface is generally physically ad-
sorbed to the chemisorbed gaseous layer. Thus, where more
than a single layer of gas is adsorbed on a surface, it is reason-
ably safe to assume that all layers other than the first layer are
physically adsorbed. In general, physically adsorbed species
can be expected to exert a relatively minor influence on the ad-
hesion, friction, and wear behavior of metal surfaces in con-
tact because of the relatively small amounts of energy required
to desorb such species and the relatively large amounts of
energy generated in the friction process which can give rise to
desorption of such species. On the other hand, chemisorbed
species can be expected to exert a very pronounced influence on
the adhesion, friction, and wear of material surfaces in contact

since these species are chemically bonded to the surfaces and require considerably more energy to desorb than is put into the surfaces by the sliding or rubbing process.

EFFECT OF ADSORBED FILMS ON FRICTION

Bowden (ref. 95) was one of the first to study the influence of chemisorbed species on the friction behavior of metal surfaces in a vacuum. In his experiments, he heated iron surfaces to high temperatures in a vacuum of 10^{-6} torr in order to clean them. With the surfaces in such a state, very high friction coefficients were obtained, in excess of 2.0 as shown by the data of figure 46. When a small concentration of oxygen was admitted to the chamber, the coefficient of friction decreased. Continued increases in the exposure of the iron surface to oxygen resulted in further decreases in the coefficient of friction. When the pressure was raised to several torr with oxygen, the friction coefficient decreased to a value of 1.0.

The surfaces in reference 95 were cleaned by simple heating in a vacuum of 10^{-6} torr. It is fairly common knowledge today that a clean iron surface cannot be obtained by simple heating in a vacuum environment (the oxides formed on iron are very stable) and that pressures of the order of 10^{-10} torr or lower are necessary to maintain the clean surface once it is achieved.
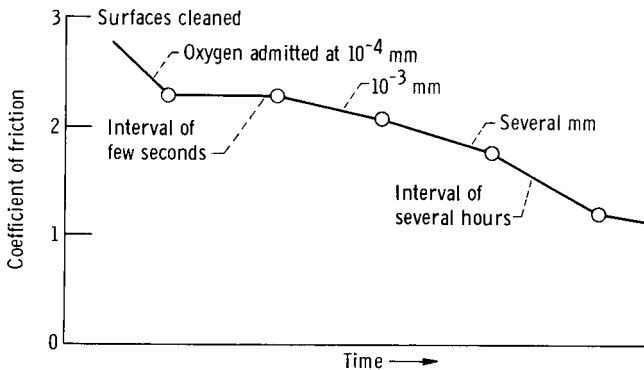

Figure 46. - Effect of oxygen on friction of outgassed iron surfaces (ref. 94).

In order to clean an iron surface it is necessary to electron beam or ion bombard the surface. Very few investigators have actually worked with clean iron surfaces. Of those who have, most studies have been done with either the field-ion microscope or with LEED (low-electron-energy diffraction) (refs. 96 to 101) to verify the state of surface cleanliness. The present author has conducted adhesion experiments in a vacuum environment with iron surfaces. These surfaces were cleaned by ion bombardment, and the state of cleanliness of the surface was determined using both LEED and Auger emission spectrometry analysis. These two devices give a very good indication of the degree of surface cleanliness at the atomic level. Figure 47 is a LEED diffraction pattern obtained for the (001) surface of iron after cleaning by ion bombardment with the surface examined in a vacuum of 10^{-10} torr. Auger emission analysis of the surface indicated only iron. Before ion bombardment, however, the surfaces were simply heated in a vacuum environment.
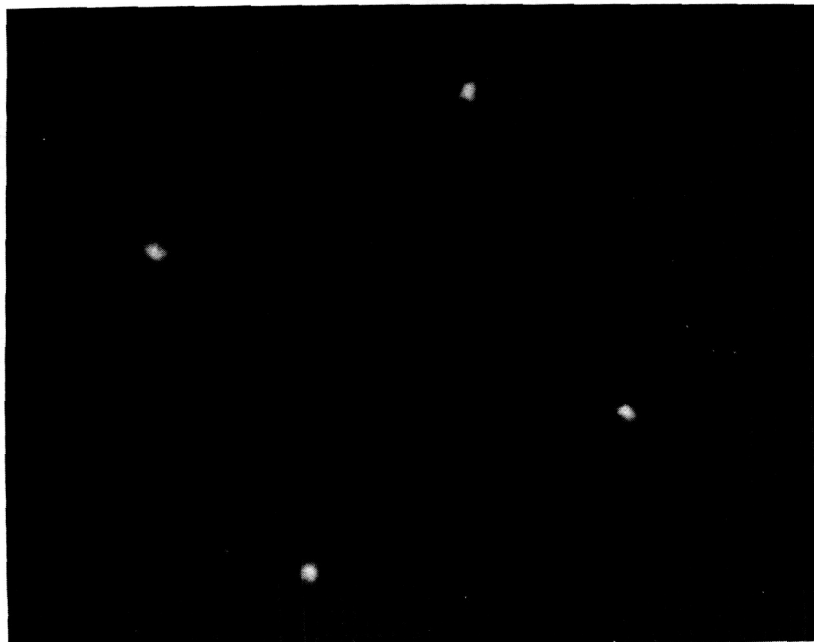

Figure 47. - LEED pattern obtained for clean iron (001) surface.

After such heating, oxygen, carbon, and sulphur, were found to
be present on the surface. Solid-state contact of iron surfaces
such as those shown in the LEED photograph of figure 47 resulted
in complete seizure. Admission of oxygen to the surfaces re-
duced the adhesion and friction between the iron surface (fig. 46)
in much that same manner as was observed by Bowden.

It was mentioned in reference to the criteria for distinguish-
ing between chemical and physical adsorption that chemisorption
was a monolayer process. It is of interest to know if fractions
of a monolayer of a chemisorbed film will have an influence on
the friction coefficient of metal surfaces in contact. Sliding
friction experiments have been conducted with tungsten single
crystals in sliding contact with themselves in the presence of
various concentrations of oxygen. Some of these data are pre-
sented in figure 48. In figure 48 the oxygen adsorption is plotted
as a function of surface exposure to oxygen. A dashed line in the
upper portion of figure 48(a) indicates the amount of oxygen that
is necessary for the formation of a complete monolayer. In fig-
ure 48(b) the friction coefficient for the tungsten sliding on itself
is plotted as a function of that same oxygen exposure.

It can be seen from figure 48(b) that, as the oxygen exposure
increases, the friction coefficient for the tungsten in contact with
itself decreases very rapidly. At oxygen exposures of approxi-
mately 2×10^{-5} torr-second sufficient oxygen is present on the
surface to reduce the friction coefficient from 3.0 to approxi-
mately 1.3. At this same oxygen exposure the surface coverage
is only approximately a half a monolayer on the tungsten. The
data indicate that half a monolayer of oxygen on a tungsten sur-
face is sufficient to reduce the friction coefficient by greater than
100 percent. Further exposure of the tungsten surface to oxygen
did not result in any marked change in friction coefficient. In
fact, the friction coefficient thereafter remained relatively con-
stant up to a complete monolayer coverage of oxygen on the tung-
sten surface. These results indicate the extreme sensitivity of
metal surfaces to the presence of chemisorbed species on their
friction properties. The friction experiments of figure 48 were
conducted with the tungsten having various fractions of a mono-

(a) Oxygen adsorption.
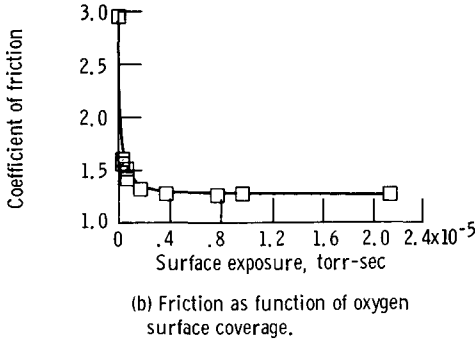
(b) Friction as function of oxygen
surface coverage.
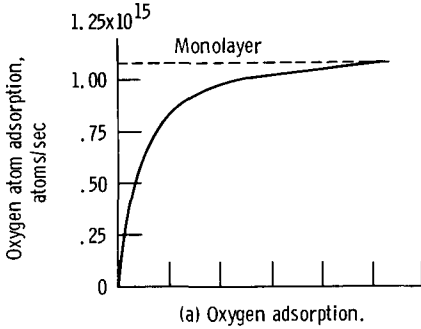
Figure 48. - Oxygen adsorption and
friction coefficient for (100) plane
of tungsten sliding on like plane.
Sliding velocity, 0.001 centimeter
per second; load, 50 grams (0.5 N);
ambient temperature, 20° C
(293 K); ambient pressure, 10^{-10} torr.

layer of oxygen on its surface in a vacuum of 10^{-10} torr with re-
peated passes of the tungsten over the same sliding surface.

The oxygen chemisorption to tungsten results in the forma-
tion of an extremely strong chemical bond. If the metal involved
formed a chemisorbed oxygen film which had appreciably weaker
binding energy, it is conceivable that during the sliding friction
process the frictional heat generated at the interface would be
sufficient to bring about desorption of the adsorbed oxygen.
This, however, did not occur for tungsten. Because frictional
energy at a sliding interface may give rise to a desorption of
chemisorbed species which are not strongly bonded to the metal

surface, it would be well to know if some type of relation exists between the metallic structure and the adsorption properties of the metal with specific gases. If this information were available and if one knew the adsorption energies of a particular gas with one particular metal, it might be possible to predict the friction behavior of another metal with the adsorption of that same gas. Haywood and Trapnell (ref. 6) have plotted the energies of chemisorption for three gases, ethylene, carbon dioxide, and hydrogen, for various metals and have grouped the metals in the transition series according to the periods. The data that they have plotted are represented in figure 49.

An examination of figure 49 indicates that at least for the three gases, ethylene, carbon dioxide, and hydrogen, the heats of chemisorption for the transition metals are related to the period in which the metals exist. For example, chromium, molybdenum, and tungsten all exhibit similar heats of chemisorption for the three gases indicated in figure 49. Thus, if one knew that hydrogen desorbed from a chromium surface during the sliding process, it would give some insight into the behavior of molybdenum and tungsten in the presence of a hydrogen adsorbed film. Note that the heats of chemisorption decrease in moving across the periodic table from left to right.

Although reasonably good correlation was obtained for the adsorption of ethylene, carbon dioxide, and hydrogen with the particular transition periods of metals, the correlation is not always quite as good. For example, with the adsorption of oxygen on these various metals surfaces, the agreement is not what is observed in figure 49. It may be that the mechanism of chemisorption of oxygen to these metal surfaces is different and that this accounts for lack of good correlation seen in figure 49 for ethylene, carbon dioxide, and hydrogen with metal period. The correlation between the heats of adsorption with the position of a metal in the periodic table seem to imply the variability of gaseous species controls the heats of adsorption, and that the surface atoms may be treated like isolated atoms.

The relative position of a metallic element in the periodic table is one factor that appears to exert an influence on the
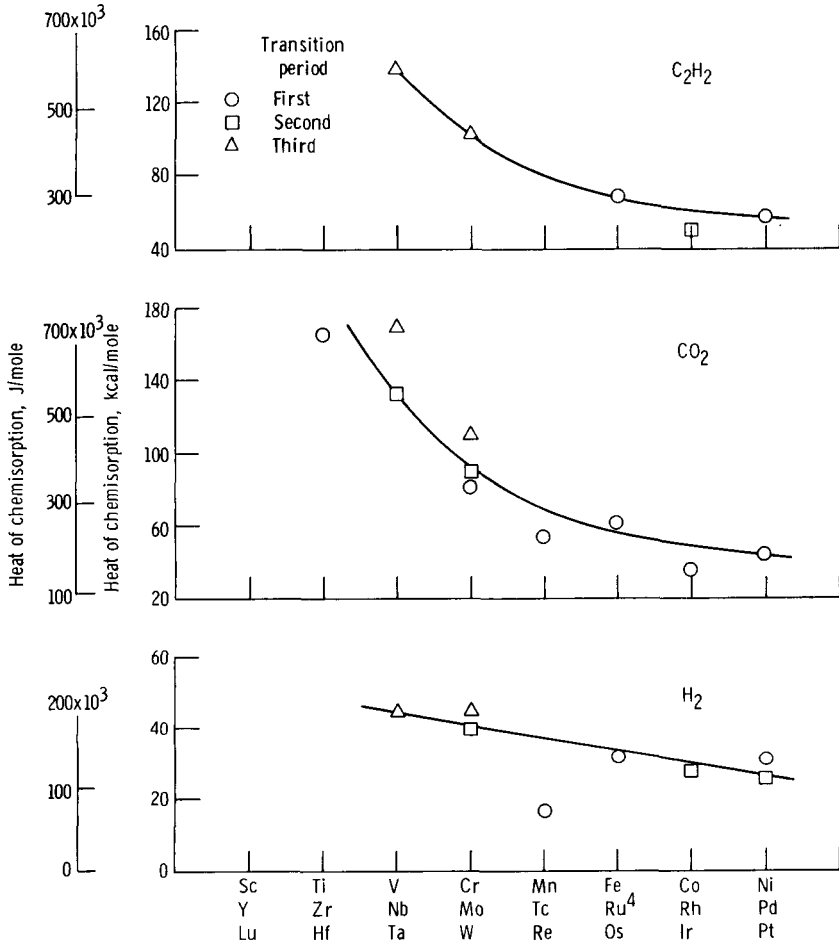
Figure 49. - Heats of chemisorption for transition metals, plotted according to periodic classification (ref. 6).

heats of chemisorption of various gases to metal surfaces. There may be other factors that also exert an influence on surfaces and the chemisorption process. For example, in reference to the discussion related to table I, it was found that the oxidation of metal crystals in air was a function of the orientation exposed. There were crystallographic planes which were very active regions with respect to interaction with oxygen and other atomic planes that were relatively inactive because of differences in the surface energies associated with the different

atomic planes. Because of the different surface energies of
the various atomic planes, it might be anticipated that the
sticking probability of gases when colliding with metal surfaces
would also be a function of the particular plane exposed. This
in turn could be expected to exert an influence on the amount of
a particular gas which would chemisorb on a surface in a fixed
exposure time. Further, since bonding of the chemisorbed
species to the metal surfaces occurs, there may be a question
of accommodation on the surface of the molecular species ad-
sorbing. Where relatively large molecules are involved, steric
hinderance may play a part in determining the concentration of
gases which may be chemisorbed to a surface.

The atomic arrangement of a particular surface will also
exert an influence on the concentration of gas that can be ac-
commodated. A question which may be posed is will this influ-
ence the friction behavior for metal surfaces in contact. Sliding
friction experiments have been conducted with tungsten in contact
with itself in a vacuum environment with various chemisorbed
gaseous species present on the surface. Three atomic planes of
tungsten were examined: the (110), the (210), and the (100) sur-
faces. Friction coefficients were measured with hydrogen, oxy-
gen, carbon dioxide, and hydrogen sulfide chemisorbed on these
three atomic planes of tungsten. The friction results obtained
are presented in table XVIII. For reference purposes the fric-
tion for the tungsten in the clean state is also presented in ta-
ble XVIII.

An examination of table XVIII indicates that orientation in-
fluences the friction properties for the clean tungsten in con-
tact, just as it did for other metal surfaces in earlier discus-
sions. An interesting result in table XVIII is that hydrogen,
present on all three atomic planes, reduced the friction coeffi-
cient for tungsten in sliding contact with itself. Table XVIII
indicates a heat of chemisorption of hydrogen to tungsten of
46 kilocalories per mole (1.93×10^6 J/mole). Thus, the hydrogen
is strongly bonded to the tungsten surface. When the two tungsten
surfaces are brought into contact, the hydrogen at the interface

TABLE XVIII. - INFLUENCE OF VARIOUS

CHEMISORBED GASES ON FRICTION

COEFFICIENT OF TUNGSTEN

IN VACUUM

[Rider specimen, (100) atomic plane of
tungsten; sliding velocity, 0.001
cm/sec; load, 50 g (0.5 N); ambient
temperature, 20° C (293 K); ambi-
ent pressure, 10^{-10} torr.]

Chemisorbed gas	Coefficient of friction		
	For (110) plane	For (210) plane	For (100) plane
None	1.33	1.90	3.00
H_2	1.25	1.33	1.66
O_2	.95	1.00	1.30
CO_2	1.15	1.15	1.40
H_2S	1.00	----	1.35

reduces the amount of metallic adhesion by satisfying some of the
unsaturated tungsten bonds. As a consequence, a friction de-
crease is observed for all three atomic planes of tungsten in the
presence of hydrogen.

The amount of reduction in friction coefficient is, however,
a function of the particular atomic plane. It can be seen by ex-
amination of table XVIII that hydrogen was much more effective
in the chemisorbed layer in reducing the friction of (100) planes
in contact than it was in reducing the friction for (210) or (110)
planes in contact. The hydrogen sticking probability for the (100)
surface of tungsten is twice that of what is observed on its (110)
surface. The time necessary to form a monolayer of hydrogen
on the (100) tungsten plane is approximately one-third the time
necessary to achieve the same surface coverage for the (110)
plane (ref. 90). With the four gases examined on the three
atomic planes of tungsten, oxygen was the most effective on all
three atomic planes in the reduction of friction coefficient.

It is interesting to compare the heats of chemisorption for these various gases with a tungsten surface with the data of table XVI and the friction coefficients of table XVIII. Oxygen, which exhibits the highest heat of chemisorption to the tungsten surface, has the lowest coefficient of friction in table XVIII. Carbon dioxide in table XVI has a slightly lower heat of chemisorption than oxygen. Tungsten, with carbon dioxide present on the surface, exhibits friction coefficients intermediate between the values obtained for oxygen and hydrogen. Hydrogen, which has the lowest heat of chemisorption in table XVI, exhibits the highest coefficient of friction in table XVIII for tungsten in sliding contact with tungsten. Although heats of chemisorption were not available for hydrogen sulfied and tungsten, an examination of the friction data of table XVIII would indicate that the heats of adsorption for hydrogen sulfide to tungsten may be fairly near that of oxygen to tungsten. Thus, the friction coefficients for metal surfaces in contact in the presence of oxides are influenced by the atomic orientation of the metal surface. The data of table XVIII indicate that the atomic orientation of the surface is also important with chemisorbed species present on the surface. Even with monolayer films atomic orientation is important in observed or measured friction behavior for metals in contact.

KINETICS OF ADSORPTION

With metal surfaces in sliding, rolling, or rubbing contact in a vacuum environment, not only is it important that the chemisorbed gases interact with the surface to form protective surface films that will reduce adhesion, friction, and wear, but also the kinetics (the rate at which these films form) is also important. Where surfaces are in sliding, rolling, or rubbing contact at relatively high surface speeds with repeated passes over the same surface, it is necessary that the protective surface film form fairly rapidly to insure that on repeated passes a film has formed which can maintain separation of the surfaces and metal-to-metal contact. If chemisorption occurs at a very slow rate,

TABLE XIX. - CHEMISORPTION ON METAL FILMS (REF. 6)

Gas	Very fast chemisorption	Slow chemisorption	No chemisorption up to 0° C (273 K)
H_2	Ti, Zr, Nb, Ta, Cr, Mo, W, Fe, Co, Ni, Rh, Pd, Rh, Pd, Pt, Ba	Mn, Ca, Ge	K, Cu, Ag, Au, Zn, Cd, Al, In, Pb, Sn
O_2	All metals except Au	------------	Au
N_2	La, Ti, Zr, Nb, Ta, Mo, W	Fe, Ca(?), Ba	As for H_2 plus Ni, Rh, Pd, Pt
CO	As for H_2 plus La, Mn, Cu(?), Ag(?), Au(?)	Al	K, Au, Cd, In, Pb, Sn
CO_2	As for H_2 less Rh, Pd, Pt	Al	Rh, Pd, Pt, Cu, Au, Cd
CH_4	Ti, Ta, Cr, Mo, W, Rh	Fe, Co, Ni, Pd(?)	------------
C_2H_6	As for CH_4 plus Ni, Pd(?)	Fe, Co	------------
C_2H_4	As for H_2 plus Cu, Au	Al	As for CO
C_2H_2	As for H_2 plus Cu, Au, K	Al	As for CO less K
NH_3	W(?), Ni(?), Fe(?)	------------	------------
H_2S	W, Ni	------------	------------

then with repeated passes in the same contact area (as might occur in a mechanical device such as a bearing or gear) the chemisorbed gas that initially formed protective surface films may be worn away, and there may be insufficient time between repeated contacts for a new film to form. Such conditions increase the metal-to-metal contact, and ultimately seizure of the components can occur. It is, therefore, important to have some concept of the rates or the kinetics of chemisorption of various gases species with those metals of interest in vacuum, friction, and wear devices. Haywood and Trapnell have indicated the tendencies for various gases to chemisorb to various metal surfaces with respect to kinetics. These data are summarized in table XIX.

Table XIX indicates the specificity of chemisorption of gases to the metals referred to earlier. As indicated in table XIX many gases will adsorb very rapidly to a wide variety of elemental metals. There are some metals, however, in which the chemisorption process occurs very slowly. With still other metals no chemisorption is observed. Oxygen will chemisorb very rapidly to almost all metals except gold. In contrast, there are a large number of metals to which hydrogen will not chemisorb. Ethane chemisorbs very slowly to iron. Ethylene and acetylene, however, chemisorb very rapidly. Friction data obtained in vacuum with iron in sliding contact with itself in the presence of these three gaseous species indicate the friction coefficient with repeated passes over the same surface to be higher (markedly so) for ethane chemisorbed to iron than for ethylene and acetylene on the same surface.

Effect of Hydrocarbon Bond Saturation

Friction experiments on the three atomic planes of tungsten the (110), (210), and (100) with the three gases ethane, ethylene, and acetylene also indicate that the degree of bond saturation may exert an influence on the coefficient of friction for tungsten as indicated in table XX. With an increasing number of carbon-to-carbon bonds, a decrease in friction coefficient was observed for

TABLE XX. - INFLUENCE OF BOND SATURATION

OF CHEMISORBED GASES ON FRICTION

COEFFICIENT OF TUNGSTEN

IN VACUUM

[Rider specimen, (100) plane of tungsten; sliding veloc-
ity, 0.001 cm/sec; load, 50 g (0.5 N); ambient tem-
perature, 20° C (293 K); ambient pressure, 10^{-10}
torr.]

Chemisorbed gas	Coefficient of friction		
	For (110) plane	For (210) plane	For (100) plane
Ethane (H_3C-CH_3)	1.10	1.10	1.25
Ethylene (H_2C=CH_2)	.88	.85	1.20
Acetylene (HC=HC)	.70	.66	1.00

all three atomic planes of tungsten. The highest friction coeffi-
cient in each case was obtained in ethane. The lowest friction
coefficients were obtained with acetylene chemisorbed to the
tungsten surfaces. Erlich (ref. 102) discusses the influence of
the atomic structure of the metals on the adsorption process.
Arthur and Hanson, (ref. 103) discuss the influence of bond sat-
uration of hydrocarbons. In their studies with ethylene and acet-
ylene chemisorbed on iridium, they found that the activation
energy for desorption of acetylene was considerably higher than
it was for ethylene, indicating stronger bonding of the acetylene
to the iridium surface than for ethylene. This may also be true
for tungsten.

The degree of bond saturation exerts an influence on the
friction behavior of metals in contact with the adsorption of hy-
drocarbons. In addition to the degree of bond saturation, how-
ever, the chain length of the hydrocarbon which is chemisorbed
to a metal surface can also exert an influence on the friction be-
havior of metals in sliding contact. The data of figure 50 indi-
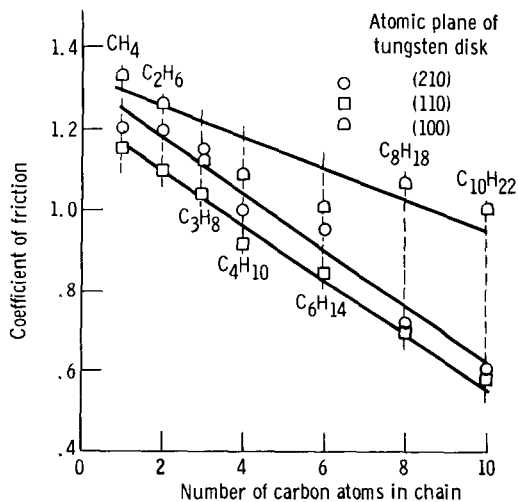cate the coefficients of friction on three atomic planes of tung-

Figure 50. - Coefficient of friction for single-crystal
tungsten rider (100) sliding on single-crystal disk
orientations (100), (110), and (210) with chemi-
sorbed monolayers of hydrocarbons. Gases,
homologous series methane through decane;
sliding velocity, 0.001 centimeter per second;
load, 50 grams (0.5 N); ambient pressure,
10^{-10} torr.

sten, the (210), (110), and (100), as functions of various hydro-
carbon chain lengths chemisorbed. The data are plotted as a
function of the number of carbon atoms in the chain length. It
can be seen from figure 50 that the friction coefficient decreases
with increasing carbon chain length in the hydrocarbons. On all
three atomic planes, the lowest coefficients of friction were ob-
tained with decane, and the highest coefficients of friction were
obtained with methane. These results were obtained with tung-
sten surfaces in a vacuum of 10^{-10} torr with the hydrocarbon
species bled into the vacuum system and allowed to chemisorb
or interact with the tungsten surfaces.

EFFECT OF HYDROCARBON CHAIN LENGTH

Hardy was one of the first to observe a relation between par-
affinic hydrocarbon chain length and the friction behavior for met-
al surfaces in contact. He conducted some sliding friction experi-

ments in air on steel surfaces with the normal oxides and surface contaminants present. Hardy was able, however, to find a relation between friction coefficient and paraffinic hydrocarbon chain length (ref. 104). Bowden and Tabor (ref. 4) later substantiated Hardy's observations. The interaction of long-chain hydrocarbons with metal surfaces and the nature of the hydrocarbon when bonded to metal surfaces has been discussed by Akhmatov (ref. 105).

Detailed examination of the physical adsorption process would indicate that physically adsorbed films do not provide the surface protection from adhesion and high friction that chemisorbed films (ref. 106) do. Gilbreath, in adhesion experiments in ultrahigh vacuum with oxygen free high conductivity copper, found, in fact, that physically adsorbed gaseous species exerted very little influence on the adhesion properties of metals. In contrast, however, he found that chemisorbed species exerted a marked influence on adhesion behavior (ref. 107).

FRICTION BEHAVIOR OF POLYMERS IN A VACUUM

There is a desire to use solid polymer compositions in many mechanical components requiring operation in a vacuum environment. The reason for the use of polymers in a vacuum environment is that some polymer compositions exhibit relatively low friction and wear behavior. Polymers such as polytetrafluoroethylene (PTFE) are known to exhibit low friction coefficients in an air environment, and it has been established that the elimination of moisture and oxygen from the environment does not appreciably alter the friction properties of PTFE. The good lubricating characteristics of PTFE bodies are inherent in the material itself.

PTFE has been used in vacuum lubrication applications as retainers for ball bearings. The bearing is normally operated without the benefit of any additional lubrication in vacuum. The PTFE cage or retainer material contacts the ball during operation. The contact of the ball with the PTFE retainer results in the transfer of PTFE from the solid body to the ball surface.

This thin transfer film is then carried to the ball-race contact zone preventing metal-to-metal contact. PTFE in such applications has proved to be a very effective lubricant. It has been found necessary, however, to include fillers in PTFE to prevent cold flow of the material.

Porous nylon is another material that has been used in a vacuum environment for the lubrication of bearings. Porous nylon has been impregnated with conventional oil lubricants and made into retainer materials for ball bearings. These impregnated retainers are used to lubricate the ball bearings in a vacuum environment. While in a vacuum and under rolling operation, the retainer continuously releases small quantities of oil from the polymer retainer which then is carried to the ball race contact zone and provides a conventional thin film of oil at the interface between the ball and race. This type of lubrication scheme was employed in the Tiros II satellite to lubricate radiometer bearings in the vacuum of space.

A relatively recent development in the field of polymer science are the polyimides. Polyimides appear to be promising materials for lubrication applications in a vacuum environment because of their extreme thermal stability. Polymers, in general, have very poor heat conduction characteristics.

In lubrication devices employing solid polymers, the generation of heat at an interface, associated with sliding or rubbing contact can produce local decomposition of the polymeric materials and severely limit the usefulness of the polymer as a lubricant in a vacuum environment. In air, heat can be dissipated from mechanical components in contact by conduction, convection, and radiation. In a vacuum environment, only radiation and conduction are available for the dissipation of frictional heat generated at the interface between sliding or rubbing surfaces. It might, therefore, be anticipated that polymers in lubrication mechanisms would be more sensitive to such parameters as load, speed, and ambient temperature when in a vacuum environment than they would be in a conventional air environment.

POLYTETRAFLUOROETHYLENE (PTFE)

Sliding friction studies have been conducted in vacuum with the most widely used polymer for lubrication application, PTFE. These experiments were conducted over a range of speeds with a glass-filled PTFE sliding on 440-C stainless steel, a conventional vacuum bearing alloy. A mass spectrometer was placed very close to the polymer metal interface, and the gaseous species generated at the interface between the two surfaces was monitored during the course of the friction experiment. The results obtained in these experiments are presented in figure 51.

In figure 51, ion concentration is plotted as a function of increasing sliding velocity for the PTFE composition sliding on 440-C stainless steel. The three mass-to-charge ratios that were monitored during the experiments were 19, 31, 50. These are some of the decomposition products which might be anticipated from PTFE. Figure 51 indicates that, with increasing sliding velocity, the concentration of decomposition products increases, indicating an increase in the amount of decomposition of the polymer at the sliding interface due to the frictional heat generated. Examination of the 440-C stainless-steel surface after sliding friction experiments indicated that a thin film of PTFE transferred to the stainless-steel surface.
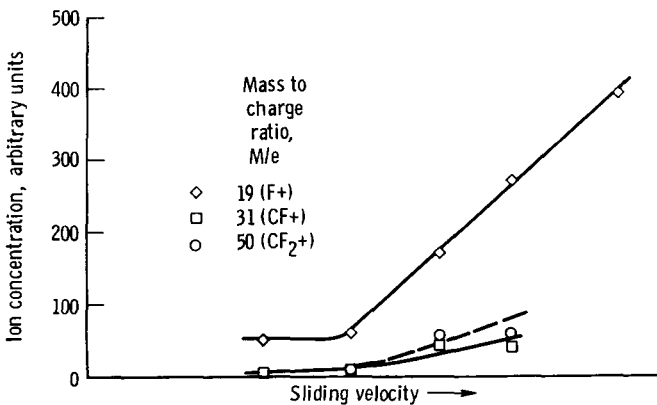

Figure 51. - Decomposition products as function of sliding velocity with 25 percent-glass - PTFE rider sliding on 440-C stainless steel.

This polymer is a poor thermal heat conductor. With the large amount of frictional heat generated at the interface with sliding, the frictional heat cannot be dissipated very readily by the polymer itself. While the metal surface would be a good conductor for heat, the presence of the transfer film of polymer to that surface inhibits its ability to dissipate the frictional heat generated during sliding. The sliding interface after a thin transfer film of polymer has developed on the 440-C stainless-steel surface is really an interface between the bulk polymer and the thin polymer film. At the interface there is polymer in contact with polymer. With increasing sliding speed, more and more frictional heat is put into the sliding system, and this frictional heat is dissipated in the decomposition of the polymeric material.

Adhesive wear normally occurs with a polymer in sliding contact with a metal surface. The polymer adheres to the metal surface, which accounts for the presence of the polymer film on the metal. Decomposition at the interface with sliding will increase the wear rate such that the total wear will reflect both adhesive wear of the polymer and wear due to the decomposition of the bulk polymer at the interface as a result of the frictional energy.

The PTFE specimen used in the sliding friction experiments of figure 51 contained 25 percent glass fibers. Some filler material is almost always used in polymers for lubrication applications because the polymer by itself is extremely susceptable to cold flow, which gives rise to a loss of dimensional stability in mechanical components. It is interesting to note that the glass actually has better conduction characteristics with respect to heat than does PTFE. The nature of the filler in PTFE can exert a marked influence on the nature of the decomposition process during sliding friction in vacuum. If 25 percent copper fibers are substituted for the 25 percent glass fibers in the PTFE composition of figure 51 and the same experiment is repeated in a vacuum sliding friction experiment on the same substrate surface, the ion concentration as a function of sliding velocity is notably different as indicated by the data of figure 52.
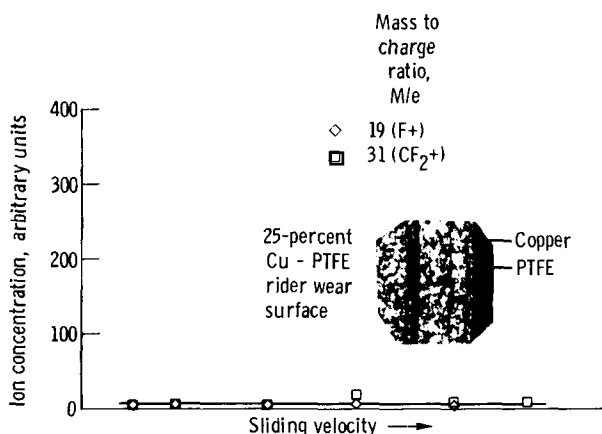
Figure 52. - Decomposition products of 25-percent-copper -
PTFE rider obtained in vacuum friction studies. Disk, 440-C
stainless steel; ambient pressure, 10^{-9} torr; no external
heating.

In figure 52 the mass spectrometer ion concentration in
arbitrary units for the m/e values of 19 and 31 are again plotted
as a function of sliding velocity. The only difference between the
experiments in figure 51 and those in figure 52 are that in fig-
ure 52 the PTFE contained 25 percent copper fiber rather than
25 percent glass fiber. In figure 52 the ion concentration was
extremely low at all sliding velocities examined. The range of
sliding velocities in figure 52 were the same as those examined
in figure 51, yet the concentration of decomposition products
from the polymer, PTFE, were markedly less in figure 52. The
difference in behavior is due simply to the substitution of copper
for glass as a filler material in the PTFE.

The photographic insert in figure 52 shows the PTFE wear
surface after completion of the sliding friction experiment in
vacuum. Microscopic examination of the surface indicated that
the copper fibers had become extremely flattened in the surficial
layer and covered a very large portion of the near surficial layer
cross-sectional area. The cross-sectional area of the wear sur-
face covered by copper was approximately 60 percent; a marked
increase over the actual composition of copper in the PTFE.
This increase in cross-sectional area was due to a deformation

of the copper increasing the contact area of the fibers by flatten-
ing the fibers. The entire surface of the PTFE specimen, how-
ever, contained a continuous film of PTFE. Thus in the sliding
process in figure 52 a thin film at the interface of PTFE was
interposed between 440-C stainless-steel surface and the bulk
polymer body just as in figure 51. In figure 52, however, the
high concentration of copper near the interface between the thin
film of PTFE and the 440-C stainless steel served as a good heat
sink to absorb the frictional heat generated in the sliding process
and thereby reduced and minimized the effect of wear by polymer
decomposition. The wear rate of the polymer in figure 52 was
markedly less than it was in figure 51 under identical mechanical
conditions of operation.

If, as figures 51 and 52 seem to indicate, the ability of the
materials at the interface to dissipate frictional heat has an in-
fluence on the behavior of the polymer in sliding contact, then
changing the subsurface containing material should also exert an
influence on the decomposition of the polymer. The substitution
of materials for 440-C stainless steel with better or poorer heat
conduction properties should then exert an influence on the ob-
served decomposition with sliding. Such experiments have been
conducted. The PTFE containing glass was made to slide on
three different substrate surfaces: An aluminum oxide disk sur-
face, which has poorer heat conduction characteristics than the
440-C stainless steel described in figures 51 and 52, and silver
and copper disk surfaces, which have markedly better heat con-
duction characteristics than the 440-C stainless steel used in
the experiments described in figures 51 and 52. Friction re-
sults obtained with glass-filled PTFE sliding on these three sur-
faces are presented in the data of figure 53.

An examination of figure 53 indicates that the concentration
of decomposition products for the mass-to-charge ratios of 12,
19, 20, 31, and 50 are somewhat greater for the aluminum oxide
than for the silver and copper disks. In light of the foregoing
discussion these results are expected. It is interesting to note,
however, that silver, which is a better heat conductor than cop-
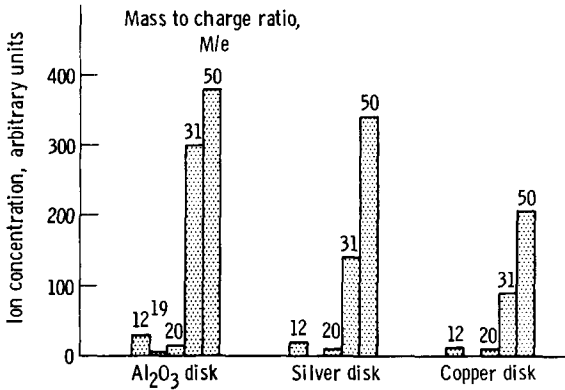per, exhibits a higher decomposition of the polymer in the slid-

Figure 53. - Mass to charge ratios for PTFE decomposition products obtained in vacuum friction studies. 15-Percent-glass - PTFE rider; sliding velocity, 216 centimeters per second; load, 1000 grams (9.8 N); ambient pressure, 10^{-9} torr; no external heating.

ing friction experiment as evidenced by the mass-to-charge ratios of figure 53 than did the sliding friction experiment with the copper. These results can be explained with the aid of figure 54. In figure 54 the coefficient of friction for the glass-filled PTFE composition sliding on the aluminum oxide, silver, and copper are presented. The data of figure 54 indicate that the friction coefficient for the polymer sliding on aluminum oxide was approximately the same as it was for copper. Thus the friction
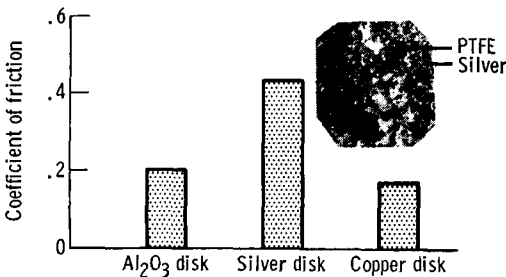

Figure 54. - Friction of 15-percent-glass - PTFE rider in vacuum. Sliding velocity, 216 centimeters per second; load, 1000 grams (9.8 N); ambient pressure, 10^{-9} torr; no external heating.

coefficients for the polymer on aluminum oxide is basically no
different from the friction coefficients obtained for the polymer
sliding on the copper surface. The reason for this similarity in
friction coefficient is as we mentioned earlier. A thin film of the
polymer transfers to the mating surface, in figure 54 to the
aluminum oxide and the copper surface. As a consequence, the
polymer is, in essence, sliding on a thin film of itself rather
than on the substrate material. The ability of that substrate
material to dissipate the frictional energy put into the interface
with sliding will, however, influence the wear as was mentioned
earlier.

The decomposition of the polymer sliding on aluminum oxide
was considerably greater than that sliding on copper. The wear
rate was correspondingly higher in that instance. While the fric-
tion coefficient in figure 54 for the PTFE sliding on aluminum
oxide and copper was essentially the same, the friction coeffi-
cient for the same glass-filled PTFE composition sliding on sil-
ver exhibited approximately twice the coefficient of friction that
it did for sliding on the other two surfaces. The reason for this
difference in friction behavior for the PTFE composition in slid-
ing contact with the silver can be explained with an examination
of the photographic insert of figure 54. The photographic insert
shows the wear surface of the PTFE composition after sliding.
A considerable amount of silver has transferred to the polymer;
approximately 80 percent of the surface of the contact region on
the polymer surface was covered with a film of silver. In the
sliding process, adhesion of the PTFE to the silver occurred
just as it did in the case of aluminum oxide and copper. Rather
than the PTFE transferring to the silver, however, the silver
transferred to the PTFE surface. As a consequence, silver was
actually sliding on silver at the interface. This accounted for
the higher coefficient of friction. The higher friction coefficient
for silver sliding on silver indicates that more frictional heat
was being put into the interface in the sliding process. This then
would account for the differences in the concentration of decom-
position products for silver and copper disks in figure 53.

One might normally anticipate that the silver would give the

lower concentration of decomposition products in figure 53. The higher friction coefficients due to metal sliding on metal with the associated higher frictional energy put into the interface accounts for the reversal of observed decomposition results of figure 53. The friction coefficients obtained for PTFE sliding on aluminum oxide and copper in figure 54 indicate that PTFE is, in fact, a good self-lubricating material for use in a vacuum environment. The friction coefficient of 0.2 or less are normally associated with effective boundary lubrication. Under equivalent conditions of sliding in air with a very good conventional boundary lubricant, such as an oil or grease, friction coefficients of 0.05 to 0.1 would normally be achieved. The data of figures 51 to 54 do indicate, however, that the presence of filler materials in the polymer composition and the nature of the mating surface with which the polymer is in contact can markedly influence the wear and friction observed. In most practical lubrication mechanisms, the friction results obtained with the silver surface in figure 54 would not be encountered. Normally, very hard steels, such as 440-C, are used in contact with the polymer.

POLYIMIDE

Polymers having the polyimide structure are promising materials for use in vacuum lubricated devices. They exhibit very good thermal stability because of their molecular structure. The polyimide molecular structure is shown in figure 55. It is a ring structure which contains both nitrogen and oxygen. The ring structure imparts good thermal stability to the material. Friction studies have been conducted with the polyimide in a vacuum
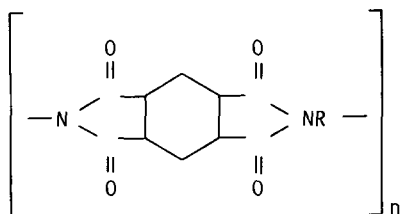

Figure 55. - Polyimide structure.

environment (ref. 108). In general, the coefficient of friction for a polyimide polymer sliding on 440-C stainless steel, the same base material that was used for the sliding of PTFE compositions, is approximately 0.2. The wear for the polyimide was considerably less than that for the PTFE. Again, just as with PTFE, the thermal conduction properties on the mating surface with which the polyimide makes contact can exert a marked influence on friction and wear behavior in a vacuum environment.

Some sliding friction experiments have been conducted with the polyimide sliding on 440-C stainless steel and on itself. The friction coefficient for the polyimide sliding on the 440-C stainless steel after a transfer film had developed was approximately 0.2. With the polyimide sliding on a mating surface of itself, the friction coefficient was 0.5. Further, the total amount of wear that occurred for the polymer sliding on itself was markedly greater. Figure 56(a) shows a photomicrograph of the 440-C disk surface in the region contacted by the polyimide. Also shown in figure 56(a) is a surface profile across the contact region after sliding. The surface profile trace indicates no evidence of a change in the nature of the surface topography of the

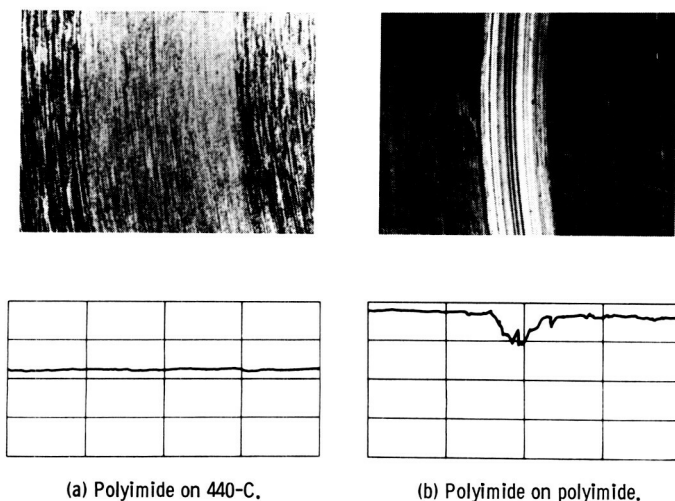(a) Polyimide on 440-C.   (b) Polyimide on polyimide.

Figure 56. - Photomicrographs and surface profile traces for polyimide sliding on 440-C stainless steel and polyimide in vacuum (10^{-9} torr). Load, 1000 grams (9.8 N); no external heating; experiment duration, 1 hour.

440-C stainless steel as a result of sliding.

In figure 56(b) a photograph and surface profile trace are presented for the polyimide after sliding on itself. With the polyimide sliding on itself, the width of the wear track was less than that observed for the polyimide sliding on the 440-C stainless steel. But, with the polyimide sliding on itself, rather than wear being detectable to the polyimide slider, both surfaces underwent wear (fig. 56(b)). The slider reflected wear, and the polyimide mating flat surface also exhibited considerable wear as indicated by the surface profile trace in figure 56(b). Note in figure 56(b) that the polymer has been removed from the surface by the flat. The friction coefficient for the polyimide sliding on itself was two and one half times that for the polyimide sliding on the 440-C stainless steel.

With the polyimide sliding on itself, its poor ability to dissipate frictional energy generated as heat at the sliding interface resulted in the localized decomposition in the interfacial layer of the polymer composition, which contributed to the wear of the polymer, just as was observed with PTFE. The presence of fillers in the polyimide will influence its friction and wear behavior. Friction studies and wear studies have been conducted in vacuum with a polyimide containing various percentages of copper fiber sliding on the bearing steel 440-C. The object of such experiments was to determine whether an improvement or reduction in wear could be achieved with the polyimide by the addition of metal filler just as was observed with PTFE. Friction results obtained in some of these experiments are presented in figure 57.

In figure 57, friction coefficient and rider wear rate in cubic centimeters per meter of sliding are plotted as a function of the copper fiber content in weight percent up to 50 weight percent of copper fibers. The friction coefficient for the unfilled polymer, as was mentioned earlier, was approximately 0. 2. With the addition of as little as 10 weight percent copper fiber to the polyimide, the friction decreased to a value of approximately 0. 05, or one fourth the value for the unfilled polymer. Further additions of copper to the polyimide did not result in any further
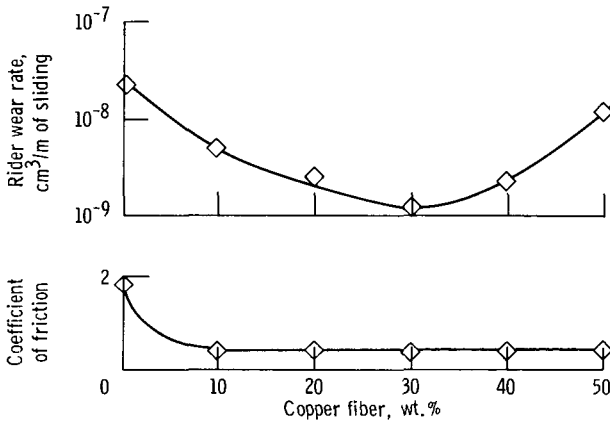
Figure 57. - Influence of copper-fiber filler in polyimide on friction and wear for polyimide sliding on 440-C stainless steel in vacuum (10^{-9} to 10^{-10} torr). Sliding velocity, 197 centimeters per second; load, 1000 grams (9.8 N); experiment duration, 1 hour.

decrease or change in the friction coefficient for the polyimide sliding on the 440-C stainless steel.

The addition of copper fiber to 30 weight percent resulted in a continuous decrease in the wear rate of the polyimide from the unfilled state. The copper acts in the same capacity in the polyimide as it did in the PTFE; it assists in the rejection of frictional heat generated at the sliding interface. At some point it might be anticipated that sufficient copper would be present at the interface such that copper would begin to contact across at least a portion of the true contact area with the 440-C stainless steel. This is what was observed. In figure 57 at copper concentrations of 40 to 50 weight percent, sufficient copper is present in the surficial region that it begins to make contact with the 440-C stainless steel and a portion of the friction force measured is due to adhesion and shearing of the copper resulting in a disruption of the polymer transfer and an increase in the wear rate. Thus, for the addition of a copper fiber to the polyimide, the presence of a copper fiber reduces friction and wear over the unfilled material. With respect to wear, however, there is an optimum concentration of metal-fiber in the polymer. From the

data of figure 57 it is 30 weight percent.

Examination with a mass spectrometer of the gaseous spe-
cies liberated from a sliding interface with the polyimide in con-
tact with 440-C stainless steel indicated that the concentration
of decomposition products liberated from the polymer with in-
creasing sliding velocity are markedly less than was observed
with PTFE in identical experiments.   The polyimide appears to
be more resistance to degradation from the frictional energy that
develops at the interface.   The data of figure 58 indicate the su-
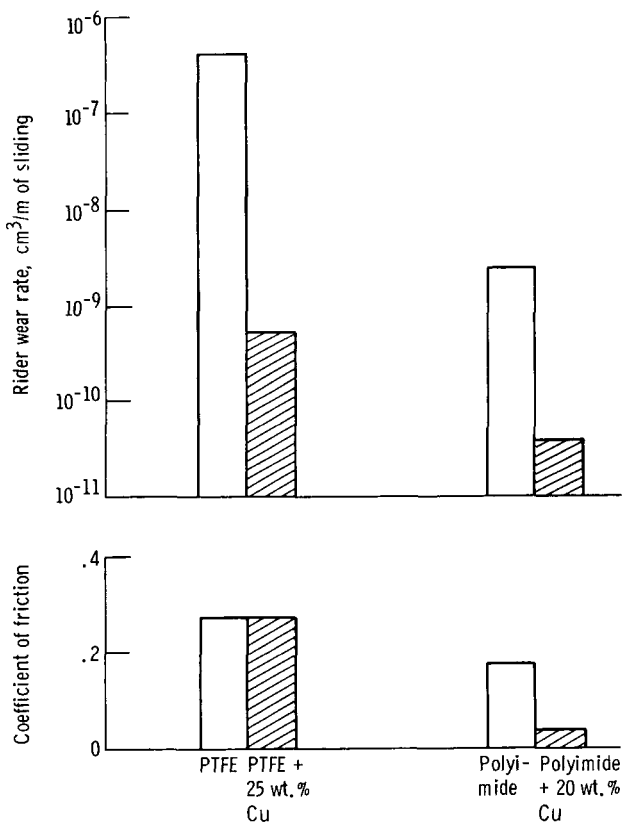perior friction and wear of polyimide, both filled and unfilled, to

Figure 58. - Comparison of coefficient of friction and rider
wear for PTFE and polyimide compositions sliding on
440-C stainless steel in vacuum (10^{-10} torr). Sliding
velocity, 197 centimeters per second; load, 1000 grams
(9.8 N); experiment duration, 1 hour; no external
heating.

that of PTFE, both filled and unfilled. Examination of figure 58
indicates that the friction coefficient for PTFE unfilled and with
copper present is approximately the same, a value slightly in
excess of 0.2. The presence of the copper filler in the PTFE
appreciably reduced wear. The addition of copper to polyimide
reduced its friction as well as its wear in sliding contact with
440-C stainless steel. The data of figure 58 indicate for both
filled and unfilled polyimides that the friction and wear behavior
are superior to that of PTFE in identical friction and wear
studies.

With polymers in sliding contact with surfaces other than
themselves, it appears that a transfer film of the polymer to the
mating surface must form to achieve an effective reduction in
friction and wear and good boundary lubrication. The presence
or absence of the transfer film on the mating surface will exhibit
a marked influence on observed friction behavior as indicated by
the data of figure 59. The data of figure 59(a) are a plot of the
coefficient of friction for a 20 percent copper filled polyimide
composition sliding on 440-C stainless steel in a vacuum of 10^{-10}
torr as a function of the number of passes over the same surface.
At a relatively low number of passes over the same surface, the
friction coefficient is extremely high, 0.6. After a certain num-
ber of passes, the friction coefficient decreased to a value of
less than 0.05 and remained low for more than 5000 passes over
the same surface. If the region of the curve near the ordinant
was expanded such that the friction coefficient is plotted as a
function of the number of passes for a relatively small number of
total passes, a gradual change and decrease in friction would be
observed as shown by the data of figure 59(b).

Figure 59(b) represents the friction coefficient for the polyi-
mide sliding on 440-C stainless steel for 13 passes. It can be
seen that, with each pass over the surface, the friction coeffi-
cient decreases for up to 11 passes. Little change in friction is
observed in the 12th and 13th passes. This general decrease in
friction coefficient with repeated passes over the same surface
reflects the development of a transfer film of a polyimide to the
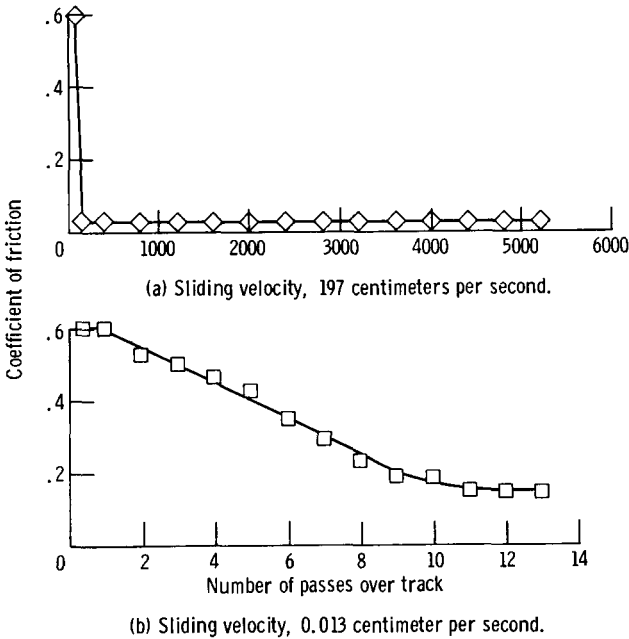440-C stainless-steel surface. In the first pass, the friction

(a) Sliding velocity, 197 centimeters per second.

(b) Sliding velocity, 0.013 centimeter per second.

Figure 59. - Coefficient of friction for 20-weight-percent copper-
powder - polyimide rider sliding on 440-C stainless steel in
vacuum (10^{-10} torr). Load, 1000 grams (9.8 N); ambient tem-
perature, 25° C (298 K).

coefficient is associated with the polyimide sliding directly on
the 440-C stainless steel. With each subsequent pass, the
amount of the true contact area covered by the polymer film in-
creases until ultimately at a certain number of passes the entire
surface becomes covered with the polymer film, and the friction
coefficient achieves some equilibrium value. These data indi-
cate that, in practical lubrication devices using polymers in a
vacuum environment, it is extremely important that a transfer
film of the polymeric material at the mating surface be devel-
oped. This frequently can be achieved by a practice which is
commonly called run-in. The running in allows for the develop-
ment of the transfer film.

ADVANTAGES OF SOLID POLYMER BODIES

Thin films of polymers deposited on metallic surfaces have

also been used to provide low friction and wear for material surfaces in contact in a vacuum environment. Such thin polymer films will provide effective lubrication by reducing friction and wear in a vacuum. However, where long endurance lives are required for mechanical components, it would appear that the use of solid polymeric bodies as one component in the system would be desirable. The advantage of using a solid polymer for such service is that the polymer body will provide a continuous supply of the polymeric material. For example, as was mentioned earlier with ball bearings in rolling contact in a vacuum, the ball of the ball bearing can, if the retainer or cage material is a polymer composition, pick up from the cage or retainer polymer and carry that polymer to the ball-race contact zone. The cage or retainer, the solid polymer body, then serves as containuous source for additional polymer should the polymer film that develops at the interface between the ball and the race of the bearing rupture or wear away. If simply a thin film of the polymer is used on the components themselves when the thin film is either ruptured or worn away, there is no source for replenishing the polymer material and the bearing may fail because of the lack of lubricant.

SOME ADDITIONAL FACTORS RELATING TO WEAR IN VACUUM

When two metal surfaces are in sliding, rubbing, or rolling contact in a vacuum environment, as has already been discussed, adhesive wear can take place because of adhesion across the interface. Adhesion occurs on the development of clean surfaces which were generated during rubbing, rolling, or sliding contact. When the two metals in contact are the same, adhesion occurs across the interface, and with tangential motion fracture may occur at the interface or subsurface in one of the two mechanical components in a manner described earlier with reference to the zones of greatest mechanical weakness. When subsurface fracture occurs, particles will generally transfer from one surface to another. The process of transfer of particles continues with

sliding, rolling or rubbing contact. In the case of mechanical devices where close tolerances are employed, this transfer will frequently result in the destruction of the operating clearance between the mechanical components and in the failure of that component.

When dissimilar metals are in contact in a vacuum environment, with sliding, rolling, or rubbing contact in the absence of a contaminating or lubricating film, the adhesion process will generally result in the transfer of particles of the cohesively weaker of the two materials to the cohesively stronger. The adhesive junctions generally being stronger than the cohesive bond of the cohesively weaker of the two materials. This transfer results in adhesive wear. If repeated contact is made over the same general area, sufficient adhesive wear particles will transfer from the cohesively weaker to the cohesively stronger material such that after a period of time the surface of the cohesively stronger material will be well populated with transferred wear particles. With continued motion over the same surface, the weaker of the two materials will begin again to transfer back to itself much as if the two materials in contact were the same metal.

With metallic alloys in sliding, rolling, or rubbing contact, even in the absence of contaminating surface films provided by the environment, adhesion and complete seizure is frequently not encountered. The absence of adhesion or complete seizure of alloys in contact in a vacuum environment in many instances is due to the presence of minor alloying constituents which can, on heating of the surfaces by the frictional energy put into the surfaces during sliding, rolling, or rubbing contact, diffuse to the surface and provide a protective surface film. Sulfur and carbon in steels as was discussed earlier will on relatively modest heating diffuse to a surface and occupy a concentration at the surface far in excess of their concentration in a bulk. Frequently, parts per million of alloying elements such as carbon and sulfur are sufficient to inhibit appreciably the adhesion of metallic alloys, thereby minimizing their friction and adhesive wear in a vacuum environment. Iron sulfide is particularly

effective in reducing adhesive wear. Sulfur-containing organic materials are frequently added to conventional lubricants to provide reaction films on steel surfaces that contain iron sulfide because of the wear resistance provided to iron-base surfaces by iron sulfide.

Vacuum not only radically affects the wear behavior of metals and alloys in contact, but it also has a pronounced influence on nonmetals as well. Mechanical carbons in the absence of adsorbed surface films, particularly moisture and hydrocarbons, exhibit extremely high rates of wear. Figure 60 presents two photomicrographs taken of different hemispherical specimens which were in sliding contact with 440-C stainless steel. In figure 60(a) the sliding experiment was conducted in air at 760 torr, the wear scar after a fixed period of sliding can be seen in the center of the photograph. When the same experiment was repeated in a vacuum environment, the wear scar increased many times as indicated by the photograph of figure 60(b). In addition, in figure 60(a) examination of the 440-C stainless steel revealed the presence of a transfer film of carbon to the 440-C stainless-steel surface with the carbon basically sliding on itself. In figure 60(b) metal was observed to transfer to the carbon surface, in addition to the high rates of wear that were observed for the graphite carbon in the absence of adsorbed moisture and hydrocarbon vapors.

Metals and carbons are quite different materials, but the mechanism which gives rise to wear of the two classes of material in a vacuum environment is not too different. For metals in contact in a vacuum environment, the absence of oxides and adsorbates gives rise to increased metal-to-metal contact, adhesion, subsurface fracture, and the generation of wear particles. If fracture occurred at the interface, no wear would occur. With carbon in sliding contact with itself, the process is somewhat similar. In the presence of adsorbates the graphitized carbon will slide on a thin transfer film of itself with a minimum in friction and adhesion. When adsorbates are removed from the graphite carbon body, however, the adhesion of the carbon to metal surface increases. The strength of the carbon-to-carbon

(a) Air (760 torr).

Metal

CS-29236
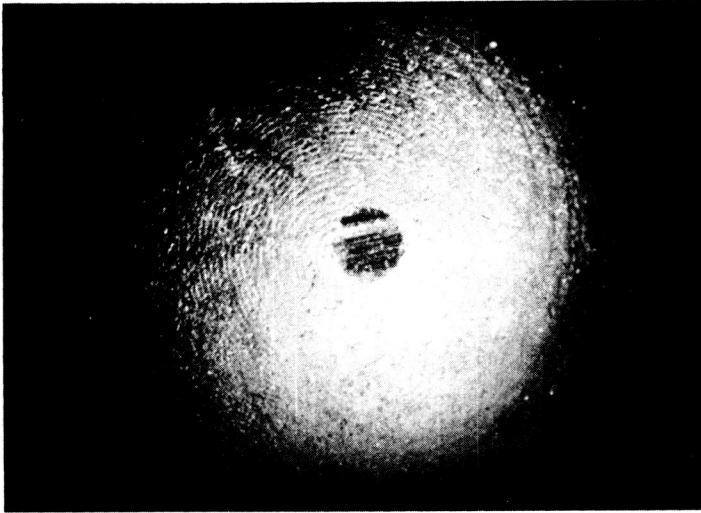
(b) Vacuum (10^{-7} torr).

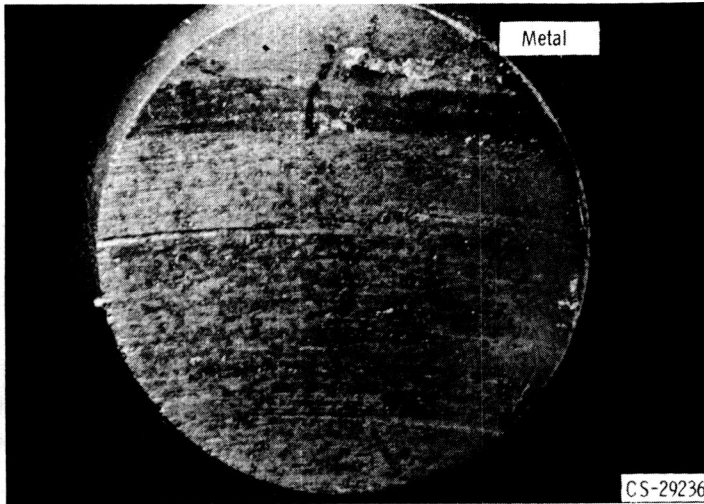Figure 60. – Photomicrographs of wear areas on 100-percent electrographitized carbon rider specimens tested in air and vacuum. Disk specimen, 440-C stainless steel; sliding velocity, 216 centimeters per second; load, 1000 grams (2.8 N); duration of experiment, 1 hour. X20.

bonds increases because of the absence of the adsorbates result-
ing in a subsurface fracture in both the metal and the carbon or

in the carbon alone depending on the relative weaknesses of the
various fracture regions.

CONVENTIONAL LUBRICATION

An area that has not been discussed thus far is the effect
that vacuum environment has on the behavior of conventional
lubricants in their lubrication of surfaces. There are many
mechanical devices in which conventional lubricants must be
used, and it is of interest to know what influence a vacuum en-
vironment will have on the lubricating ability of these materials.
The first point of consideration is the volatility of the lubricant
in the vacuum environment. Most conventional lubricants will
exhibit relatively high evaporation rates in a vacuum environ-
ment; for example, the conventionally used ester aircraft lubri-
cant diethylhexylsebacate will boil when it is placed in an open
vacuum chamber. Thus, in a relatively short period of time the
lubricant could be lost from the surface due to evaporation and
ineffective lubrication provided for the surfaces in contact. In
general, the evaporation of the bulk fluid from the system may be
relatively high. The last chemisorbed monolayer, however, may
require a greater amount of energy for its removal from the sur-
face than the evaporating bulk fluid.

In devices where sliding, rubbing, or rolling contact are in-
volved, the frictional heat generated from frictional energy put
into the surfaces can bring about desorption of these species and
ultimately lead to solid material contact. Those fluids that have
relatively low vapor pressures may be useful, however, to lubri-
cate mechanical devices in relatively modest vacuum environ-
ments. Reichenbach (ref. 109) has conducted experiments with
fluid lubricants in air and in vacuum to determine the influence
of a modest vacuum on the wear behavior of 52100 bearing steel.
The experiment consisted of cross cylinders in contact with one
of the rotating cylinders. After rotating in contact under fixed
load for a set period of time, the wear scars on the cylinders
were measured. The wear scar diameters on the cylinders with
refined mineral oil lubricating 52100 bearing steel in air and in

a modest vacuum of 10^{-5} torr are presented in figure 61(a). The wear scar diameter is plotted in figure 61(a) as a function of contact load on the two cross cylinders in kilograms. With the increase in contact load in air, the wear scar diameter increases as one might expect. In a vacuum of 10^{-5} torr the wear scar diameter is greater at all loads than it was in air.

The modest vacuum was sufficient to cause the refined mineral oil to degas, which resulted in an increase in the rider
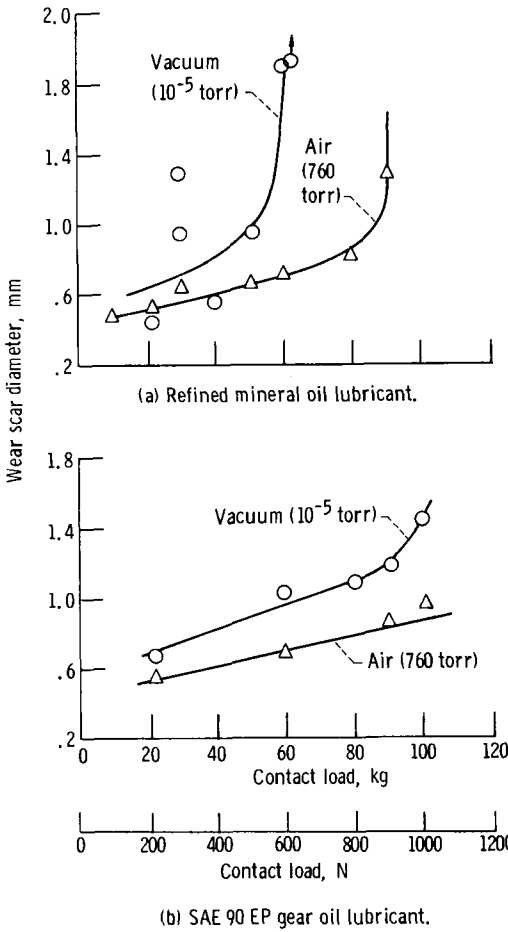
Figure 61. - Cross-cylinder load-carrying tests. Hardened 52100; diameter, 0.64 centimeter; cylinder speed, 95 rpm; experiment duration, 1 hour; ambient temperature, 20° C (293 K) (ref. 108).

wear. Gases entrained in conventional oil lubricants include oxygen, water vapor, and nitrogen. Oxygen and water vapor help protective surface films to form on the steel surfaces. These films minimize wear for two solid surfaces in contact. When the fluids are degased and the oxygen and water vapor are lost from the fluid, the beneficial effects of oxygen and water vapor are lost, and an increase in wear of the surfaces in contact is observed. The lubricant becomes less effective in a vacuum environment than it was in air.

The lubricant used to obtain the data of figure 61(a) was a simple paraffinic, refined mineral oil lubricant with no additives. A refined mineral oil which contained additives that would assist in the formation of protective surface films on the metal surfaces was used to produce the data of figure 61(b). The same wear experiments were performed for both lubricants. The lubricant in figure 61(b) was a SAE 90 EP gear oil. (The EP indicates that an additive has been placed in the oil to provide effective boundary lubrication under extreme loading conditions.) An examination of the wear data in figure 61(b) indicates that the presence of the additive does improve the load carrying capacity of the fluid. In figure 61(b) the wear scar diameter was measured in air to contact loads of 100 kilograms. In figure 61(a) the wear scar diameter has become appreciable at such loads. Thus, the EP additive in air reduces the wear scar diameter by providing a reactive surface film which minimized the adhesive metal-to-metal contact at the interface between the two metal surfaces.

Comparing the wear scar diameters in figure 61(b) with those of 61(a) in a vacuum of 10^{-5} torr shows that the wear scar diameter in a vacuum environment in the presence of an EP oil was less than that in the absence of the surface active agent. Thus, the extreme pressure, which is added to the fluid to provide a protective surface film, still operates in this capacity even at reduced ambient pressures. The selection of the additive is extremely critical. The extreme pressure additive, must have a relatively low vapor pressure. If the additive is highly volatile (higher than that of the base lubricant fluid), the additive could be lost from the fluid just as were oxygen and water vapor

in figure 61(a). The data of figure 61 indicate the importance of
adding materials to conventional lubricants that have relatively
low volatility and can prevent adhesive wear from occurring when
those fluids are to be used as lubricants in a vacuum environ-
ment. When it is desirable to use conventional lubricants, mo-
lecular flow seals can be provided to minimize losses of the
fluids due to evaporation to the vacuum environment.

There are many techniques that can be employed to reduce
the friction and wear between solid surfaces in contact in a vac-
uum environment. The most obvious is the use of some conven-
tional oil or grease lubricant to reduce friction, adhesion, and
wear. Where conventional organic lubricants such as oils and
greases are used in a vacuum environment, the factor of great
importance is the volatility or the evaporation rate behavior of
that particular lubricant in a vacuum environment. In experi-
ments with various organic fluids in a vacuum environment, for
any particular class of fluids the molecular weight will have an
influence on the volatility of the fluid. Thus, if a particular
class of fluids is to be used, for example, the glycols, then it is
advantageous to use a high molecular weight fluid. At a fixed
temperature in the vacuum environment the higher the molecular
weight the lower will be the rate of evaporation.

Nearly all conventionally used organic fluid lubricants con-
sist of a fluid which is representative of a range of molecular
weights rather than a specific molecular weight. There is a mo-
lecular weight distribution then in the fluid. As a consequence,
when the fluid is used in a vacuum environment, the initial evap-
oration rates will, very frequently, be higher than the rates after
prolonged evaporation when the lighter molecules or fragments
have been lost. When greases are used in a vacuum environ-
ment, the evaporation rates of the grease will be dictated gener-
ally by the evaporation rate of the base fluid or oil used in that
grease because the base fluid will generally have a higher vola-
tility than will the thickener.

Evaporation rate experiments conducted with a grease con-
taining a chloromethylphenylsilicone base fluid and a lithium
stearate thickener have indicated that in a vacuum the evapora-

tion rates at various temperatures for the grease were basically the same as that for the base fluid chloromethylphenylsilicone. When the base fluid had been lost because of evaporation, a change in the slope of the rate of evaporation with temperature occurred because of the evaporation of the less volatile lithium stearate thickener. It is conceivable that in some situations the thickener might have a higher volatility than the base fluid in which case the thickener would volatilize before the base fluid.

The evaporation rate of conventional organic lubricant films in a vacuum environment is a function of the area of the film exposed to the vacuum. Thus, the loss of conventional organic oils and greases from devices in a vacuum environment can be minimized if the area exposed to a vacuum environment is appreciably reduced. This can be achieved by a number of techniques. One such technique is that of employing molecular flow seals to minimize the loss of the oil in such mechanical components as rolling element bearings. The necessary equations for calculating losses when utilizing molecular flow seals to inhibit the loss of volatile materials from a system can be obtained from the literature (ref. 110).

Another method that has been used to reduce the loss of conventional organic oils in a vacuum environment has been to impregnate porous materials such as polymeric structures with an oil. This will reduce or inhibit the loss of the fluid to the vacuum environment and provide a continuous reservoir for the fluid to the solid surfaces in contact.

SOLID FILM LUBRICANTS

Although conventional organic oil and grease films have been effectively used in a vacuum environment to reduce friction and wear, there are many areas in which conventional organic fluids cannot be used. One area, for example, may be where the temperatures are above the normal ambient. Under such conditions the volatility of many fluids at temperatures slightly above ambient in a vacuum environment may be high enough to prohibit their use. Another area where conventional lubricants

are difficult to use exists where there are devices in the same
system that cannot tolerate contamination by the condensation of
organic films. In the areas just mentioned, it is the practice to
use inorganic solid-film lubricants. The advantage of inorganic
solid-film lubricants is that in general they have lower volatility
and higher dissociation temperatures. Inorganic compounds such
as molybdenum disulfide, tungsten disulfide, molybdenum di-
selenide, and niobium diselenide are frequently used in vacuum
lubrication systems to inhibit adhesion, friction, and wear.

LAYERED LATTICE COMPOUNDS

Compounds such as molybdenum disulfide have low volatility
rates in a vacuum environment and do not begin to dissociate
until temperatures of 730° C (1003 K) are achieved. Thus, such
inorganic compounds provide a very useful source of materials
to lubricate solid surfaces over a broad temperature range in a
vacuum environment (ref. 111). Graphite, when rubbed on solid
surfaces, is a good lubricant in an air environment, but it is in-
effective as a thin-film lubricant in a vacuum as indicated by the
data of table XXI taken from reference 112.

In table XXI friction data are presented for both natural and
pyrolitic graphite in air and in a vacuum of 10^{-9} torr. The fric-
tion coefficients for both natural and pyrolytic graphite are more
than two times higher in vacuum than they are in air. This is
due to the adhesion of graphite to itself as was mentioned earlier.

TABLE XXI. - FRICTION DATA FOR GRAPHITE

AND BORON NITRIDE (REF. 112)

Solid	Coefficient of friction		Pressure, torr
	Air	Vacuum	
Natural graphite compact	0.19	0.44	6×10^{-9}
Pyrolytic graphite	.18	.50	2×10^{-9}
Hot-pressed boron nitride	.25	.70	2×10^{-9}

Boron nitride, which has a layer lattice structure much like that of graphite, exhibits in air a friction coefficient of 0.25. In a vacuum environment, however, the friction coefficient is 0.70 (see table XXI). Thus graphite and boron nitride, although they are layer lattice compounds, do not have inherently good lubricating characteristics. Their lubricating characteristics depend on the presence of adsorbates that come from the environment. In the absence of these adsorbates, graphite and boron nitride should not be used in vacuum lubrication applications. Even in air boron nitride's ability to lubricate surfaces is questionable and therefore should definitely be avoided in vacuum.

Although a layer lattice structure itself does not determine that a material will be a good lubricant, many of the inorganic compounds possessing a layer lattice structure are, in fact, good lubricants in vacuum. Flom and Haltner (ref. 112) have obtained friction data in air and vacuum for a number of inorganic compounds possessing a layer lattice structures. Some of these data are presented in table XXII. If an arbitrary friction coefficient of 0.2 is assumed to be associated with effective boundary lubrication, the friction properties of many of the compounds in table XXII would qualify as effective boundary lubricants for vac-

TABLE XXII. - FRICTION DATA FOR SOME

LATTICE COMPOUNDS (REF. 112)

Solid	Crystal system	Coefficient of friction		Pressure, torr
		Air	Vacuum	
MoS_2	MoS_2	0.18	0.07	2×10^{-9}
WS_2	MoS_2	.17	.13	3×10^{-9}
WS_2	MoS_2	.17	.08	1×10^{-5}
BiI_3	AsI_3	.34	.39	5×10^{-7}
LiOH	LiOH	.37	.21	2×10^{-9}
$CdCl_2$	$CdCl_2$	.35	.16	2×10^{-9}
CdI_2	CdI_2	.24	.18	2×10^{-9}
$CdBr_2$	CdI_2	.22	.15	2×10^{-9}
Phthalocyanine	-----	.35	.33	1×10^{-6}

uum. The two materials in table XXII that exhibit friction coeffi-
cients markedly higher than 0. 2 are bismuth iodide and phthal-
ocyanine. In table XXII all the solid lubricants except bismuth
iodide and phthalocyanine exhibit a lower friction coefficient in
vacuum than in air.

It is interesting to contrast the data of table XXII with that of
table XXI. In table XXI materials such as graphite and boron
nitride require adsorbates for their lubricating properties, and
the friction coefficients increase when these materials are used
as thin films in a vacuum because the adsorbed surface films are
lost. With the materials in table XXII the loss of adsorbed sur-
face films, principally water vapor, actually enhances the lubri-
cating properties of the layer lattice compounds. The influence
of adsorbed films on the lubricating behavior of layer lattice
compounds has been thoroughly investigated (refs. 113 to 119).
Not only do many of the compounds in table XXII provide more
effective boundary lubrication and lower friction in vacuum than
in air, but many of these compounds encountered in air are
actually corrosive to the surfaces that they are lubricating be-
cause of the presence of adsorbed water vapor. Thus, as shown
in table XXII a vacuum environment is actually advantageous to
friction behavior of materials surfaces in contact.

Molybdenum disulfide is probably the first inorganic solid
to be suggested as a lubricant for a vacuum environment
(ref. 120). Since its initial recommendation for use in vacuums,
considerable research has been put into studying the lubrication
behavior of molybdenum disulfide in a vacuum environment.
References 113, 114, 117, 119, 121, and 122 all concern the
lubrication behavior of molybdenum disulfide and molybdenum
disulfide films in a vacuum environment. The references cited
are by no means inclusive. The total number of research papers
that have been devoted to this subject are too numerous to cite
here.

Brainard (ref. 111) measured the friction properties of
metal surfaces lubricated with molybdenum disulfide and other
dichelconides in a vacuum environment over a range of temper-
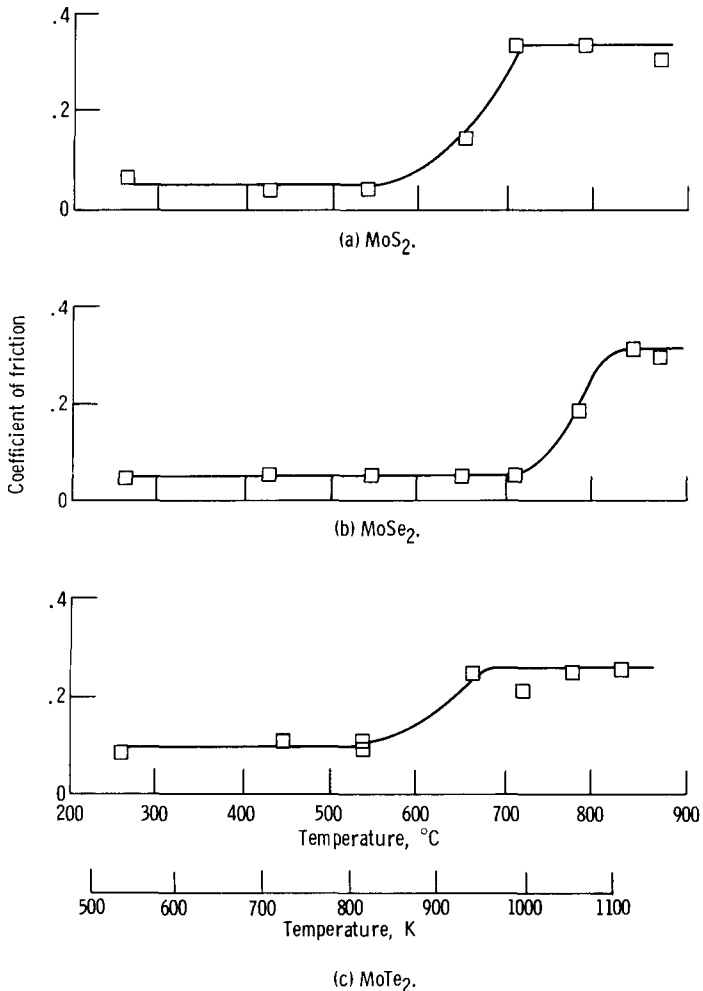atures. Some of the data he obtained are presented in figures

Figure 62. - Coefficient of friction for MoS_2, $MoSe_2$, and $MoTe_2$ film
lubrication at various temperatures. Exposure time, 60 minutes
in vacuum (10^{-8} to 10^{-6} torr); sliding velocity, 2.0 centimeters
per second; load, 100 grams (1.0 N) (ref. 110).

62 and 63.   In figure 62 the friction coefficient is plotted as a
function of temperature for three inorganic compounds present
on metal surfaces as thin rubbed films.   The compounds are
molybdenum disulfide in figure 62(a), molybdenum diselenide in
figure 62(b), and molybdenum ditelluride in figure 62(c).   It can
be seen from figure 62 that for all three inorganic compounds
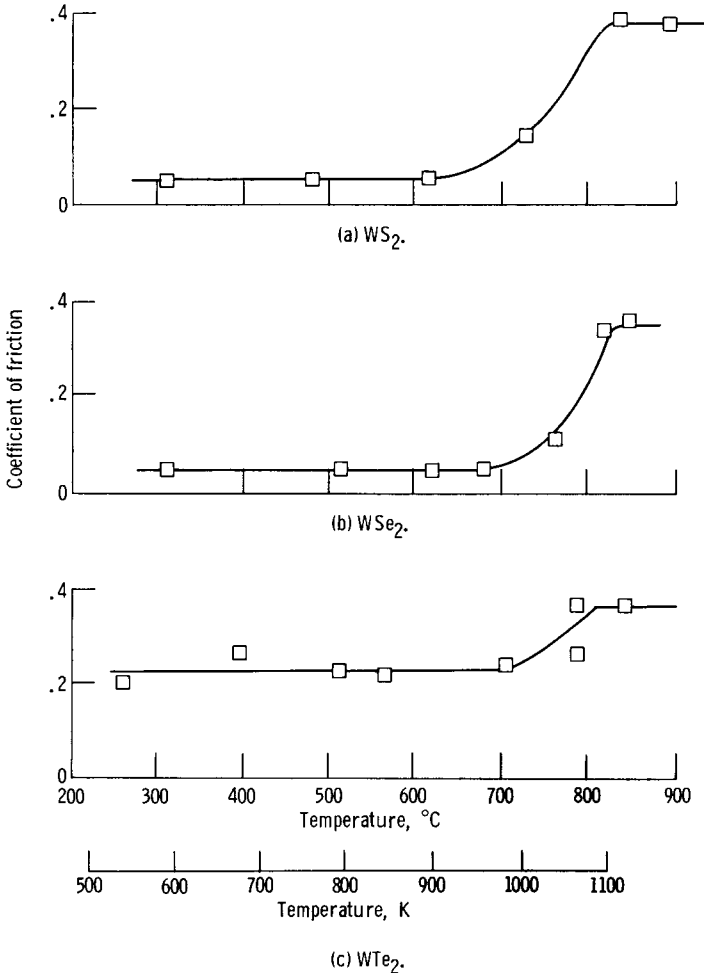the friction coefficients were less than 0.1 at 20° C (293 K).

Figure 63. - Coefficient of friction for WS_2, WSe_2, and WTe_2 film lubrication at various temperatures. Exposure time, 60 minutes in vacuum (10^{-8} to 10^{-6} torr); sliding velocity, 2.0 centimeters per second; load, 100 grams (1.0 N) (ref. 110).

With molybdenum disulfide the friction coefficient remained low at temperatures to 550° C (823 K) at which time the friction coefficient began to increase ultimately reaching a value of 0.4. The increase in friction coefficient at about 550° C (823 K) is associated with the dissociation of molybdenum disulfide into molybdenum and sulfur. Brainard measured with a vacuum dissociation apparatus the temperatures at which dissociation com-

menced for these various inorganic compounds and found that
molybdenum disulfide begins to dissociate at 730° C (1003 K) in
a vacuum environment (ref. 110).   The increase in friction be-
ginning at 550° C (823 K) in figure 62 indicates the influence of
the input of frictional heat on the dissociation of the molybdenum
disulfide.   With X-ray examination of the surface after operating
at temperatures above 730° C (1003 K), Brainard confirmed the
dissociation of molybdenum disulfide during the sliding friction
experiment into molybdenum and sulfur.

Molybdenum diselenide is slightly more stable in vacuum
than molybdenum disulfide.   It will be noted that the friction
coefficient in figure 62(b) for molybdenum diselenide remained
relatively low and constant to 750° C (1023 K) at which time it
began to increase.   Dissociation studies conducted in refer-
ence 111 indicate that molybdenum diselenide is thermodynam-
ically more stable than molybdenum disulfide and that the fric-
tion results are as might be anticipated.   The friction results
of molybdenum ditelluride in figure 62(c) indicate that it ex-
hibits about the same stability as molybdenum disulfide in vac-
uum friction experiments.   The friction coefficient, however,
was slightly higher for the molybdenum ditelluride than it was
with molybdenum disulfide on the same metal surface.   The data
of figure 62 indicate the relatively broad temperature range
over which some of the inorganic solid films may be useful as a
lubricant to reduce friction and wear of material surfaces in
contact.

In figure 63 friction coefficients are plotted for the three
analogous tungsten compounds to the molybdenum compounds
examined in figure 62: tungsten disulfide, tungsten diselenide,
and tungsten ditelluride.   The experiments were conducted under
conditions identical to those in figure 62.   The films were rubbed
films of the solid-film lubricant on a metal substrate.   The con-
tacting surface was also a metal.   A comparison of figures 63(a)
and 62(a) shows that molybdenum disulfide is stable at slightly
lower temperatures than tungsten disulfide.   Tungsten diselenide
exhibited very low friction coefficients over the same tempera-
ture range examined with molybdenum diselenide in figure 62(b).

Figure 63(b) indicates that molybdenum diselenide and tungsten diselenide may be useful over a broader temperature range in a vacuum environment than the most commonly used solid-film inorganic lubricant, molybdenum disulfide.

The poorest film in preventing adhesion and metal-to-metal contact was tungsten ditelluride. Friction coefficients obtained with tungsten ditelluride as a solid-film lubricant were relatively high compared with the other solid films (fig. 63(c)). The friction coefficient for tungsten ditelluride at temperatures below 700° C (973 K) was in excess of 0.2. The data of figures 62 and 63 indicate in general that the lubricating properties of the dichelcoanides of molybdenum and tungsten are very good with the exception of tungsten ditelluride.

Another layer lattice compound with very good friction properties in a vacuum environment is cadmium iodide. Flom and Haltner (ref. 113) investigated the friction behavior of cadmium iodide in detail in a vacuum environment. They conducted sliding friction experiments in both air and vacuum at various sliding speeds to contrast the friction behavior of cadmium iodide in those environments. Some of their friction results are reproduced in figure 64. In figure 64(a) friction coefficient is plotted as a function of sliding speed. The friction coefficient for cadmium iodide increased with increasing sliding speed. Identical experiments were conducted in a vacuum environment with cadmium iodide. Again, an increase in friction coefficient with sliding speed was observed (fig. 64(b)). The friction coefficient over the entire range of sliding speeds examined in figure 64(b) were lower than the friction coefficients in air in figure 64(a). Flom and Haltner attributed the general decrease in friction coefficient change in environment from air to vacuum to the loss of water vapor. The friction properties of the cadmium iodide are better in the absence of water vapor than in the presence of it just as is the case with molybdenum disulfide. The increase in friction coefficient with increasing sliding speed in both environments is unusual. With the more conventional solid-film lubricants (e.g., molybdenum disulfide), no such speed discrepancy is observed. The dependency of friction coefficient on speed in
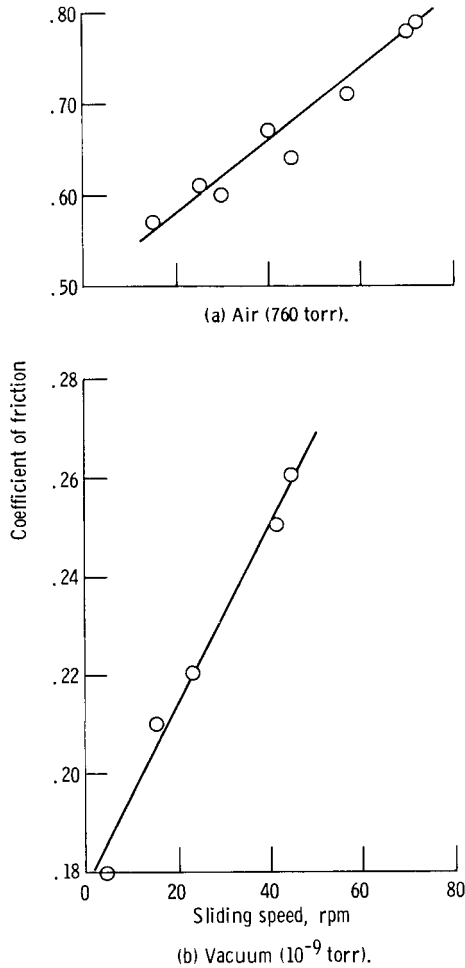
Figure 64. - Coefficient of friction as function
of sliding speed for cadmium iodide in
vacuum and in air (ref. 112).

both air and vacuum may be related to the stability of the crystal structure itself with sliding. With increased sliding speeds, increased frictional energy is supplied to the interface, and this may alter the stability of the cadmium iodide.

METHODS OF APPLICATION

The method of applying the solid-film lubricants to surfaces in order to inhibit adhesion, friction, and wear can be achieved

by several methods. Such solid-film lubricants as molybdenum disulfide have been applied by many different techniques. Burnishing, that is, mechanically rubbing the inorganic solid film onto the surface has been a common technique. In general, those who have used this method have found that, if the surface were slightly roughened, rather than highly polished, a better protective surface film of the lubricant was obtained.

Probably the most common method of applying such solid-film lubricants is to mix the solid film lubricant with some binder material (something which will enhance the adhesion of the solid film lubricant to the substrate material). Binders have included inorganic compounds such as sodium silicate and organic materials such as epoxy and resins. There is a wide range of materials that have been used as binders to achieve the adhesion of the solid-film lubricants to the substrate surface. In general the binder is not itself a lubricant; it is undesirable from the view point of lubrication but is nonetheless necessary in order to accomplish adhesion to the surface.

Sputtering, both radiofrequency (rf) and direct current (dc) have recently been used to apply molybdenum disulfide films to solid metal surfaces (refs. 123 and 124). The use of sputtering has eliminated the need for a binder. Further, very strong adhesion of the molybdenum disulfide to the substrate can be achieved with sputtering. In the sputtering process, argon ion plasma is used to bombard the surfaces to be coated. In the argon-ion bombardment process, the adsorbed surface films on the components to be coated are removed by the impinging argon ions. Thus, the specimen surface can be ionically cleaned in a vacuum environment. Molybdenum disulfide is then deposited by either rf or dc sputtering on to the freshly cleaned surface. The entire operation is conducted in a vacuum. The cleaning procedure with argon ions before the deposition of the molybdenum disulfide insures strong adhesion because of the electron interaction between the clean metal and the molybdenum disulfide being deposited.

In general, it has been found that the film thickness required for effective boundary lubrication with molybdenum disulfide

films applied by sputtering can be extremely thin.   Spalvins
(ref. 124) applied films that were typically 2000 Å (200 nm) thick
and achieved effective boundary lubrication (see fig. 65).   The
friction coefficient is plotted for niobium in sliding contact with
niobium in the absence of a lubricating film on the left side of
figure 65.   The friction coefficient is high and erratic, indicat-

(a) No lubricant.   (b) Sputtered MoS_2 film lubricant 2000 Å (0.2 μm) thick.
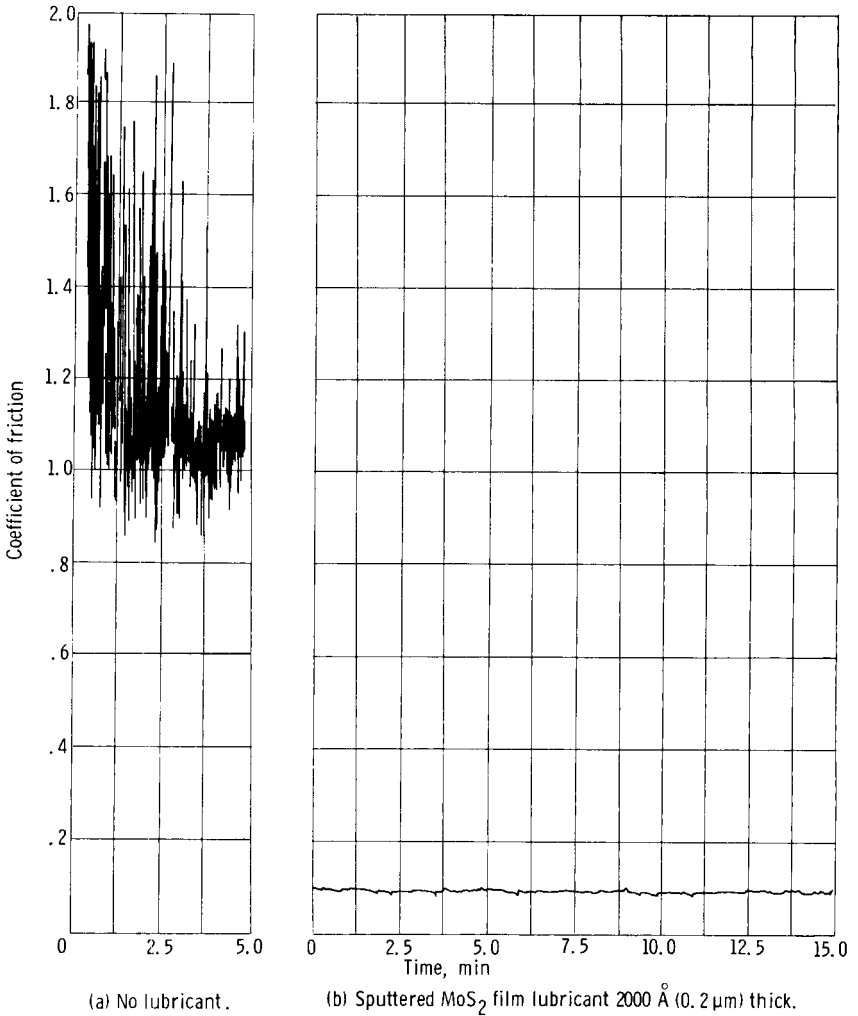
Figure 65. - Actual friction traces of niobium sliding on niobium with and without sputtered
MoS_2 film. Sliding velocity, 2.5 centimeters per second; load, 25 grams (0.25 N); pres-
sure, 10^{-11} torr (ref. 123).

ing marked stick-slip during the sliding process due to the adhe-
sion of the niobium to itself. When the surface is coated by
sputtering with 2000 Å (200 nm) of molybdenum disulfide, the
friction coefficient decreases to a value of less than 0.1 and
remains relatively low for long periods of time. Repeated cy-
cles over the same surface have indicated that thin films of the
order of 2000 Å (200 nm) of molybdenum disulfide can provide
effective surface protection against adhesion for as much as one
half of a million repeated cycles.

The effectiveness of the application technique in providing
surface protection by the solid-film lubricant, molybdenum di-
sulfide, is shown in figure 66. There, the cycles to failure are
shown for films of molybdenum disulfide that have been applied
by three methods. The first application method, burnishing,
yields the shortest endurance of molybdenum disulfide films.
The second method and that most commonly used for applying
solid film lubricants is resin bonding. This 130 000-Å (13-μm)
thick film exhibited endured approximately 100 000 cycles over
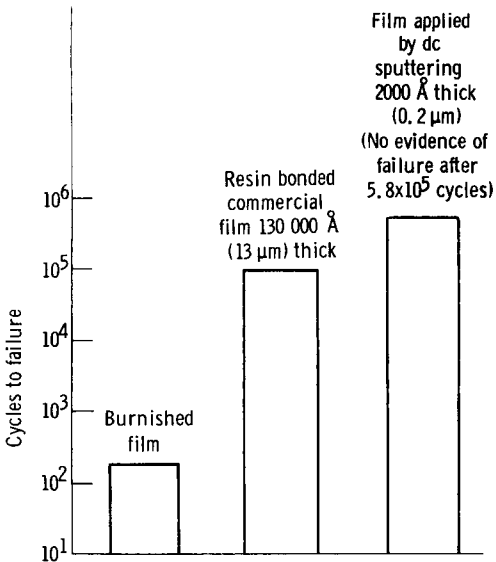the same surface. The film which provided the greatest endur-

Figure 66. - Endurance lives of MoS_2 films applied
by various techniques (ref. 123).

ance was that applied by d-c sputtering. It lasted more than
500 000 cycles. Note in figure 66 that the molybdenum disulfide
film applied by sputtering was only 2000 Å (200 nm) thick and
that the commercial resin bonded film has a thickness of
130 000 Å (13 μm). These results indicate that extremely thin
films may provide effective boundary lubrication to minimize
adhesion, friction, and wear for solid surfaces in contact over
prolonged periods of time.

SOFT METAL FILMS

The critical factor in the lubrication efficiency of solid-film
lubricants in a vacuum environment appears to be the adhesion
of the lubricant to the substrate.

Another class of materials that are effective as boundary
lubricants in a vacuum environment are thin, soft-metal films.
These films have been used for many years in more conventional
environments to minimize friction and wear between two solid
surfaces. If a thin, soft-metal film is applied to a very hard
substrate material and if the two surfaces are brought into con-
tact under a load, the load will be supported by the high-strength
substrate material. As a consequence, the true contact area may
be relatively small. When tangential motion is imposed either in
sliding, rubbing, or rolling contact, shear will take place at the
interface. If a soft, thin-metal film is interposed between the
two hard surfaces, shear will occur in the weakest region in the
surficial area. This will occur then in the soft-metallic film.
The friction force will be determined by the shear strength of
the soft-metal film present at the interface. Metals such as
gold, silver, indium, tin, lead, and zinc as well as cadmium
have been used as thin, soft, lubricating metal films.

In general, because the soft metals will have higher shear
strength than inorganic compounds, such as molybdenum disul-
fide, the friction coefficients for soft-metal films will generally
be slightly higher than for some of the inorganic compounds.
Friction coefficients for such soft-metal films as gold or silver
may be 0. 1. Gold is one of the most widely used soft-metal

films in an air environment (refs. 125 and 126). The conven-
tional method for the application of gold films as lubricants to
the substrate surfaces has been by electro-deposition (refs. 125
and 126). When electro-deposited gold films are placed in a
vacuum and when two surfaces are brought into rubbing or slid-
ing contact, the frictional heat generated in the process of roll-
ing, sliding, or rubbing is generally sufficient to cause the coat-
ings to blister because of gases trapped at the interface between
the substrate and the coating film. The gases cannot escape
from the coating material rapidly enough, and the coating blis-
ters on the surface. With sliding or rubbing contact, the blis-
ters are broken and metal-to-metal contact of the base mate-
rials will occur through the lubricating film.

In order to avoid the relatively weak interface and to avoid
contaminants in the coating and at the interface between gold and
the substrate surface, various vacuum deposition techniques
have been used to achieve the deposition of gold lubricating films
on various substrates (refs. 127 to 129). One method of applying
the gold films is sputtering. Gold films have been sputtered onto
various substrate surfaces to provide surface protection and re-
duce the adhesion, friction, and wear of various surfaces. The
sputtered gold films do not contain the contaminants normally
associated with conventional electrodeposited films because the
entire coating process is accomplished in vacuum.

The electron photomicrograph of figure 67 shows a typical
sputtered gold film on a nickel substrate. The deposited gold
crystals are very small; but the film is principally gold, and
its adherence to the nickel surface is good. In the sputtering
process for the deposition of a soft-metal film such as gold,
argon-ion bombardment is used to clean the substrate surface
just as it is for the deposition of molybdenum disulfide films.
This gives rise to good metal-to-metal bonding because the soft-
metallic film is depositing on a clean metallic substrate. Slid-
ing friction experiments conducted on such films in a vacuum
environment indicate that they have very good adhesion. The
coatings do not blister as is normally encountered with elec-
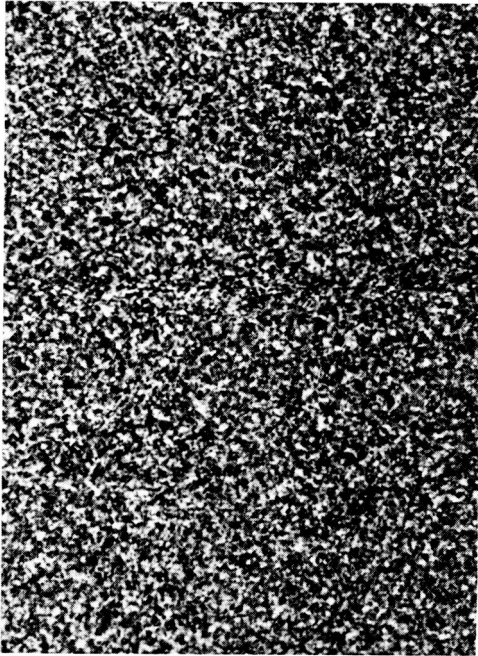trodeposited films, and they afford very good surface protec-

Figure 67. - Electron transmission micrograph of sputtered gold film on nickel surface (ref. 123). X87 000.

tion giving minimum friction coefficients.

Figure 68 presents the coefficient of friction for a nickel chrome alloy in sliding contact with niobium. The friction coefficient is plotted in figure 68 for the bare metals in contact and a friction coefficient of 1.2. Friction is also plotted for a conventional vacuum vapor deposited film. The adhesion is not as good as that obtained with sputtering. Also presented in figure 68 are the friction data for gold films, which have been applied by sputtering on the nickel-chrome substrate. The data of figure 68 indicate that the friction coefficient is markedly reduced by the presence of gold, whether applied by vapor deposition or by sputtering. The better adhesion of the film sputtered to the substrate results in longer endurance for the sputtered coating. The results obtained with molybdenum disulfide and gold using sputtering as a method of application indicate that such techniques improve the adhesion of the coating material to the
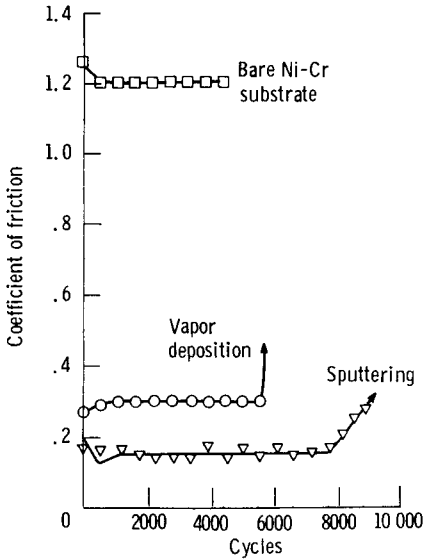
Figure 68. - Coefficient of friction of niobium sliding on Ni-Cr alloy with gold deposited by vapor deposition and sputtering about 2000 Å (0.2 μm) thick. Sliding velocity, 2.5 centimeters per second; load 250 grams (2.5 N); ambient pressure, 10^{-11} torr (ref. 123).

substrate, and offer considerable promise for the application of solid-film lubricants.

Another metal that has demonstrated an ability to provide effective boundary lubrication with solid surfaces in contact in a vacuum is gallium (ref. 130). Gallium has a very low vapor pressure. Its melting point is near room temperature; therefore, it can lubricate much as a conventional oil. Friction and wear studies conducted in reference 130 with gallium as a boundary lubricant for various materials indicate that it offers considerable promise as a material to reduce adhesion, friction, and wear in vacuum.

REFERENCES

1. da Vinci, Leonardo (Edward MacCurdy, trans.): Notebooks. Jonathan Cape, London, 1938.

2. Amontons, G.: Histoire de l'Academic Royale des Sciences avec les Memoires de Mathematique et de Physique. 1699, p. 206.

3. Coulomb, C. A.: Memoires de Mathematique et de Physique de l'Academic Royale des Sciences. 1785, p. 161.

4. Bowden, F. P.; and Tabor, D.: The Friction and Lubrication of Solids. vol. I. Clarendon Press, Oxford, 1950.

5. Gwathmey, Allan T.; Leidheiser, Henry, Jr.; and Smith, G. Pedro: Influence of Crystal Plane and Surrounding Atmosphere on Chemical Activities of Single Crystals of Metals. NACA TN 1460, 1948.

6. Hayward, D. O.; and Trapnell, B. M. W.: Chemisorption. Second ed., Butterworths & Co., 1964.

7. Kramer, Irvin R.; and Demer, Louis J.: Effect of Environment on Mechanical Properties of Metals. Progr. Materials Sci., vol. 9, 1961, pp. 133-199.

8. Westwood, A. R. C.; and Stoloff, N. S., eds.: Environment-Sensitive Mechanical Behavior. Gordon and Breach Science Publ., 1966, p. 35.

9. Likhtman, V. I.; Rebinder, P. A.; and Karpenko, G. V.: Effect of Surface-Active Media on the Deformation of Metals. Chemical Publishing Co., 1960.

10. Westwood, A. R. C.: Sensitive Mechanical Properties. Chemistry and Physics of Interfaces. American Chemical Society Publ., 1965.

11. Rebinder, P. A.; and Likhtman, V. I.: Effect of Surface-Active Media on Strains and Rupture in Solids. Proc. 2nd Inter. Cong. Surface Activity, London, No. 3, 1957, pp. 563-580.

12. Bridgman, P. W.: Effects of High Shearing Stress Combined with High Hydrostatic Pressure. Phys. Rev., vol. 48, no. 10, Nov. 15, 1935, pp. 825-847.

13. Bridgman, P. W.: Shearing Phenomena at High Pressures, Particu-
    larly in Inorganic Compounds. Proc. Am. Acad. Arts Sci.,
    vol. 71, 1937, pp. 387-460.

14. Ernst, H.; and Merchant, M. E.: Surface Friction Between Metals -
    A Basic Factor in the Metal Cutting Process. Proceedings of the
    Special Summer Conferences on Friction and Surface Finish. Mur-
    ray Printing Co., 1940, pp. 76-101.

15. Joffe, Abram F.: The Physics of Crystals. McGraw-Hill Book Co.,
    Inc., 1928.

16. Roscoe, R.: The Plastic Deformation of Cadmium Single-Crystals.
    Phil. Mag., vol. 21, 1936, pp. 399-406.

17. Harper, S.; and Cottrell, A. H.: Surface Effects and the Plasticity
    of Zinc Crystals. Proc. Phys. Soc., ser. B, vol. 63, pt. 5, May
    1950, pp. 331-338.

18. Westwood, A. R. C.: The Rebinder Effect and the Adsorption-
    Locking of Dislocations in Lithium Fluoride. Phil. Mag., vol. 7,
    no. 76, Apr. 1962, pp. 633-649.

19. Westwood, A. R. C.; Goldheim, D. L.; and Lye, R. G.: Rebinder
    Effects in MgO. Phil. Mag., vol. 16, no. 141, Sept. 1967, pp.
    505-519.

20. Kramer, I. R.: The Effect of Surface-Active Agents on the Me-
    chanical Behavior of Aluminum Single Crystals. Trans. AIME,
    vol. 221, no. 5, Oct. 1961, pp. 989-993.

21. Westbrook, J. H.; and Jorgense, P. J.: Indentation Creep of
    Solids. Trans. AIME, vol. 233, no. 2, Feb. 1965, pp. 425-438.

22. Kennedy, Alfred J.: Processes of Creep and Fatigue in Metals.
    John Wiley & Sons, Inc., 1963.

23. Dokos, S. J.: Sliding Friction Under Extreme Pressures. J.
    Appl. Mech., vol. 13, no. 2, June 1946, pp. 148-156.

24. Ishlinski, A. Y.; and Kraghelsky, I. V.: On Stick-Slip in Friction.
    Zh. Tekn. Fiz., vol. 14, 1944, pp. 276-282.

25. Whitehead, J. R.: Surface Deformation and Friction of Metals at
    Light Loads. Proc. Roy. Soc. (London), ser. A, vol. 201,
    no. 1064, Mar. 7, 1950, pp. 109-124.

26. Barwell, Frederick T.: Lubrication of Bearings. Butterworth &
    Co., 1956.

27. Kruschov, M. M.; and Babichev, M. A.: Investigations Into the Wear of Metals. U. S. S. R. Academy of Sciences, Moscow, 1960.

28. Scott, V. D.; and Wilman, H.: Surface Re-Orientation Caused on Metals by Abrasion - Its Nature, Origin and Relation to Friction and Wear. Proc. Roy. Soc. (London), ser. A, vol. 247, no. 1250, Sept. 30, 1958, pp. 353-368.

29. Spretnak, J. W.: A Summary of the Theory of Fracture in Metals. DMIC Rep. 157, Battelle Memorial Inst., Aug. 7, 1961.

30. Buckley, Donald H.: Effect of Various Properties of FCC Metals on Their Adhesion as Studied with LEED. J. Adhesion, vol. 1, Oct. 1969, pp. 264-281.

31. Buckley, Donald H.: Effect of Orientation on Friction Characteristics of Single-Crystal Beryllium in Vacuum (10^{-10} Torr). NASA TN D-3485, 1966.

32. Buckley, Donald H.: Effect of $3\frac{1}{2}$ Percent Silicon on Adhesion, Friction, and Wear of Iron in Various Media. NASA TN D-5667, 1970.

33. Tipper, C. F.: The Brittle Fracture of Metals at Atmospheric and Sub-Zero Temperatures. Met. Rev., vol. 2, no. 7, 1957, pp. 195-261.

34. Zener, Clarence: The Micro-Mechanism of Fracture. Fracturing of Metals. American Society for Metals, 1948, pp. 3-31.

35. Cottrell, A. H.: Theoretical Aspects of Fracture. Fracture. B. L. Averbach, D. K. Felbeck, G. T. Jahn, and D. A. Thomas, eds., MIT Press and John Wiley & Sons, Inc., 1959, pp. 20-53.

36. Petch, N. J.: The Ductile-Cleavage Transistion in Alpha-Iron. Fracture. B. L. Averbach, D. K. Felbeck, G. T. Jahn, and D. A. Thomas, eds., MIT Press and John Wiley & Sons, Inc., 1959, pp. 54-67.

37. Cottrell, A. H.: Theory of Brittle Fracture in Steel and Similar Metals. Trans. AIME, vol. 212, no. 2, Apr. 1958, pp. 192-203.

38. Griffith, A. A.: The Phenomena of Rupture and Flow in Solids. Roy. Soc. Phil. Trans., vol. 221A, 1921, pp. 163-198.

39. Irwin, G. R.: Onset of Fast Crack Propagation in High Strength Steel and Aluminum Alloys. Rep. 4763, Naval Research Lab., May 24, 1956.

40. Irwin, George R.: Fracture Dynamics. Fracturing of Metals. American Society of Metals, 1948, pp. 147-166.

41. Irwin, George R.; and Kies, J. A.: Critical Energy Rate Analysis of Fracture Strength. Welding J. Res. Suppl., vol. 33, no. 4, Apr. 1954, pp. 193s-198s.

42. Stoloff, N. S.: Fracture of Iron-Base Solid-Solution Alloys. Physical Basis of Yield and Fracture. Stickland, A. C., eds., Institute of Physics and Physical Society, 1966, pp. 68-76.

43. van der Merwe, J. H.: On the Stresses and Energies Associated with Inter-Crystalline Boundaries. Proc. Phys. Soc., vol. A64, pt. 6, June 1950, pp. 616-637.

44. van der Merwe, J. H.: On the Structure of Epitaxial Bicrystals. Surfaces and Interfaces. I. John J. Burke, Norman L. Reed and Volker Weiss, eds., Syracuse University Press, 1967, pp. 361-381.

45. van der Merwe, J. H.: Crystal Interfaces. Part I. Semi-Infinite Crystals. J. Appl. Phys., vol. 34, no. 1, Jan. 1963, pp. 117-122.

46. Matthews, J. W.: Accommodation of Misfit Across the Interface Between Single-Crystal Films of Various Face-Centered Cubic Metals. Phil. Mag., vol. 13, no. 126, June 1966, pp. 1207-1221.

47. Rabinowicz, Ernest: Friction and Wear of Materials. John Wiley & Sons, Inc., 1965.

48. Radchik, A. S.; and Radchik, V. S.: Deformation of Surface Layers During Sliding. Dokl. Akad. Nauk SSSR, vol. 119, 1958, p. 933.

49. Cottrell, A. H.; and Hull, D.: Extrusion and Intrusion by Cyclic Slip in Copper. Proc. Roy. Soc. (London), ser. A, vol. 242, no. 1229, Oct. 29, 1957, pp. 211-213.

50. Mott, N. F.: A Theory of the Origin of Fatigue Cracks. Acta Met., vol. 6, no. 3, Mar. 1958, pp. 195-197.

51. Kennedy, Alfred J.: Processes of Creep and Fatigue in Metals. John Wiley & Sons, Inc., 1963.

52. Gilman, John J.: Cleavage, Ductility, and Tenacity in Crystals. Fracture. B. L. Averbach, D. K. Felbeck, G. T. Jahn, and D. A. Thomas, eds., MIT Press and John Wiley & Sons, Inc., 1959, pp. 193-224.

53. Wood, W. A.: Mechanism of Fatigue. Fatigue in Aircraft Stuctures. Alfred M. Feudenthal, ed., Academic Press, 1956, pp. 1-19.

54. May, A. N.: A Model of Metal Fatigue. Nature, vol. 185, 1960, pp. 303-304.

55. Thompson, N.: Some Observations on the Early Stages of Fatigue Fracture. Fracture. B. L. Averbach, D. K. Felbeck, G. T. Jahn, and D. A. Thomas, eds., MIT Press and John Wiley & Sons, Inc., 1959, pp. 354-375.

56. Orowan, E.: Theory of Fatigue of Metals. Proc. Roy. Soc. (London), ser. A, vol. 171, no. 944, May 1, 1939, pp. 79-106.

57. Hamilton, G. M.; and Goodman, L. E.: The Stress Field Created by a Circular Sliding Contact. J. Appl. Mech., vol. 33, no. 2, June 1966, pp. 371-376.

58. Buckley, Donald H.: Influence of Surface Active Agents on Friction, Deformation, and Fracture of Lithium Fluoride. NASA TN D-4716, 1968.

59. Buckley, Donald H.: Effect of Surface Active Media on Friction, Deformation, and Fracture of Calcium Fluoride. NASA TN D-5580, 1969.

60. Glenny, E.; and Taylor, T. A.: A Study of the Thermal-Fatigue Behavior of Metals. J. Inst. Metals, vol. 88, 1959-1960, pp. 449-461.

61. Savage, Robert H.: Graphite Lubrication. J. Appl. Phys., vol. 19, no. 1, Jan. 1948, pp. 1-10.

62. Smith, R. Nelson; Pierce, Conway; and Joel, Cliffe D.: The Low Temperature Reaction of Water with Carbon. J. Phys. Chem., vol. 58, no. 4, Apr. 1954, pp. 298-302.

63. Snow, C. W.; Wallace, D. R.; Lyon, L. C.; and Crocker, G. R.: Reaction of Carbon Blacks with Oxygen. Proceedings of the Third Conference on Carbon. Pergamon Press, 1957, pp. 279-287.

64. Bowden, F. P.; and Hanwell, A. E.: The Friction of Clean Crystal Surfaces. Proc. Roy. Soc. (London), Ser. A, vol. 295, no. 1442, Dec. 6, 1966, pp. 233-243.

65. Buckley, Donald H.: Friction Characteristics in Vacuum of Single and Polycrystalline Aluminum Oxide in Contact with Themselves and with Various Metals. ASLE Trans., vol. 10, no. 2, Apr. 1967, pp. 134-145.

66. Roberts, R. W.: Clean Surfaces, Their Preparation and Characterization. Adhesion or Cold Welding of Materials in Space Environments. Spec. Tech. Publ. 431, ASTM, 1967, pp. 20-66.

67. Tabor, D.: Junction Growth in Metallic Friction: The Role of Combined Stresses and Surface Contamination. Proc. Roy. Soc. (London), Ser. A, vol. 251, no. 1266, June 9, 1959, pp. 378-393.

68. Keller, D. V.: The Adhesion Between Solid Metals. Wear, vol. 6, 1963, pp. 353-365.

69. Taylor, Norman J.: A LEED Study of the Epitaxial Growth of Copper on the (110) Surface of Tungsten. Surface Sci., vol. 4, no. 2, 1966, pp. 161-194.

70. Spedding, Frank H.; and Daane, A. H.; eds.: The Rare Earths. John Wiley & Sons, Inc., 1961.

71. Hampel, Clifford A.; ed.: Rare Metals Handbook. Second ed., Reinhold Pub. Corp., 1961.

72. Bridgman, P. W.: Shearing Phenomena at High Pressures, Particularly in Inorganic Compounds. Proc. Am. Acad. Arts Sci., vol. 71, 1937, pp. 387-460.

73. Buckley, Donald H.; and Johnson, Robert L.: The Influence of Crystal Structure on Friction Characteristics of Rare-Earth and Related Metals in Vacuum 10^{-10} MM of Mercury. ASLE Trans., vol. 8, no. 2, Apr. 1965, pp. 123-132.

74. Wonsiewicz, B. C.; and Backofen, W. A.: Plasticity of Magnesium Crystals. Trans. AIME, vol. 239, no. 9, Sept. 1967, pp. 1422-1431.

75. Burke, E. C.; and Hibbard, W. R., Jr.: Plastic Deformation of Magnesium Single Crystals. J. Metals, vol. 194, no. 3, Mar. 1952, pp. 295-303.

76. Hauser, F. E.; Landon, P. R.; and Dorn, J. E.: Deformation and Fracture Mechanisms of Polycrystalline Magnesium at Low Temperatures. Trans. ASM, vol. 48, 1956, pp. 986-1002.

77. Buckley, Donald H.: Influence of Number of Operable Slip Systems on Friction Characteristics of Single-Crystal and Polycrystalline Magnesium. NASA TN D-4351, 1968.

78. Schmid, E.; and Boas, W.: Kristallplastizitat. Springer-Verlag, Berlin, 1935.

79. Teutonico, L. J.: The Dissociation of Dislocations on (112) Planes
    in Anisotropic B.C.C. Crystals. Acta. Met., vol. 13, no. 6,
    June 1965, pp. 605-610.

80. Seitz, Frederick: Modern Theory of Solids. McGraw-Hill Book
    Co., Inc., 1940.

81. Bowden, F. P.; and Hanwell, A. E.: The Friction of Clean Crys-
    tal Surfaces. Proc. Roy. Soc. (London), ser. A, vol. 295, no.
    1442, Dec. 6, 1966, pp. 233-243.

82. Bowden, F. P.; and Hanwell, A. E.: Friction and Wear of Diamond
    in High Vacuum. Nature, vol. 201, no. 4926, 1964, pp. 1279-
    1281.

83. Bowden, F. P.; and Hughes, T. P.: The Friction of Clean Metals
    and the Influence of Adsorbed Gases. The Temperature Coefficient
    of Friction. Proc. Roy. Soc. (London), ser. A, vol. 172, no.
    949, Aug. 3, 1939, pp. 263-279.

84. Bowden, F. P.; and Young, J. E.: Friction of Clean Metals and the
    Influence of Adsorbed Films. Proc. Roy. Soc. (London), ser. A,
    vol. 208, no. 1094, Sept. 7, 1951, pp. 311-325.

85. Harris, L. A.: Analysis of Materials by Electron-Excited Auger
    Electrons. J. Appl. Phys., vol. 39, no. 3, Feb. 15, 1968, pp.
    1419-1427.

86. Harris, L. A.: Some Observations of Surface Segregation by Auger
    Electron Emission. J. Appl. Phys., vol. 39, no. 3, Feb. 15,
    1968, pp. 1428-1431.

87. Taylor, Norman J.: Auger Electron Spectrometer as a Tool for Sur-
    face Analysis (Contamination Monitor). J. Vac. Sci. Tech.,
    vol. 6, no. 1, 1969, pp. 241-245.

88. Gibbs, J. W.: Thermodynamics. Vol. 1 of The Collected Works.
    Yale University Press, 1906.

89. Buckley, Donald H.: Influence of Chemisorbed Films on Adhesion
    and Friction of Clean Iron. NASA TN D-4775, 1968.

90. Buckley, Donald H.: Influence of Chemisorbed Films of Various
    Gases on Adhesion and Friction of Tungsten. J. Appl. Phys.,
    vol. 39, no. 9, Aug. 1968, pp. 4224-4233.

91. Bowden, F. P.; and Childs, T. H. C.: The Friction and Deformation of Clean Metals at Very Low Temperatures. Proc. Roy. Soc. (London), ser. A, vol. 312, no. 1511, Sept. 30, 1969, pp. 451-466.

92. Semenov, A. P.: The Bonding of Metals in the Basis of Cold Welding. Automatic Welding, no. 5, 1964, pp. 3-7.

93. Beebe, Ralph A.; and Dowden, Dennis A.: Heats of Adsorption of Gases on Chromic Oxide at Low Temperatures. J. Am. Chem. Soc., vol. 60, no. 12, Dec. 1938, pp. 2912-2922.

94. Trapnell, B. M. W.: Adsorption on Evaporated Tungsten Films. II. The Chemisorption of Hydrogen and the Catalytic Parahydrogen Conversion. Proc. Roy. Soc. (London), ser. A, vol. 206, no. 1084, Mar. 22, 1951, pp. 39-50.

95. Bowden, F. P.: The Influence of Surface Films on the Friction, Adhesion, and Surface Damage of Solids. Ann. N. Y. Acad. Sci., vol. 53, 1951, pp. 805-823.

96. Cooper, Earl C.; and Muller, Erwin W.: Field Desorption by Alternating Fields. An Improved Technique for Field Emission Microscopy. Rev. Sci. Instr., vol. 29, no. 4, Apr. 1958, pp. 309-312.

97. Richter, E. L.; and Schmidt, W. A.: Field Emission Studies of Iron. Surface Sci., vol. 15, no. 3, July 1969, pp. 498-506.

98. Benjamin, M.; and Jenkins, R. O.: The Distribution of Autoelectronic Emission From Single Crystal Metal Points. I. Tungsten, Molybdenum, Nickel in the Clean State. Proc. Roy. Soc. (London), ser. A, vol. 176, no. 965, Oct. 9, 1940, pp. 262-279.

99. Muller, E. W.; and Nishikawa, O.: Atomic Surface Structure of the Common Transition Metals and the Effect of Adhesion as Seen by Field Ion Microscopy. Adhesion or Cold Welding of Materials in Space Environments. Spec. Tech. Publ. 431, ASTM, 1967, pp. 67-87.

100. Pignocco, A. J.; and Pellissier, G. E.: Low-Energy Electron Diffraction Studies of Oxygen Adsorption and Oxide Formation on a (001) Iron Surface. J. Electrochem. Soc., vol. 112, no. 12, Dec. 1965, pp. 1188-1194.

101. Pignocco, A. J.; and Pellissier, G. E.: LEED Studies of Oxygen Adsorption and Oxide Formation on an (011) Iron Surface. Surface Sci., vol. 7, no. 3, July 1967, pp. 261-278.

102. Ehrlich, Gert: Adsorption on Clean Surfaces. Ann. N. Y. Acad. Sci., vol. 101, 1963, pp. 722-755.

103. Arthur, John R., Jr.; and Hansen, Robert S.: The Adsorption and Surface Reactions of Hydrocarbons on Clean Iridium. Ann. N. Y. Acad. Sci., vol. 101, 1963, pp. 756-765.

104. Hardy, William B.: Collected Scientific Papers. Cambridge University Press, 1936.

105. Akhmatov, A. S.: Molecular Physics of Boundary Friction. Israel Program for Scientific Translations, 1966. (Russian Original Published 1963.)

106. Young, David M.; and Crowell, A. D.: Physical Adsorption of Gases. Butterworth & Co., 1962.

107. Gilbreath, W. P.: Definition and Evaluation of Parameters Which Influence the Adhesion of Metals. Adhesion or Cold Welding of Materials in Space Environments. Spec. Tech. Publ. 431, ASTM, 1967, pp. 128-148.

108. Buckley, Donald H.: Friction and Wear Characteristics of Polyimide and Filled Polyimide Compositions in Vacuum (10^{-10} mm Hg). NASA TN D-3261, 1966.

109. Reichenbach, George S.; Shaw, Robert, Jr.; and Foster, Robert G.: Lubricant Behavior in High Vacuum. ASLE Trans., vol. 7, no. 1, Jan. 1964, pp. 82-90.

110. Dushman, Saul; and Lafferty, J. M.: Scientific Foundations of Vacuum Technique. Second ed., John Willey & Sons, Inc., 1962.

111. Brainard, William A.: The Thermal Stability and Friction of the Disulfides, Diselenides, and Ditellurides of Molybdenum and Tungsten in Vacuum (10^{-9} to 10^{-6} Torr). NASA TN D-5141, 1969.

112. Flom, D. G.; and Haltner, A. J.: Lubricants for the Space Environment. Presented at the AIChE Materials Conference, Symposium on Materials for Re-Entry and Spacecraft Systems - Spacecraft Materials, Part 2, Philadelphia, Pa., Mar. 31-Apr. 4, 1968.

113. Flom, D. G.; Haltner, A. J.; and Gaulin, C. A.: Friction and Cleavage of Lamellar Solids in Ultrahigh Vacuum. ASLE Trans., vol. 8, no. 2, Apr. 1965.

114. Haltner, A. J.: An Evaluation of the Role of Vapor Lubrication Mechanisms in MoS_2. Wear, vol. 7, 1964, pp. 102-117.

115. Savage, R. H.: On the Friction and Wear of Graphite and Other Layer-Latticed Solids. Fundamentals of Friction and Lubrication in Engineering American Society of Lubrication Engineers, 1954, pp. 161-164.

116. Johnson, Virgil R.; Lavik, Melvin T.; and Vaughn, George W.: Mechanism of WS_2 Lubrication in Vacuum. J. Appl. Phys., vol. 28, no. 7, July 1957, p. 821.

117. Johnson, Virgil R.; and Vaughn, George W.: Investigation of the Mechanism of MoS_2 Lubrication in Vacuum. J. Appl. Phys., vol. 27, no. 10, Oct. 1956, pp. 1173-1179.

118. Lavik, M. T.; Gross, G. E.; and Vaughn, G. W.: Investigation of the Mechanism of Tungsten Disulfide Lubrication in Vacuum. Lubr. Eng., vol. 15, no. 6, June 1959, pp. 246-249.

119. Lavik, Melvin T.; Daniel, T. Bruce; and Abbott, A. Neal: Friction of Molybdenum Diselenide. J. Appl. Phys., vol. 32, no. 9, Sept. 1961, p. 1795.

120. Bell, M. E.; and Findlay, J. H.: Molybdenite as a New Lubricant. Phys. Rev., vol. 59, no. 11, June 1, 1941, p. 922.

121. Devine, M. J.; Lamson, E. R.; and Bowen, J. H., Jr.: The Effect of the Chemical Composition of Metals in Solid Lubrication. Presented at the USAF Aerospace Fluids and Lubricants Conference, San Antonio, Texas, Apr. 16-19, 1963.

122. Craig, W. D., Jr.: Friction Variation of PTFE and MoS_2 During Thermal Vacuum Exposure. Lubr. Eng., vol. 20, no. 7, July 1964, pp. 273-277.

123. Spalvins, T.: Deposition of MoS_2 Films by Physical Sputtering and Their Lubrication Properties in Vacuum. ASLE Trans., vol. 12, no. 1, Jan. 1969, pp. 36-43.

124. Spalvins, T.: Sputtering of Solid Lubricants. Presented at the Third Symposium on Deposition of Thin Films, Rochester, N.Y., Sept. 9-10, 1969.

125. Antler, Morton: The Wear of Electrodeposited Gold. ASLE Trans., vol. 11, no. 3, July 1968, pp. 248-260.

126. Takagi, Rutsu, and Liu, Tung: The Lubrication of Steel by Electroplated Gold. ASLE Trans., vol. 10, no. 2, Apr. 1967, pp. 115-123.

127. Spalvins, T.; and Buckley, D. H.: Importance in Lubrication of Various Interface Types Formed During Vacuum Deposition of Thin Metallic Films. Transactions of the International Vacuum Metallurgical Conference, 1967, pp. 247-260.

128. Spalvins, T.; and Buckley, D. H.: Vapor-Deposited Gold Thin Films as Lubricants in Vacuum (10^{-11} mm Hg). J. Vac. Sci. Tech., vol. 3, no. 3, May/June 1966, pp. 107-113.

129. Spalvins, Talivaldis; Przybyszewski, John S.; and Buckley, Donald H.: Deposition of Thin Films by Ion Plating on Surfaces Having Various Configurations. NASA TN D-3707, 1966.

130. Buckley, D. H.; and Johnson, R. L.: Gallium-Rich Films as Boundary Lubricants in Air and in Vacuum to 10^{-9} mm Hg. ASLE Trans., vol. 6, no. 1, Jan. 1963, pp. 1-11.